ANALYSIS OF REGENERATION SYSTEM OF METRO TRAIN AND USE OF TECHNOLOGY ENHANCEMENT TO IMPROVE REGENERATION AND ENERGY SAVING MEASURES IN METRO TRAIN SYSTEM

A Project Report submitted in partial fulfillment of the requirements for the Degree of

MASTER OF TECHNOLOGY

IN

Power Electronics System (PES)

Submitted by:

ANAND KUMAR TIWARI

2K13/PES/501

Under the esteem guidance of:

Dr. Vishal Verma

Professor, DTU

Department of Electrical Engineering

Delhi Technological University

(Formerly Delhi College of Engineering)

July, 2016

Department of Electrical Engineering
Delhi Technological University
(Formerly Delhi College of Engineering)

CERTIFICATE

This is to certify that this project entitled "Analysis of Regeneration system of Metro Train and use of Technology Enhancement to improve Regeneration and Energy Saving Measures in Metro Train system" submitted by **Anand Kumar Tiwari, University Roll No. 2K13/PES/501**, student of Master of Technology (Power Electronics System) in Electrical Engineering department from Delhi Technological University (Formerly Delhi College of Engineering), is a dissertation work carried out by him under my guidance during session 2015-2016 towards the partial fulfillment of the requirements for the award of the degree of Master of Technology in Power Electronics System. Any material borrowed or referred to is duly acknowledged.

I wish his all the best in his endeavors.

Date: July 2016

ANAND KUMAR TIWARI
2K13/PES/501
M Tech (Power Electronics System)

Dr. VISHAL VERMA
Professor.
Electrical Engineering Department
Delhi Technological University

ACKNOWLEDGEMENT

While bringing out this report to its final form, I came across a number of people whose contributions in various ways helped my field of research and they deserve special thanks. It is a pleasure to convey my gratitude to all of them.

First and foremost, I would like to express my deep sense of gratitude and indebtedness to my project guide **Prof. Vishal Verma**, for his invaluable encouragement, suggestions and support from an early stage of this work and providing me an opportunity to work under his guidance and extraordinary experiences throughout entire period of the project. His continued cooperation, never-ending encouragement, meticulous guidance and uninhibited support at various stages helped me in preparation of this research study.

I specially acknowledge him for his advice, supervision, and the vital contribution as and when required during this research. His involvement with originality has triggered and nourished my intellectual maturity that will help me for a long time to come. I am proud to record that I had the opportunity to work with an exceptionally experienced Professor like him.

I am highly grateful to the **Mr. Amritesh Kumar**, Faculty of DTU, for his cooperation and kind support throughout the work.

I would also like to acknowledge the vital role of my present organization Delhi Metro Rail Corporation Ltd., in providing me with sectorial insights into the Train systems Technology and its Energy data of Train system.

I would also wish to express my gratitude to my family members and friends specially my wife **Ms. Saruka Rani** for their continuous support, which enabled me to take up the M. Tech. course.

Date: July 2016

ANAND KUMAR TIWARI
2K13/PES/501
M Tech (Power Electronics System)

ABSTRACT

The global energy scenario and climatic changes have forced mankind to reorient the development model for minimizing energy needs and energy consumption. Energy conservation grows in importance worldwide in terms of preventing of global warming.

The Transportation sector is one of the largest consumers of energy, with significant contribution to CO_2 emissions. Transport emissions of today are over 30% higher than in 1990. By using energy efficient electric traction with regeneration capability and optimal vehicle design, Metro and Railway operators are continuously improving specific energy consumption and their environmental commitments. Adoption of multipronged strategies for minimizing energy consumption by analyzing each and every consumption point right from the vehicle manufacturing to its ultimate utilization and recycling is now considered essential. Since the subject is very wide in its scope, this paper covers those critical areas which need the attention of the designers and operators.

For a well-integrated public transport system it is imperative that travel be as seamless as possible and offers a simple Integrated Reliable Energy Efficient Train System and operation. This is especially true when new modes of public transport such as BRT, Light Rail, and Mono Rail are introduced. To execute a seamless multi-modal integration, an electronic system for unified fare collection and indisputable settlement among operators is essential.

Traction accounts for about 60-80% of the total energy consumption in a Metro system. The quantity of energy consumed by trains is influenced by a wide range of factors, train design being one of them. Hence, optimization of the overall system design in order to control consumption of electricity becomes essential. The modern design of Metro Rolling Stock incorporating three phase induction motors and Converter Inverters enable recovery of a major portion of consumed electricity by way of using regenerative braking. Metro railways worldwide have reported an average of about 20% saving in traction energy on account of regeneration. Regeneration also helps to reduce heat load inside tunnel and thus reduce Air Conditioning load. With increased awareness and commitment for the environment, Metros have also taken it as Green House Gas reduction initiative. Regenerated energy is mostly used by other trains powering in the network. The quality of regenerated power is important since the injected harmonics effect signalling, communication system and other loads connected on the grid.

Power electronics contribute to saving energy with their highly efficient power conversion technologies, where power devices play central roles. Therefore, one design goal in Power Electronics is the reduction of losses in power devices. Silicon (Si) has been used as a conventional material for power devices. However, power devices fabricated using Si are approaching their performance limits. Silicon carbide (SiC) power devices are expected as next-generation alternatives to conventional Si power devices because they demonstrate overwhelming characteristics in terms of loss reduction for their exceptional material properties, such as a wider band gap, a higher critical electric field strength, and a higher thermal

conductivity.

At present, most rail car inverters use Si diodes in an attempt to deliver both higher energy savings and enhanced performance. However, in order to achieve even higher performance gains, expectations have turned to SiC because it offers high voltage resistance, having 10 times greater dielectric breakdown strength. This enables the creation of thinner devices and, in turn, reduces resistance loss when developing the new compact SiC hybrid inverter.

This paper will report on the status of a present system and provide a detailed analysis and proposed solution. The goal of the project is to propose how to utilize the new technology available and save the Energy to the extent possible.

Contents

CHAPTER-1

1. Introduction

1.1 General

Environmental measures have played, and continue to play an important role on a global scale to achieve a low carbon society and prevent future global warming. There is a growing demand for the rail transport systems with low environmental impact. By producing rail car inverters which are reduced in size and weight, increased energy efficiency can be achieved.

Silicon-based power devices have long dominated the power electronics and power systems applications. Silicon-based power semiconductor devices, ranging from diodes, thyristors, gate turn-off thyristors, metal–oxide–semiconductor field-effect transistors, and, more recently, insulated-gate bipolar transistors (IGBT), integrated gate-commutated thyristors, and metal–oxide–semiconductor turn-off thyristors, are the workhorse of power electronic systems and circuits. Large-area devices that are capable of handling thousands of amperes and kilovolts are now available from a large number of manufacturers. MOS-gated devices such as IGBTs are now able to handle voltages up to 6 kV and currents up to 1200 A. IGBTs are being widely used for motor drives, resonant converters, and power supplies. IGBTs offer low switching losses, high switching frequency operation, and a simplified gate circuit. IGBT is one of the most popular silicon power high-voltage, high-current application devices and widely used for Traction Inverters. Silicon offers multiple advantages to power circuit designers, but at the same time suffers from limitations that are inherent to silicon material properties, such as low bandgap energy, low thermal conductivity, and switching frequency limitations. With IGBTs, switching performance is required to achieve low resistance at high breakdown voltage. On contrary, recently developed SiC is a compound semiconductor which is comprised of Silicon (Si) and Carbon (C). SiC is different than any other Si material in terms of breakdown field strength, band gap, thermal conductivity etc.

The need for faster devices with high voltage and high switching frequency capability is growing, especially for advanced power conversion. Applications where devices are required to operate at higher than 150C junction temperature, high voltages, high switching frequencies, and high power densities are growing, especially for Traction applications. Silicon-based devices are not able to meet these stringent requirements without costly cooling systems, large number of devices in series and parallel, and costly active or passive snubbers. The latter adds to the overall size and weight, a mostly undesirable feature of silicon-based power converters. Wide-bandgap-based semiconductor devices such as silicon carbide and gallium nitride offer multiple advantages for power electronic designers. The superior physical properties of these semiconductors offer a lower intrinsic carrier concentration (10–35 orders of magnitude), a higher electric breakdown field (4–20 times), a higher thermal conductivity (3–13 times), a larger saturated electron drift velocity (2–2.5 times), when compared to silicon. Silicon carbide in particular has been the focus of a number of research groups and

organizations in the past 15 years. Its wide bandgap energy of 2.2–3.3 eV is larger than the 1.1-eV bandgap of silicon. In addition, SiC has a higher electric breakdown field of $3X10^6$ V/cm, which is an order of magnitude larger than that of silicon. The higher breakdown field allows a ten times reduction in drift layer thickness; hence, lessening the minority carrier charge storage and greatly increasing the switching frequency of bipolar devices. Its high carrier saturation velocity of $2X10^7$ cm/s is also an order of magnitude larger than silicon's. Its high thermal conductivity of 4.9 W/cm.K enhances heat dissipation and coupled with the wide bandgap energy allows for power efficient high temperature operation up to 350ºC. According to various figures of merit, SiC comes out on top of silicon and gallium arsenide as the material of choice for power devices.

Power electronics converters for transportation applications have to comply with strict requirements because of space and weight limitations and extremely harsh operating conditions. In a vehicle, there is limited space for the electrical and/or mechanical units; therefore, all the units have to be compact, occupying as little volume as possible. Moreover, they are expected to be lightweight so that the weight of the vehicle stays constrained. A lighter vehicle means less load on the engine and/or motor, faster acceleration, and higher efficiency. Higher efficiency results in less fuel or battery charge consumption. Finally, converters have to be able to function at high temperatures for long periods of time without failure— i.e., they have to be highly reliable, and they must be available at a reasonable price.

In summary, the general requirements for any power converter in a transportation application are compactness, lightweight, high power density, high efficiency, and high reliability under harsh conditions.

1.2 Statement of Problem

As per Energy conservation law,

Energy cannot be created and it cannot be destroyed, it can be only transformed from one form to other form. Applying same logic in Metro system, The electrical energy required for propel the train can be converted back in electrical energy back by means of Regeneration using suitable power electronic devices.

Electrical Energy for propulsion (Acceleration) of Train

↓

Kinetic Energy (Train movement)

↓

Regenerated Electrical Energy for Braking (Deceleration) of Train

In lossless system

Input Electrical Energy = Regenerated Electrical Energy

But practical regenerated Energy is only some percentage (typically varies from 20% to 40%) of Input electrical energy.

With smaller inter-station distances, Metro operation is essentially of start/stop nature. Due to frequent acceleration & de-acceleration requirements, energy demand is very high. Traction accounts for about 60-80% of total energy consumption in a Metro system. The quantity of energy consumed by trains is influenced by a wide range of factors, which can be grouped as

(i) Design of network,

(ii) Design of trains &

(iii) Service planning operation.

Hence, optimization of overall system design in order to control consumption of electricity becomes essential.

This need to be analyzed to know the potential of energy loss. It could be

(i) losses at source level (OCS and RSS)

(ii) losses in between OCS and Converter

(iii) losses at Converter level

(iv) limitation of Power Electronic devices

(v) losses in between Converter and load

(vi) losses at load level (Traction Motors)

1.3 Scope of Project

The scope of the project would be to

1. Find out the key components/equipments responsive for Energy losses/ Less Regeneration as described above

   (i) losses at source level (OCS and RSS)

   (ii) losses in between OCS and Converter

   (iii) losses at Converter level

   (iv) limitation of Power Electronic devices

   (v) losses in between Converter and load

   (vi) losses at load level (Traction Motors)

2. Design modification to improve regeneration of Metro system

The scope of this project is limited to one of design aspect of trains i.e. regenerative braking. The modern

design of Metro Rolling Stock incorporating three phase induction motors and Converter Inverter enables recovery of a major portion of consumed electricity by way of using regenerative braking. Metro railways worldwide have reported an average of about 20% saving on account of regeneration.

Tangible benefits

Saving of Energy.

(i) By using intelligent blending of regenerative and pneumatic braking, optimization of energy recovery as well as accurate control of train movement can be achieved.

(ii) In addition to saving of electricity, regenerative braking provides additional benefits in form of lesser wear of wheel and brake pads.

(iii) In Metro applications, there is likelihood of having a considerable area of underground operation. An efficiently employed regenerative braking system helps to reduce heat load inside tunnel and thus reduce Air Conditioning load.

(iv) Regenerative braking helps in mitigating Global Warming by way of reducing carbon emissions due to reduced electricity requirements from grid.

Intangible benefits

(v) Environmental friendly system

(vi) Technology driven system

(vii) Increase in customer satisfaction

(viii) Improvement in image

(ix) Improvement in knowledge & skill

1.4 Background of Metro system

With the proliferation of economic development in countries in Middle East, East Asia and South East regions, the transportation needs of people have suddenly taken a quantum jump. The energy consumed by the new developing economies is naturally showing a distinct increase every year. The trend in the past indicates that the energy consumption increases at the highest pace in the field of transport since most energy is consumed by automobiles for private use. This may further accentuate the green house and may accelerate the associated problems of rising sea level and arable land desertification more serious. Therefore it has now become essential to globally undertake measures to restrict energy consumption in transportation sector.

The energy consumed by automobiles accounts for the majority of the total energy consumed in passenger and freight transport in the domestic transport industry. In terms of the energy consumption per

passenger – kilometer in passenger transport, railways consumes only 1/6 of energy consumed by cars for private use and 3/5 that of the busses. For freight transport, Railway consumes only 1/20 of energy consumed by private trucks and 1/6 that of commercial trucks (calculated in terms of energy consumed per ten-kilometer). It may, therefore, be appreciated that energy consumed by cars for private use and trucks will be cut by 80% if railways are used to replace these road vehicles. Typical value of CO_2 emission for an Aircraft is 23KgCO_2/100ppm as compared to aprox. 4.8 Kg CO_2/100ppm for Rail. Electric Railways reduce environmental contamination by avoiding SO_2 & NOx emissions. This inter-alia means an energy efficient electric railway transport system would provide an effective means to optimally use limited energy resources and simultaneously provided a solution to environmental problem.

CO_2 Emissions

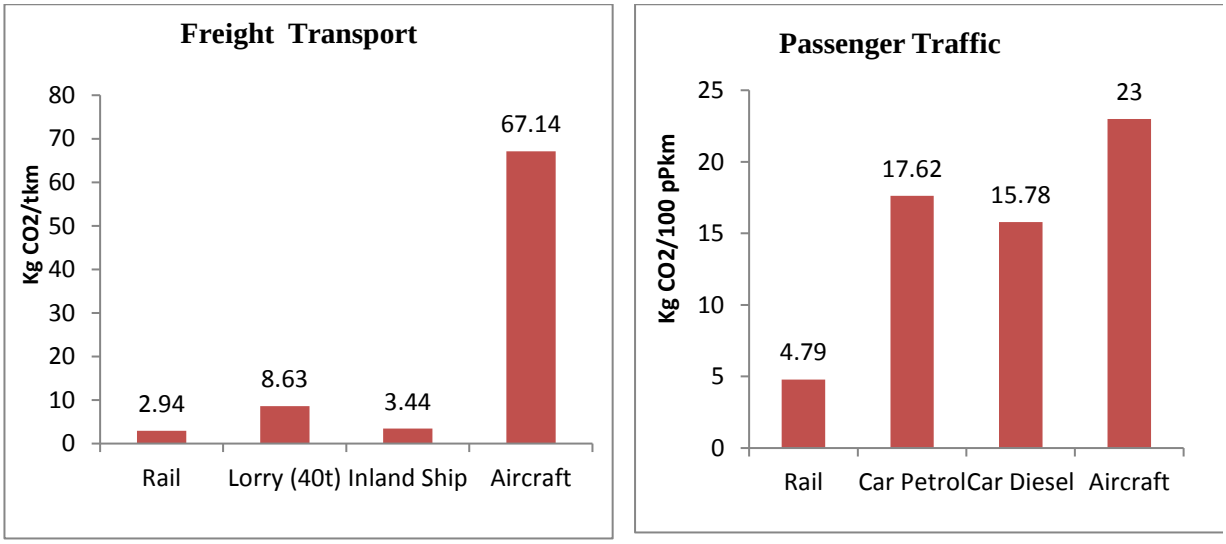

As compared to other industries, though the energy consumption by Railways is rather small, there is still tremendous scope to reduce energy consumption especially because of reduced losses between iron wheel and rail as compared to tyre and road surface and possibility of recovery of kinetic energy of trains. Research efforts are now being focused on the specific areas which can yield energy saving. Development of technologies for storage of energy such as lithium batteries, fly wheels and fuel cells is an effort in this direction.

CHAPTER-2

2. Literature Survey

2.1 General:

Use of SiC based power electronic devices is highly popular subject now-a-days, since Si base devices are reaching at their performance limits due to diversified and extremely harsh operating requirements. At the same time energy saving approaches are also being discussed.

Silicon carbide (SiC) is a wide-bandgap semiconductor, which compared to silicon has superior physical and electrical properties especially at high temperature [1, 2]. SiC power devices are considered to be one of the enabling technologies for future power dense DC-DC converters, as they can be operated at very high switching frequencies which reduces the size of the magnetic components. The fast switching transitions of these devices do however create design issues for the converter, including parasitic current and voltage oscillations, electromagnetic interference (EMI) effects and control complexities.

2.2 Reviews of Literature:

A large number of publications have appearing in the field of SiC based devices, it's used and comparison with conventional Si based devices.

To understand the SiC MOSFET static and dynamic behaviour, several modelling approaches have been proposed, including semiconductor physics models and behavioural models. Most of the models are complex or poorly incorporate the circuit parasitic components, and so produce inaccurate circuit waveforms. Analytical modelling of the switching transients can be a good approach to understand the switching behaviour of SiC MOSFETs. The models can then be extended to incorporate circuit parasitics and also soft-switching of the power devices.

Switching test results of SiC MOSFETs in converter circuits have shown that their switching losses can significantly limit the operating frequency. Soft switching techniques can be employed to minimize the switching losses.

Sic-based power switches can be used in both electric traction drives and other automotive electrical subsystems with many benefits compared with Si based switches. With less than 1/100 the conduction drop, Sic-based devices have reduced conduction losses. Consequently, the efficiency of the power converter is higher. In addition, Sic-based semiconductor switches can operate at high temperatures (up to 600°C reported in [I]) without much change in their electrical properties. Thus the converter has a higher reliability. Reduced losses and allowable higher operating temperatures. result in smaller heatsink size. Moreover, the high frequency operating capability of Sic converters lowers the filtering requirement and the filter size. As a result, they are compact, light, reliable, and

efficient and have a high power density. These qualities satisfy the requirements of the automotive industry for power converters.

2.2.1 Design of Traction System (Simulation) for Dhaka Metro

Mathematical calculation

(i) Weight of a Crush-loaded 8 car train = 305.28 tons

(ii) (305.28 tons) x (1000kg/ton) = 305280 kg weight = 3053600 kg

(iii) (3053600 kg mass) x (0.92 m/sec^2) = 280857 Newtons (N) where N = kg m/sec^2

(iv) Required Constant Acceleration to a velocity of 11.16 m/sec, or 40 km/hr

(v) (280857 N) x (11.16 m/sec) = 3134370 kg m^2/sec^3 = 3134370 watts (W) where W = kg m^2/sec^3

(vi) (3134370 W) / 16 Traction Motors = 195898 W/Traction Motor

(vii) Traction Motor Power = 200 kW / motor

(viii) (3134370 W) / (1500 VDC OCS Line Voltage) = 2090 Amps (OCS Line Current)

Design using Mathematica (Simulation)

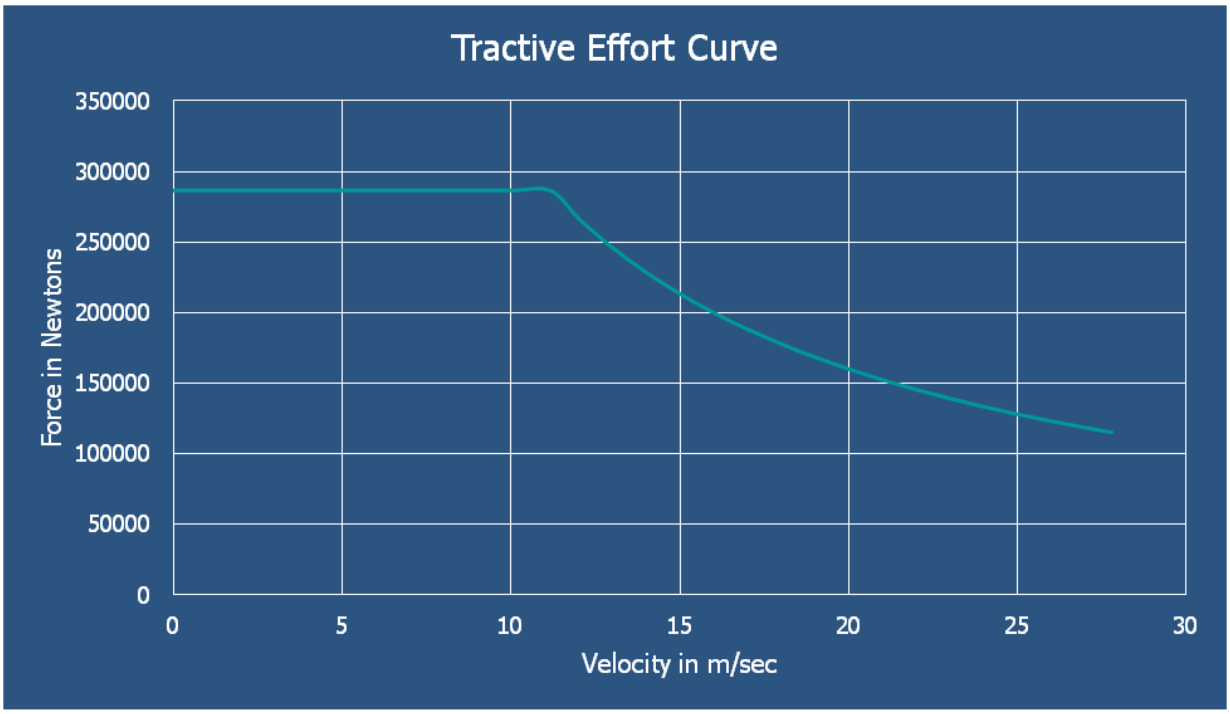

Figure 2.1

(i) VVVF output voltage = 0 V AC to 1100 V AC Line to Line

(ii) VVVF output current at 11.16 m/sec velocity = (200000 W/motor) / √3 X 1100 V AC @.85 PF) = 123.5 Amps Line to Line per motor.

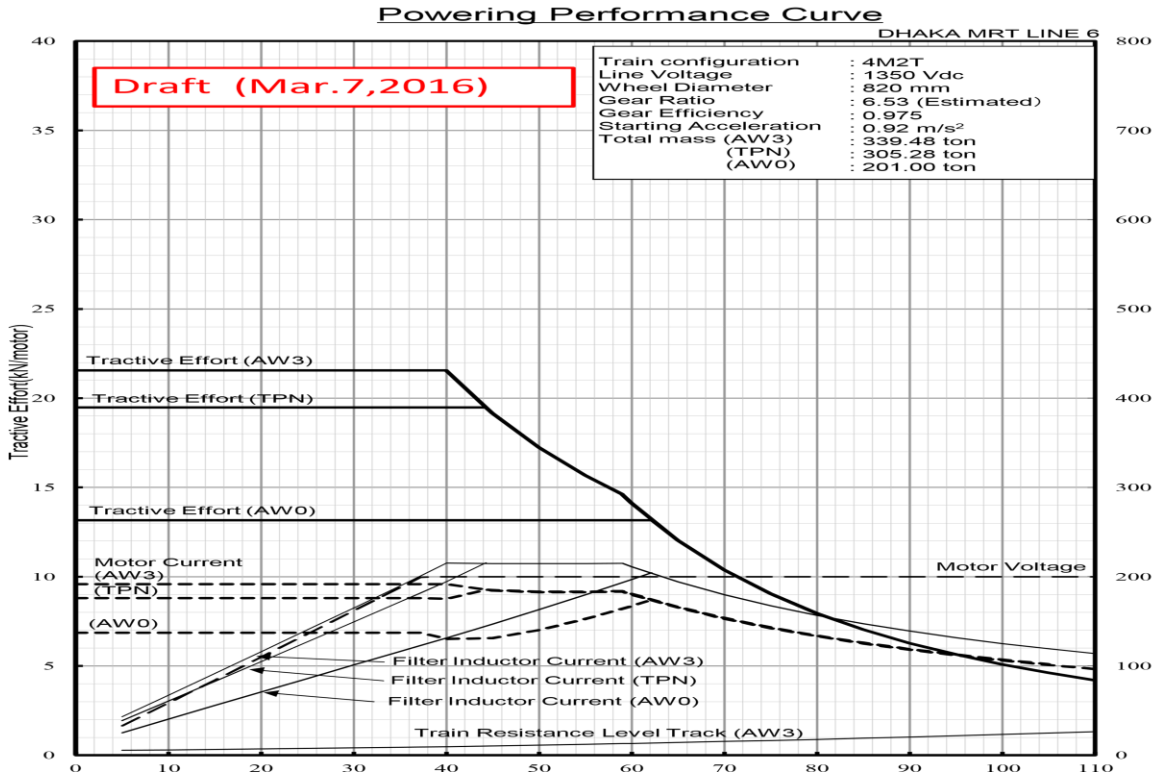

Figure 2.2 Power Performance Curve

2.2.2 Comparison of Silicon Carbide MOSFET and IGBT based Electric Vehicle Traction Inverters

There is an increasing demand for electrical and hybrid electrical vehicles on the market. All over the world governments are giving great support for the electrical vehicles to launch them on the market rapidly since most of the countries depend on the foreign sources for fuel and fuel sources seems to be under risk of diminishing. Besides, countries should reduce the fuel use as a main energy source in order to stop climate change. Electric vehicles give significant contribution for resolving these vital problems with zero emission. But, the driving range and cost of EVs are major obstacles to generalize the usage of the EVs. The inverter is the one of main parts of the traction system of the EVs to enhance vehicle performance with reasonable cost. The limited battery energy is transferred to electric motor through traction inverter and the cost of the traction inverter can be considered as the major cost of the traction system of the EV.

In recent years, SiC based MOSFET switches with high current and voltage ratings are manufactured and they could be a good candidate for the EV traction inverter. In literature, SiC semiconductor materials have inherent advantages compared to Si materials and they are about the replace Si-based power switches. The effect of using SiC devices on EVs is investigated. An integrated Matlab/Simulink simulation for Hybrid EV (HEV) traction inverter is described. The inverter includes SiC MOSFET and

SiC diodes and subjected to a real driving cycle. The range extension is analyzed for EVs by adopting SiC devices for the traction inverter. An accumulation channel concept is adapted to SiC trench MOSFET to have lower on-resistance and high breakdown voltage for EV motor drive systems. SiC MOSFET and IGBT based inverters are designed to measure power losses. The inverters are controlled with SPWM. Simulation model with VEHLIB and physical measurements of SiC MOSFET based inverter are compared. Two commercially available devices, SiC MOSFET and Si IGBT are modeled in PSCAD and Matlab/Simulink and an experimental model is designed to compare simulation results with experimental measurements. Si and SiC device technologies are compared for the use of HEVs traction inverters to find optimum chip area for each of them in.

In this study, SiC MOSFET and IGBT based traction inverters are simulated in PSIM and the performance of these inverters are compared. The comparison includes efficiency and cost of these inverters. Commercially available Powerex IGBT module, PM50RL1A120 and a Cree SiC MOSFET module, CCS050M12CM2, are modeled in detail using PSIM. They are simulated under different load conditions to obtain their efficiency curves. Then, obtained efficiency curves together with the vehicle kinematic model are used to evaluate energy requirements under three different drive cycles. Energy losses of these two inverters are compared.

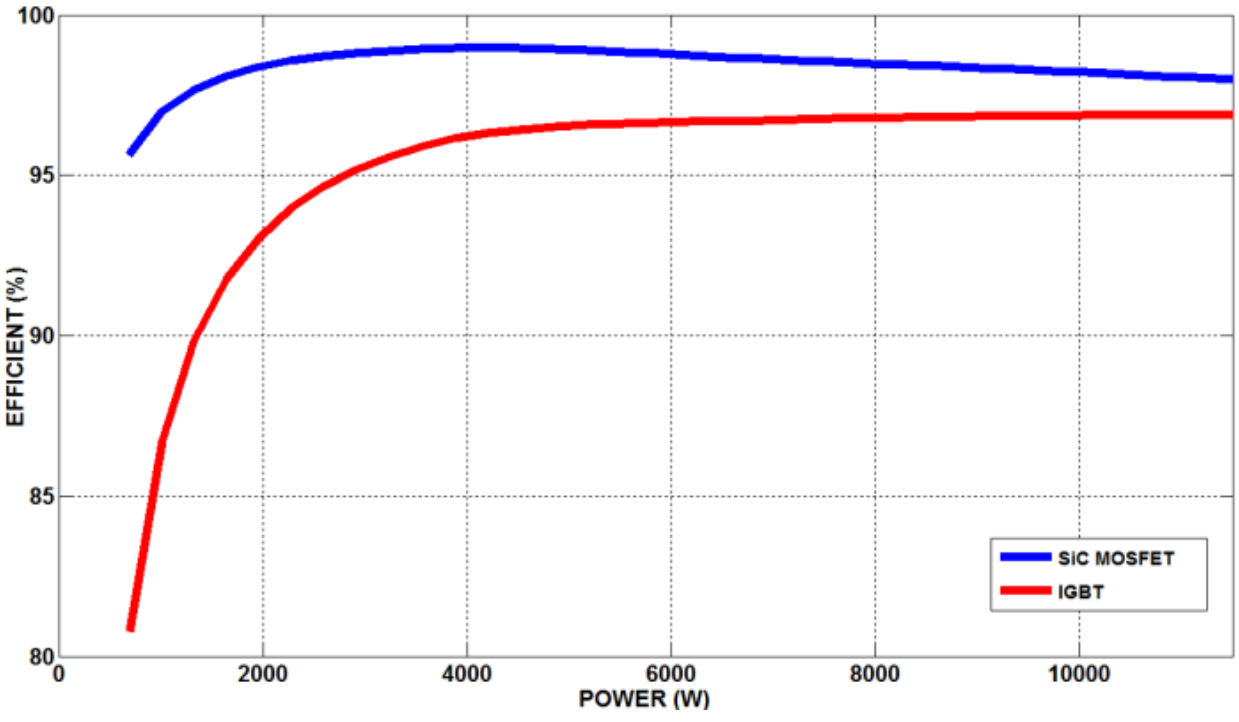

Fig. 2.3 Efficiency curves of IGBT and SiC MOSFET inverters: - Full scale

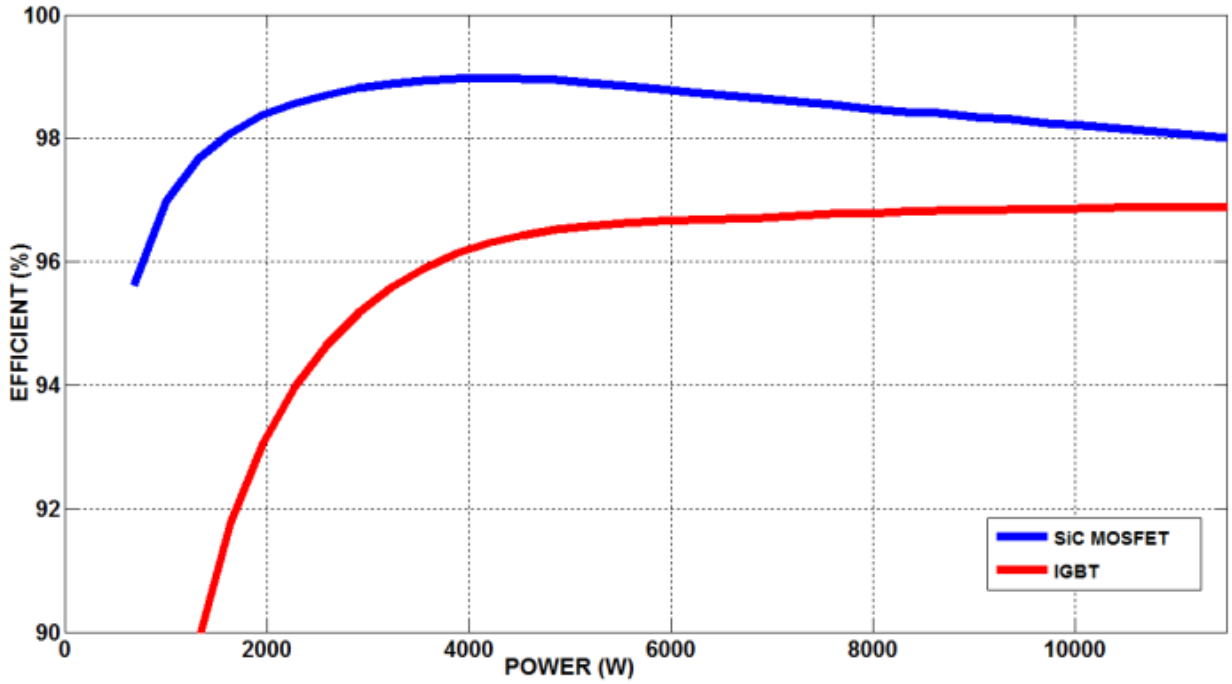

Fig. 2.4 Efficiency curves of IGBT and SiC MOSFET inverters: - Zoomed between %90-%100

2.2.3 Advantage of SiC based device

SiC is a compound semiconductor which is comprised of Silicon (Si) and Carbon (C). SiC is different than any other Si material in terms of breakdown field strength, bandgap, thermal conductivity etc.

Dielectric breakdown field strength is approximately ten times higher than that of Si. SiC can reduce the resistance per unit area of the drift layer up to 1/300 compare to Si at the same breakdown voltage.

IGBT is one of the most popular silicon power high-voltage, high-current application devices. But with IGBTs, switching performance is required to achieve low resistance at high breakdown voltage. On the other hand, MOSFETs are majority carrier devices. As a result, they can take advantages of Sic's higher breakdown field and higher carrier concentration to achieve high voltage, low on-resistance and fast switching speed.

SiC devices also ensures thermal reliability of the packages. They can operate at 200 degree celcius or higher, if properly packaged. Due to the larger bandgap, SiC devices are capable of operating is such high temperature which normally ranges from 150-175 degree celcius.

Some graphical advantages of SiC over IGBT is shown below:

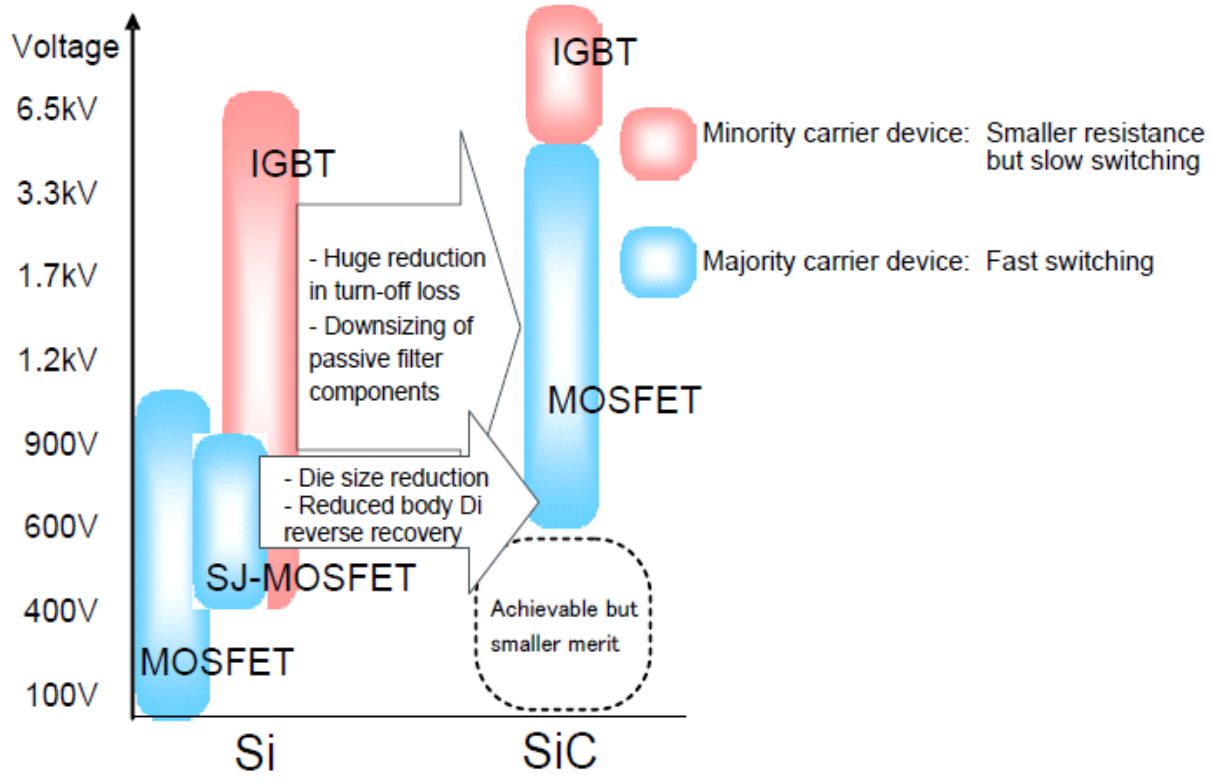

Figure 2.5

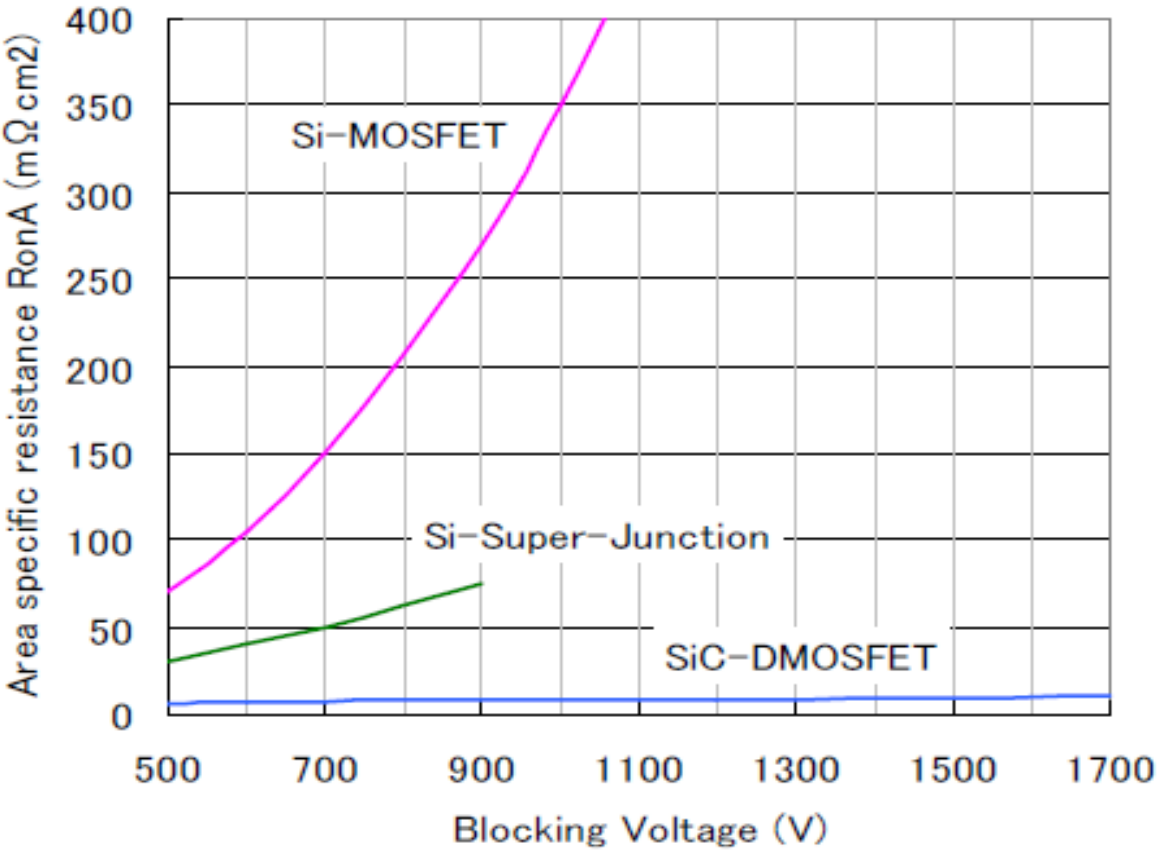

2.2.4 Application of SiC-based Power electronics in Traction

system in Train

As per Japanese journal referred at (2), they have already commercialized large-capacity hybrid SiC power modules with 1.7kV SiC Schottky barrier diodes (SBDs) and Si-insulated gate bipolar transistors (IGBTs).

The traction inverter system incorporating these modules was mounted on a Japanese subway and demonstrated 38.6% energy reduction compared with the conventional system. Also, efficiency improvement and miniaturization of power inverters and converters by embedding SiC power devices have been reported.

They have successfully developed a 3.3kV=1500A power module consisting of 16 SiC-MOSFETs and 16 SiC-SBDs with a rated voltage of 3.3kV connected in parallel.

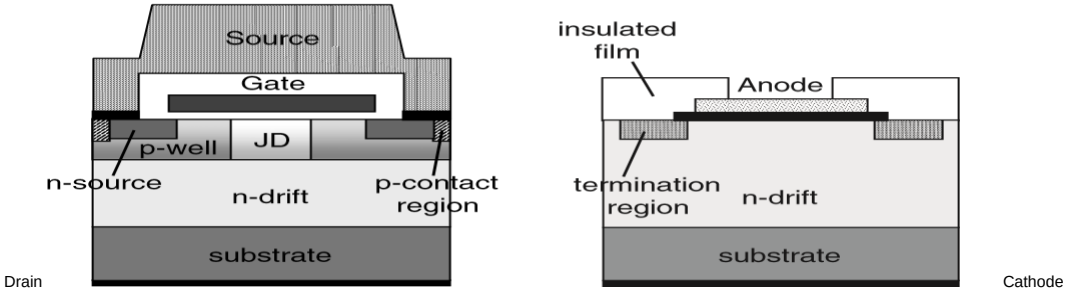

Fig. 2.7 Cross-sectional structures of (a) MOSFET and (b) SBD.

Switching Loss

Figures 2.8 and 2.9 show the measured turn-on and turn-off waveforms of the module at 175°C with gate resistances of 2.4 and 4.1Ω, respectively. The larger gate resistance was employed during turn-off so that the ringing voltage does not overshoot the breakdown voltage. The switching voltage= current and gate drive voltage were set to 1.8kV=1500A and ±15V, respectively. The turn-on and turn-off power losses of the module were calculated to be 1.44 and 0.53J, respectively. The loss of the SiC module is reduced by approximately 55% compared with those of the Si counterparts. These results surely demonstrate the superiority of SiC devices for high-power systems with a rated voltage of 3.3kV.

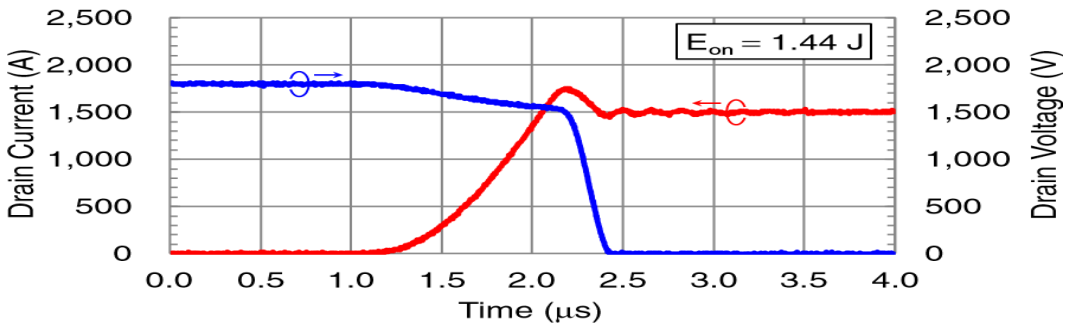

Fig. 2.8. Turn-on waveform of 3.3kV=1500A all-SiC power module (V_{DS} = 1.8kV, I_{DS} = 1500A, V_{GS} = ±15V, T_j = 175°C, and R_G = 2.4Ω).

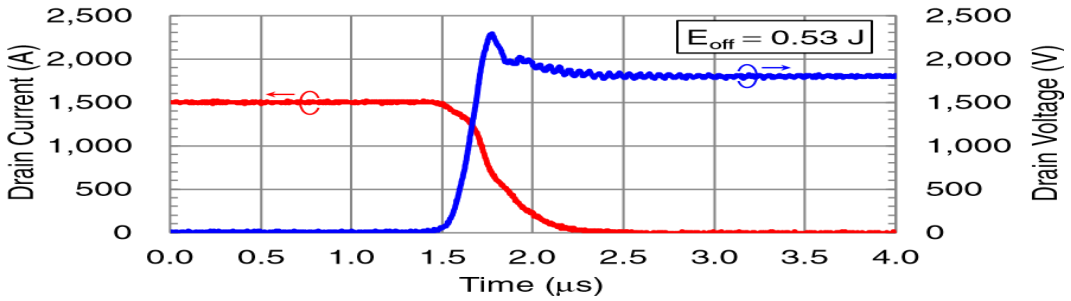

Fig. 2.9. Turn-off waveform of 3.3kV=1500A all-SiC power module (V_{DS} = 1.8kV, I_{DS} = 1500A, V_{GS} = ±15V, T_j = 175°C, and R_G = 4.1Ω).

Conduction Loss

The conduction loss of the SiC-MOSFET with JFET doping was reduced to a value as low as that of Si-IGBT. The JFET doping technique is effective in reducing the temperature coefficient of JFET resistance, leading to the decreased on-resistance of the SiC-MOSFET at high temperatures.

CHAPTER-3

3. Train Design and Energy Consumption

3.1 Analysis of Train Energy Consumption and Regeneration

Three years (2013, 2014 & 2015) energy data have been analyzed and observations are as follow (Calculation sheets are attached herewith)

1. Average consumption for 4 car train set in KWh/Km

Head	KWh/Km
Traction Consumption (A)	10.96
Auxiliary Consumption (B)	3.96
Total Consumption (A+B)	14.92
Regeneration (C)	5.70
Net Consumption (A+B-C)	9.22

2. Average regeneration figure is 38% of total consumption. Regeneration figure varies from 35% to 44% as it depends on Auxiliary figure. This figure excludes the losses beyond Converter/Inverter.

3. Average Auxiliary consumption is 26% of total consumption, which consumption depends mainly on Air conditioning use. It figures vary from 17-20% in winter (December/January) to 31-32% in summer (June/July).

4. Regeneration %age figure changes based on Auxiliary consumption:

Month	Auxiliary consumption	Regeneration
Winter (Dec/Jan)	17-20%	41-44%
Summer (June/July)	31-32%	34-36%

5. Traction Figure and Regeneration figure are almost uniform throughout the year (varies across the stocks and with combination of Car).

Energy Consumption per 2-Car for year 2015

Year/Month	Consumption			Regeneration	Net
	Traction	Auxilliary	Total		
2015	5.48	1.98 (26.54)	7.46	2.85 (38.20)	4.61
January	**5.50**	**1.38 (20.04)**	**6.88**	**2.9 (42.20)**	**3.97**
February	**5.50**	**1.49 (21.28)**	**6.98**	**2.9 (41.57)**	**4.08**
March	**5.44**	**1.64 (23.20)**	**7.08**	**2.87 (40.50)**	**4.21**
April	**5.46**	**2.01 (26.88)**	**7.47**	**2.87 (38.42)**	**4.60**
May	**5.50**	**2.32 (29.62)**	**7.82**	**2.83 (36.17)**	**4.99**
June	**5.55**	**2.51 (31.11)**	**8.06**	**2.87 (35.59)**	**5.18**
July	**5.52**	**2.55 (31.60)**	**8.07**	**2.84 (35.20)**	**5.22**
August	**5.53**	**2.51 (31.23)**	**8.04**	**2.84 (35.36)**	**5.19**
September	**5.50**	**2.37 (30.12)**	**7.88**	**2.82 (35.84)**	**5.04**
October	**5.49**	**1.99 (26.66)**	**7.48**	**2.88 (38.46)**	**4.60**
November	**5.26**	**1.56 (22.88)**	**6.82**	**2.69 (39.43)**	**4.13**
December	**5.53**	**1.4 (20.19)**	**6.93**	**2.9 (41.91)**	**4.02**

Energy Consumption per 2-Car for year 2014

Year/Month	Consumption			Regeneration	Net
	Traction	Auxilliary	Total		
2014	5.50	1.97 (26.37)	7.47	2.89 (38.66)	4.58
January	**5.59**	**1.16 (17.17)**	**6.74**	**2.98 (44.19)**	**3.76**
February	**5.58**	**1.23 (18.12)**	**6.81**	**2.98 (43.83)**	**3.83**
March	**5.50**	**1.50 (21.41)**	**7.00**	**2.89 (41.28)**	**4.11**
April	**5.44**	**1.77 (24.58)**	**7.21**	**2.81 (38.93)**	**4.41**
May	**5.48**	**2.16 (28.24)**	**7.64**	**2.82 (36.92)**	**4.82**
June	**5.52**	**2.66 (32.49)**	**8.17**	**2.80 (34.24)**	**5.37**
July	**5.53**	**2.60 (31.99)**	**8.14**	**2.82 (34.60)**	**5.32**
August	**5.52**	**2.56 (31.69)**	**8.08**	**2.82 (34.92)**	**5.26**
September	**5.54**	**2.38 (29.99)**	**7.92**	**2.84 (35.89)**	**5.08**
October	**5.44**	**1.94 (26.27)**	**7.38**	**2.83 (38.32)**	**4.55**
November	**5.51**	**1.39 (20.14)**	**6.90**	**2.89(41.92)**	**4.01**
December	**5.48**	**1.17 (17.53)**	**6.64**	**2.84(42.81)**	**3.80**

3.2 Main factors for Energy Consumption

Three major factors have major contribution to the improvement in energy efficiency of commuter trains. These are

(i) Light weight cars which can be achieved through lighter car body shells, lighter bogies and lighter electrical equipment.

(ii) Intensive use of regenerative braking – a boon of 3-phase technology and enhanced efficiency of traction equipment. This is achievable through improved system design, optimization of traction motor design and providing need based energy storage arrangement.

(iii) Improved aerodynamics reduce train resistance.

Energy cost accounts for 5% to 15% of operating cost in most of metros. 60% to 80% of this energy is used in Traction while auxiliary loads in station area i.e. lighting, air-conditioning, lifts, escalators etc. accounts for 20% to 40%. In DMRC energy cost is almost 30% of operating cost and auxiliary loads accounts for 50% of this due to adverse ratio of underground stations. Metros have taken several energy saving initiatives like regenerative braking, rationalization of trains during off peak hours, building energy management etc. It is found that saving due to regenerative braking amounts to an average of about 20% of traction energy and is the most important energy saving initiative and obviously almost all metros have implemented regenerative braking in various degrees depending on age & technology of stock in use. Quantum of energy regenerated varies from 5% in Hong Kong KCRC to 30% in Lisbon Metro and 34% in Delhi Metro.

3.3 Overall Description of DMRC Traction System

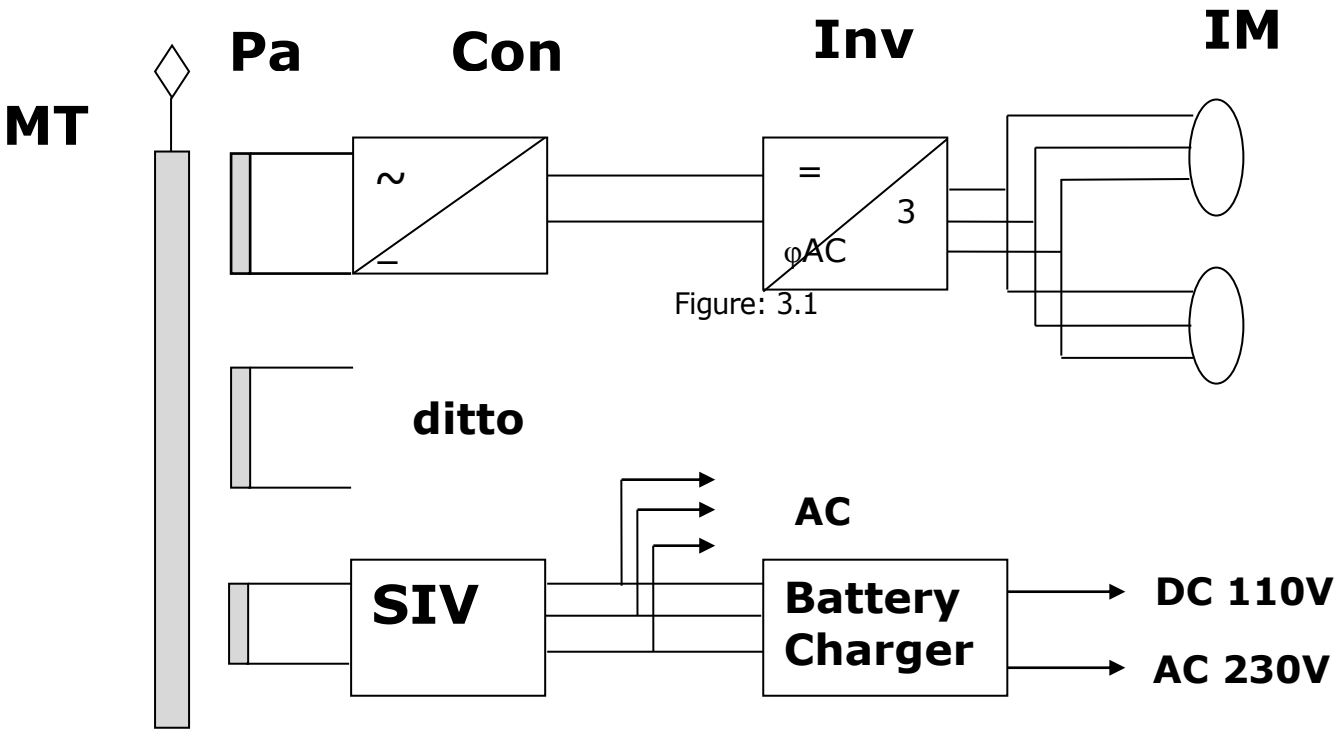

Figure: 3.1

The Converter and inverter are operated with Pulse Width Modulation (PWM) using Insulated Gate Bipolar Transistors. "Three-phase Drive" with Variable Voltage and Variable Frequency (VVVF) control is applied for the propulsion system.

The Converter unit consists of the IGBT modules, also called IPMs, with control and self- protection functions incorporated. The IGBT modules used consist of the High Power High Voltage IGBT, Gate drive circuit, and its own protection circuits against Over current, Short circuit, Over temp and Low Power supply detection. The Converter unit carries out PWM control, making it possible to attain Zero phase difference between the primary voltage and current of the Main transformer. In other words, a unity power factor can be achieved.

The Converter unit converts 1058V AC obtained in the Secondary windings of the Main transformer to a constant DC voltage of 1900V. During regenerative brake operation, the Converter unit is also capable of inversely converting 1900V DC to 1058V AC, providing efficient powering and regenerative operations without switching the main circuit.

The Inverter unit converts the output of Converter ie.DC power supply at 1900V DC into AC power supply at a desired output voltage and frequency. The Inverter unit controls the voltage applied to the Traction Motors to obtain the desired level of tractive effort and the frequency to change the Traction motor speed. This VVVF control is achieved by sequencing the on/off timings and adjusting the voltage to the IGBT`s through a microcomputer in the Inverter control circuit.

Optical fibre cables are used to connect the Gate control unit to the Gate interface of Converter / Inverter units. The Optical fibre cable transmits the Gate signal to the drive the IGBT via gate interface. The Optical fibre cables provide electrical isolation between the IGBT and the Gate control unit and are thus impervious to electrical interference.

Function of Converter /Inverter

The function of Traction Converter / Inverter set (C/I) is to control Train acceleration and deceleration according to driving commands from the Driver’s Cab through Master controller and Mode selector by suitably converting the power drawn from the Main Transformer to operate the Traction motors. One Converter / Inverter Box houses two Converter / Inverter sets. Each C/ I feeds power to two Traction Motors. Each Converter / Inverter set is controlled independently by one Gate control unit ie Computer based control system that effectively and efficiently controls the Operation of C/I.

The Function of C/I can best be understood by understanding the functions of Main Power circuit , Control Circuit and Input /Output signals pertaining to C/I.

Table1: Technical details of Traction Controller

No	Item	Description
1	Circuit form	Converter：2-level Inverter：2-level
	Main switching device	IPM (Intelligent Power Module) 3300V 1200A IGBT, FWD and gate circuit with self–protection function are installed .
3	Range of input voltage of converter	Input voltage (Catenary voltage)
	Nominal input voltage Operation guaranteed Output performance guaranteed	AC 1058V (25kV) 1Φ AC741V ~ AC1270V (17.5kV~30kV) AC952V ~ AC1164V (22.5kV~27.5kV) (AC741V~AC952V: power limited mode)
4	Input frequency of converter	48Hz～52Hz
5	DC link voltage	1900Vdc max
6	Ripple voltage at DC stage Method of reduction for affection by 100Hz ripple	±100V ±5% Beatless control
7	Initial charging circuit	Charging from tertiary winding
8	Maximum output voltage of inverter	1450V 3Φ
9	Maximum output current of inverter	Powering(max) : Approx. 163A ×2 3Φ Braking(max) : Approx. 135A×2 3Φ For High acceleration mode 191Amax
10	Maximum output frequency	Powering :Approx. 137Hz
11	Rated output current of inverter	Approx.AC 113Arms×2 3Φ
12	Modulation frequency	Converter : 450Hz Inverter : 800Hz max
13	Efficiency of converter/inverter	Above 0.97
14	Power factor	Above 0.99

15	Continuous rating power of converter	423kVA (= 404A×952V×1.1)
16	Maximum rating power of converter	Approx. 566kVA 6 sec
17	Control system	Block diagram of the control circuit Converter:
18	Components	No.1 power unit, No.2 power unit
19	Ambient temperature	3 degree Celsius to 47 degree Celsius
20	Voltage of control circuit	110V dc +25%, -30% (77V to 137.5V)
21	Cooling method	Natural air ventilation
22	IGBT junction temperature	Margin for maximum rating is above 10℃

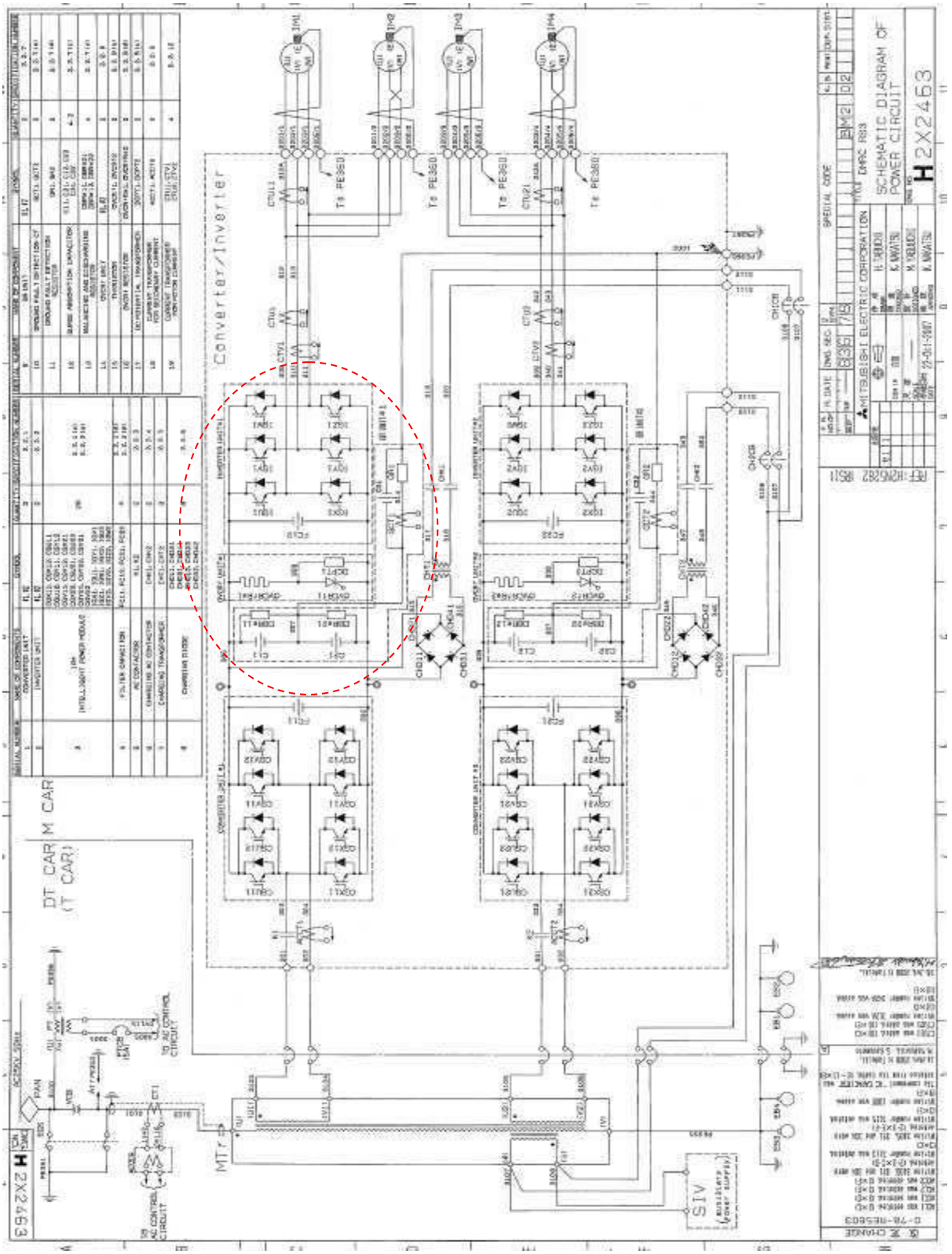
Converter/Inverter
DT CAR M CAR
(T CAR)
MITSUBISHI ELECTRIC CORPORATION
SCHEMATIC DIAGRAM OF
POWER CIRCUIT
H2X2463

Figure 3.2

3.4 Regenerative Braking

The rotor always tries to match the rotational speed of the stator magnetic field. If two speeds are matched than there is no interaction between the stator and the rotor, and hence no torque develops. The performance of Induction motor is maximum when the difference between the rotational speed of the rotor and the rotating magnetic field of the stator or the slip is less than 10 percent. For large induction motors, the ideal slip may be around 1 %.

When the slip is positive, i.e. rotor rotational speed is less than the speed of magnetic field of stator, the motor drives the mechanical load that is motor is powering and a characteristic curve shown in Figure 3.3

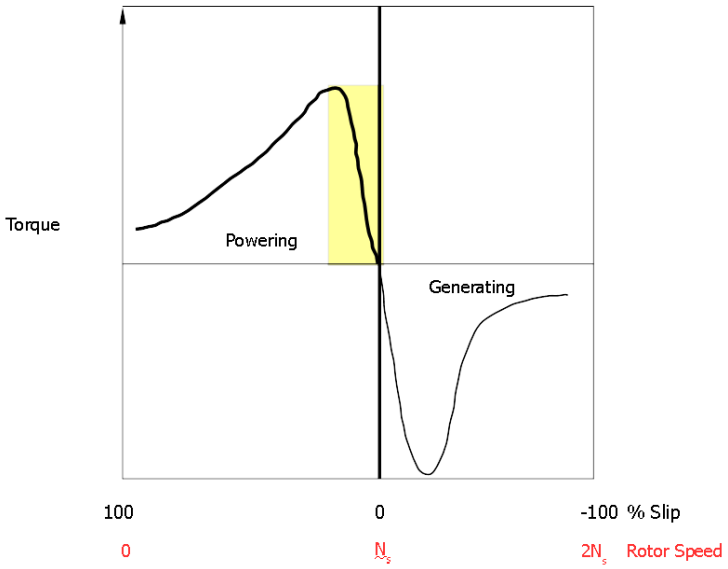

Figure 3.3: Torque – Speed Curve in Powering

For power frequency of 50 Hertz, the stator of a three-phase 4 pole induction motor will have a magnetic field rotating at synchronous speed $N_s = (120x50) / 4$ rpm = 1500 RPM. 4 percent slip = 1500 RPM x .04 = 60 RPM. The rotor rotational speed at 4% slip will be (1500 – 60) RPM = 1440 RPM. The rotor will continuously try to increase the speed and match it's rotational speed with the synchronous speed of the stator magnetic field, thereby producing the positive motoring torque.

When slip is negative, that is, the rotor is rotating faster than the stator magnetic field, the motor is generating power back into the system. A characteristic generating curve is shown in Figure 3.4.

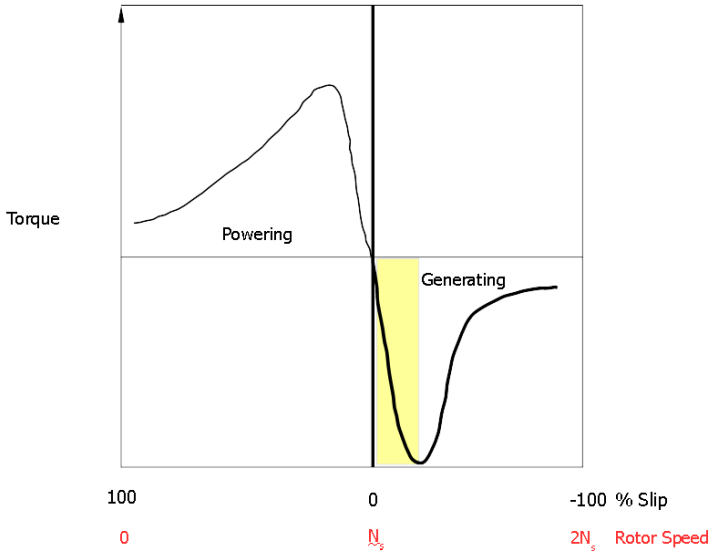

Figure 3.4: Torque Speed Curve in Generating

In this case the rotor is trying to reduce it's rotational speed to match the rotational speed of the stator magnetic field. For a 50 Hertz power frequency, the stator of a three-phase 4 pole induction motor will have a magnetic field rotating at synchronous speed N_s = (120x50) / 4 rpm = 1500 RPM. A negative 4 percent slip = 1500 RPM x -.04 = -60 RPM. The rotor rotational speed at -4% slip will be (1500 – -60) RPM = 1560 RPM. The rotor will continuously try to slow down to match it's rotational speed with the synchronous speed of the stator magnetic field, producing the negative (braking) torque.

Figure 3.5 shows a curve for an induction motor in which the control unit is reducing the synchronous speed N_s so that the rotor speed is always greater than synchronous speed N_s. In this manner the braking force is continuously applied down to a train speed less than 8 km/hr.

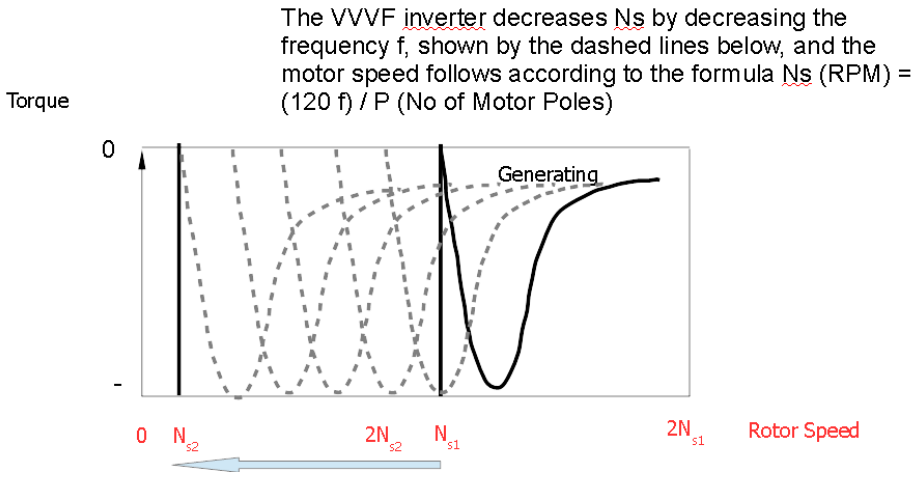

Figure 3.5: Reduction of Synchronous Speed (N_s) by the VVVF Inverter

In braking, the induction traction motor consumes reactive power that magnetizes the stator and rotor windings and generates real power back to the system. The process of generating power places a drag on the rotor that slows the rotor down and produces the braking force. In theory, 100 per cent of the energy regenerated by the induction motor is recoverable. In practice, the amount of energy that can be used

through regenerative braking is totally dependent upon the load. With regenerative power, the load is known as the receptivity of the line.

3.5 Speed Control of Traction Motor

The two factors on which the speed of Induction motor depends are number of poles and frequency of applied power supply which is governed by the following relation Induction motor depends only on number of poles and frequency of applied power supply from the formula

$$\omega_s=120f/p$$

Supply voltage also affects the speed of induction motor since generated torque depends upon supply voltage. Reduction in supplied voltage results in reduction of generated torque which in turn results in reduction of speed. There is no universal application of these speed control measures for any meaningful gain. Many different methods of speed control are employed based on requirement, for example use of pole change from four to six pole for double speed vacuum exhauster used on many types locomotive for instant creation of vacuum after application of brakes.

With technological advancement many advance power devices are fabricated such as thyrister, GTO and IGBT, through which frequency control became possible.

Speed-torque characteristics of Induction motor derives the Tractive effort vs speed characteristics of three phase Induction Motor.

3.5.1 Constant Torque Zone

Now $I_r \propto f_{sl}\Phi_{ag}$ and $T_{em} \propto \Phi_{ag} I_r$ we get $T_{em} \propto (\Phi_{ag})^2 f_{sl}$; from this equation it may be derived that with f_{sl} kept constant and if we keep the air gap flux at the maximum permissible limit and constant, motor will deliver maximum torque which will be at constant level. Torque speed curve at different frequencies is shown below. Here T_{max} is the maximum torque motor can deliver for a short duration without increasing the temperature beyond permissible limits.

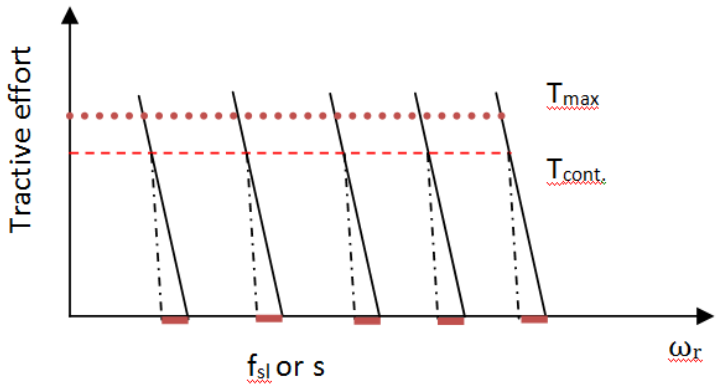

Constant Air gap Flux and Constant f_{sl} = sf results constant torque up to rated frequency

3.5.2 Constant Power Zone

When voltage is increased in proportion to frequency, Φ_{ag} can be maintained constant. This is possible up to rated voltage thereafter; air gap flux reduces as shown below

$\Phi_{ag}=E_{ag}/f$; $T_{em} \propto (\Phi_{ag})^2 f_{sl}$ or $T_{em} \propto (E_{ag}/f)^2 f_{sl}$ or $\propto E_{ag}^2 f_{sl}/f^2$ or $\propto f_{sl}/f^2$ or $\propto sf/f^2$ or $\propto s/f$

From above it can be concluded that torque varies inversely proportion to frequency by keeping slip constant.

3.5.3 Reduced Power Zone

Torque reduces with reduction of slip and therefore slip can only be reduced to the limit of minimum torque which is essentially required by load. Thereafter slip reduces in proportion to frequency, keeping sf constant and in this situation T_{em} is in inverse proportional to square of frequency.

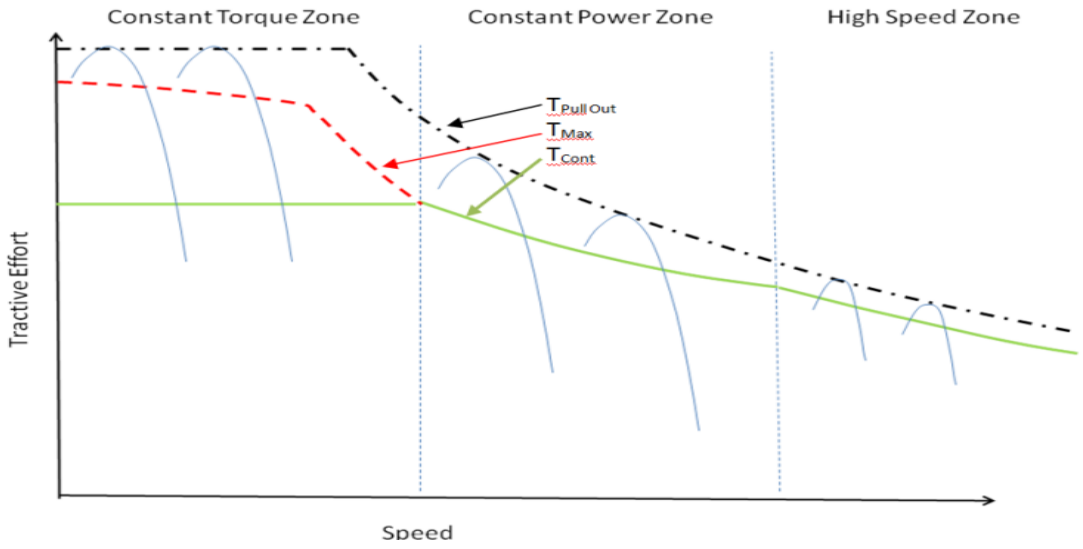

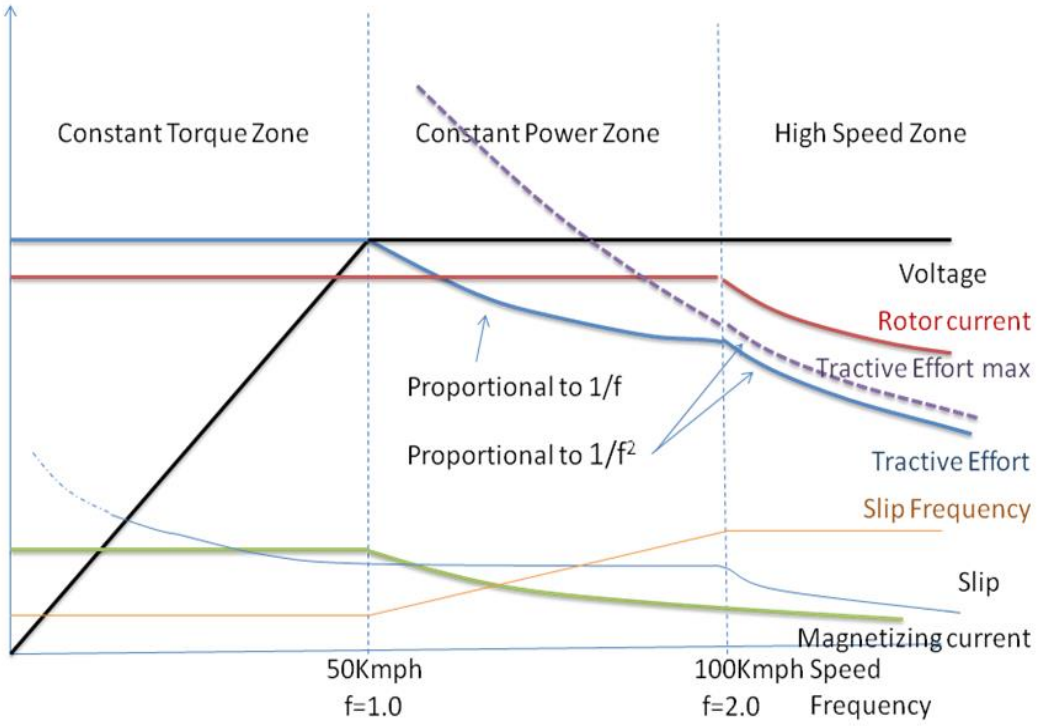
Constant Torque Zone
Constant Power Zone
High Speed Zone
Voltage
Rotor current
Tractive Effort max
Proportional to 1/f
Proportional to 1/f2
Tractive Effort
Slip Frequency
Slip
Magnetizing current
50Kmph
f=1.0
100Kmph Speed
f=2.0
Frequency

CHAPTER-4

4 Selection of Power Electronic Device

4.1 Limitation of Silicon based Devices

The electronics in a vehicle are subjected to adverse environmental conditions and they are supposed to operate under these conditions without appreciable deterioration in performance. The most detrimental environmental factor in this regard is high temperature.Since heat is generated by multiple sources such as, the motor, engine, the semiconductor device losses, and the environment itself is source of heat, the electronics have to be cooled so that they will continue to perform without derating. The maximum permissible junction temperature for most Si based devices is 150°C; therefore, the temperature of the Si chips and power devices should remain under this value. Even then, the variation in the electrical characteristics of Si devices with temperature and time remains a substantial reliability issue.

There are three standard options for cooling power devices i.e. natural air, forced air, or water-cooled heat sinks. However, as the temperature of the environment increases, the capacity of the cooling system decreases. The type of heat sink to use depends upon the power rating of the converter. High-power converters require the more expensive, but smaller liquid-cooled heat sinks, whereas for low-power converters, bulky, natural-air heat sinks are sufficient,. However, the former require a radiator and a fan to cool the coolant as well as a pump to circulate it. Typically, one-third of the total volume of a power converter is occupied by heat sink and it usually weighs more than the converter itself. One way of decreasing the cooling requirements, size, and cost of the converter is by building electronics that can withstand higher temperatures is, but Si devices have reached their theoretical temperature limits.

Heat generated by the semiconductors themselves is a major source of heat affecting vehicular electronics. Losses associated with conducting and switching high currents are the source of heat in these power devices. The amount of loss depends on the type of power devices used. In applications like the traction drive, which comes under high-power transportation, insulated gate bipolar transistors(IGBT) and PiN diodes are presently used. Both these devices are bipolar devices and have higher losses compared to their unipolar counterparts, such as metal oxide semiconductor field effect transistors (MOSFET) and Schottky diodes. Although, these unipolar devices have superior properties compared to bipolar devices, they do not comes at high power ratings hence they are not used in traction drives.For unipolar devices as above, as the breakdown voltage increases, the device requires a large silicon die area, and this results in reduced manufacturing yields and increased costs.Hence Building higher-voltage-rating MOSFETs and Schottky diodes would not be feasible For higher breakdown voltages, a material with a higher electric breakdown field is required.

The switching frequency of the devices is also a limiting factor because of the heat generated by the devices, primarily the switching losses. Higher-frequency operation is preferred because of smaller filter requirements, generation of less audible noises, and smaller passive component requirements. The

outputs of high-frequency power converters are smoother, and a small filter is sufficient to filter the harmonics. Additionally, with high frequency, the size of the passive components decreases, this results in an overall gain in size and weight. Additionally, with higher frequency, the noise generated by converter operation is in an inaudible frequency range, which would be comfortable for the user.

4.2 Why SiC based Devices?

As we have seen above, the effectiveness of Si can't be increased to meet the requirements of modern transportation industry because it has reached its theoretical limits. On the other hand, it is already established that even the specifications of first SiC-based power devices are above Si's theoretical limits. SiC power devices, have far superior characteristics and hence they offer great performance improvements and can work in adverse environmental conditions where Si power devices cannot function. Some of the advantages of SiC based devices over Si based power devices are as follows:

- SiC -based unipolar devices have lower on-resistances because they are thinner which translate into lower conduction losses; hence, higher overall converter efficiency is achieved.
- SiC-based power devices because of their higher electric breakdown field, have higher breakdown voltages; thus, while Si Schottky diodes are commercially available typically at voltages lower than 300 V, the first commercial SiC Schottky diodes are already rated at 600 V.
- SiC-based devices have a higher thermal conductivity (4.9 W/cm-K for SiC as opposed to 1.5 W/cm-K for Si). Hence, SiC-based power devices have a lower junction-to case thermal resistance, $R_{th\text{-}jc}$ as compared to Si devices . This means easy transfer of heat out of the device, resulting in slower rate of temperature increase.
- The operating temperature of SiC-based power devices is higher than Si based devices. The literature notes operation of SiC devices up to 600°C. Si devices, on the other hand, can operate at a maximum junction temperature of only 150°C.
- The variation of Forward and reverse characteristics of SiC-based power devices with temperature and time is also less; therefore, they are more reliable.
- SiC-based bipolar devices have excellent reverse recovery characteristics which reduces the switching losses and electromagnetic interference (EMI), and hence there is less or no need for snubbers. As a result, the requirement of soft-switching techniques to reduce switching losses does not arise.
- SiC-based devices can operate at higher frequencies (>20 kHz) because of low switching losses, which is not possible with Si-based devices in power levels of more than a few tens of kilowatts.

In spite of having many advantages over Si based devices, SiC based semiconductor power devices do not find widespread use because of some disadvantages. Some of these disadvantages are

- low processing yield because of defects for SiC and processing problems for GaN and diamond; hence, high cost;
- limited availability, with only SiC Schottky diodes that too at relatively low power are commercially available; and
- fabrication of SiC devices needs high-temperature packaging techniques that have not yet been developed fully.

These drawbacks are to be expected, given that SiC-based semiconductor technology has not yet matured.

4.3 Reason for selection of SiC based Devices

SiC based semiconductor materials have superior electrical characteristics compared with Si. Some of these characteristics for the most popular WBG semiconductors and Si are shown in Table 4.1.

Table 4.1. Physical characteristics of Si and the major WBG semiconductors

Property	Si	GaAs	6H-SiC	4H-SiC	GaN	Diamond
Bandgap, E_g (eV)	1.12	1.43	3.03	3.26	3.45	5.45
Dielectric constant, ε_r	11.9	13.1	9.66	10.1	9	5.5
Electric breakdown field, E_c (kV/cm)	300	400	2,500	2,200	2,000	10,000
Electron mobility, μ_n ($cm^2/V \cdot s$)	1,500	8,500	500 80	1,000	1,250	2,200
Hole mobility, μ_p ($cm^2/V \cdot s$)	600	400	101	115	850	850
Thermal conductivity, λ (W/cm·K)	1.5	0.46	4.9	4.9	1.3	22
Saturated electron drift velocity, v_{sat} ($\times 10^7$ cm/s)	1	1	2	2	2.2	2.7

Two SiC polytypes that are popular in SiC research presently,viz : 6H-SiC and 4H-SiC. Before the introduction of 4H-SiC wafers in 1994, 6H-SiC was the dominant polytype. Since then, both of these polytypes have been used in research, but recently 4H-SiC has become the more dominant polytype. Although both of these polytypes have similar properties, 4H-SiC is preferred over 6H-SiC because the mobilities in 4HSiC are identical along the two planes of the semiconductor, whereas 6H-SiC exhibits anisotropy, which means the mobilities of the material in the two planes are not the same.
The most important properties of the SiC-based semiconductors are explained in the following sections.

a) High Saturated Drift Velocity

The high-frequency switching capability of a semiconductor material is directly proportional to its drift velocity. The drift velocities of SiC materials are more than twice the drift velocity of Si (1×10^7); therefore, it is expected that SiC-based power devices could be switched at higher frequencies than their Si counterparts. Moreover, higher drift velocity allows charge in the depletion region of a diode to be removed faster; therefore, the reverse recovery current of SiC-based diodes is smaller, and the reverse recovery time is shorter.

b) Wide Bandgap

In a solid, electrons exist at energy levels that combine to form energy bands. A simplified energy band diagram is shown in Fig. 8. The top band is called the conduction band, and the next lower one is called the valence band. The region between the valence band and the conduction band is called the forbidden band, where, ideally, no electrons exist. (There are other bands below the valence band, but these are not important for this study.)

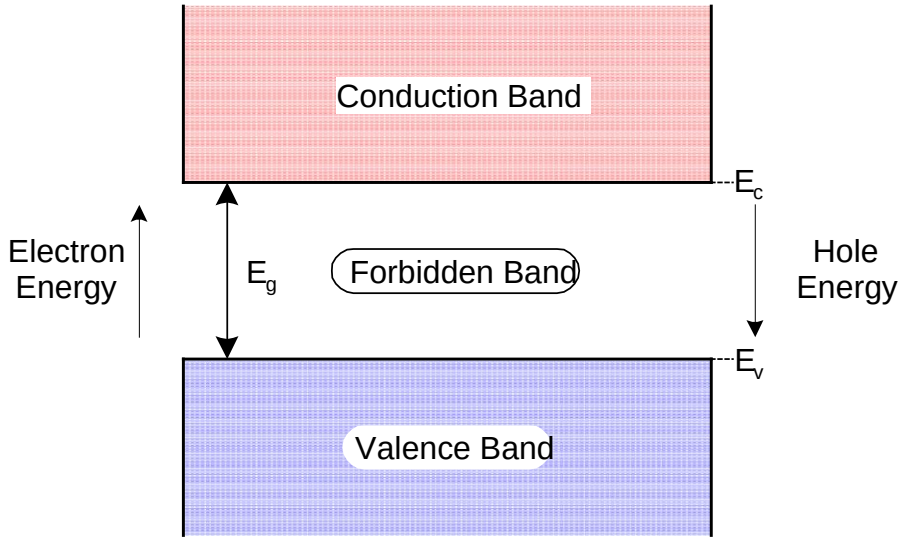

Fig. 4.1 Simplified energy band diagram of a semiconductor.

If the electrons in the valence band are excited externally, they can move to the conduction band. In the valence band, they have energy of E_v. In order to move to the conduction band, they need an $E_g = E_c - E_v$ amount of energy, where E_g is the bandgap.

For a conductor like copper, the forbidden band does not exist, and the energy bands overlap. For an insulator, on the other hand, this band is so wide that the electrons need a lot of energy to move from the valence band to the conduction band. For semiconductors, the gap of the forbidden band is smaller than for an insulator.

Some semiconductors are classified as “wide-bandgap” semiconductors because of their wider bandgap. Silicon has a bandgap of 1.12 eV and is not considered a wide-bandgap semiconductor. The bandgaps of SiC-based semiconductors are about three times or more that of Si as can be seen in Table 4.1. Among these semiconductors, diamond has the widest bandgap; consequently, it also has the highest electric breakdown field.

SiC-based semiconductors have the advantage of high-temperature operation and more radiation hardening. As the temperature increases, the thermal energy of the electrons in the valence band increases. At a certain temperature, they have sufficient energy to move to the conduction band. This is an uncontrolled conduction that must be avoided. The temperature at which this happens is around 150°C for Si. For SiC-based semiconductors, the bandgap energy is higher; therefore, electrons in the valence band need more thermal energy to move to the conduction band. This intrinsic temperature for SiC is around 900°C, and this value is much higher for diamond.

The wider the bandgap is, the higher the temperatures at which power devices can operate; therefore, diamond power devices have the capability to operate at higher ambient temperatures than power devices based on other WBG materials.

The above reasoning is also true for radiation hardening. Radiation energy can also excite an electron like the thermal energy and make it move to the conduction band.

As a result of the wide bandgap, devices built with SiC-based semiconductors can withstand more heat and radiation without losing their electrical characteristics. They can be used in extreme conditions where Si-based devices cannot be used.

c) High Thermal Stability

As explained earlier, because of the wide bandgap, SiC-based devices can operate at high temperatures. In addition to this, SiC has another thermal advantage not mentioned previously — its high thermal conductivity. As seen in below Equation, junction-to-case thermal resistance, $R_{th\text{-}jc}$, is inversely proportional to the thermal conductivity.

$R_{th\text{-}jc} = \mathrm{d}/\ \Upsilon \mathrm{A}$

where Υ is the thermal conductivity, d is the length, and A is the cross-sectional area. Higher thermal conductivity means lower $R_{th\text{-}jc}$, which means that heat generated in a SiC-based device can more easily be transmitted to the case, heatsink, and then to the ambient; thus, the material conducts heat to its surroundings easily, and the device temperature increases more slowly. For higher-temperature operation, this is a critical property of the material.

d) High Electric Breakdown field

Wider band gap results in a larger electric breakdown field (E_c). A higher electric breakdown field results in power devices with higher breakdown voltages. Much higher doping levels can be achieved with a high electric breakdown field; thus, for the same breakdown voltage levels device layers can be made thinner. The resulting SiC-based power devices are thinner than their Si-based counterparts and have

smaller drift region resistances.

The width of the drift region was calculated for all the semiconductors in Table 4.1, and the results are plotted in Fig. 4.2. for a breakdown voltage range of 100 to 10,000 V.

Compared to these, Si requires a drift region approximately 10 times thicker.

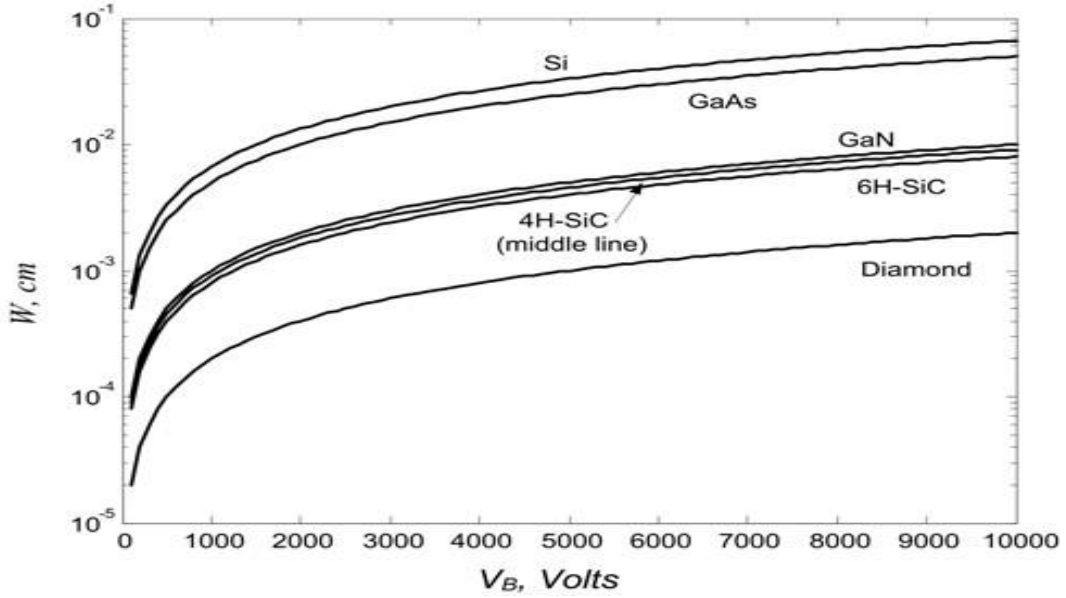

Fig. 4.2 Width of the drift region for each material at different breakdown voltages.

The on-resistance of the drift region for the Si device is approximately 10 times more than for the SiC polytypes and GaN devices. As the breakdown voltage increases, more doping can be applied to WBG semiconductors than to Si, so the specific on-resistance ratio between Si and WBG semiconductors increases further.

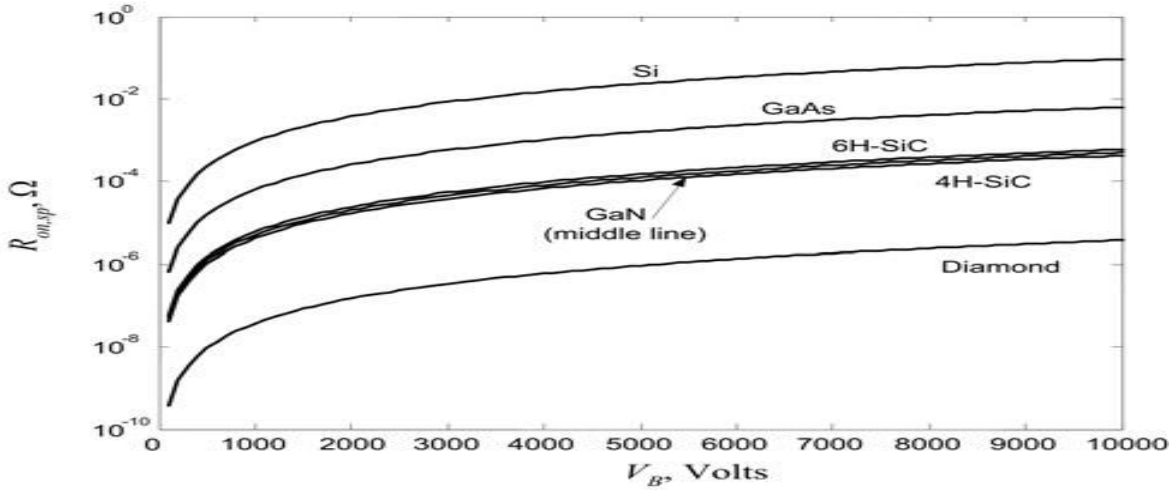

Fig. 4.3 Resistance of the drift region for each material at different breakdown voltages.

The storage of the minority carriers (Q_{rr} in diodes) is also reduced because of the thinner layers. Therefore, reverse recovery losses of WBG semiconductor-based diodes decrease, and this decrease allows higher-frequency operation.

CHAPTER-5

5 MATLAB Simulation Model & Performance Evaluation

The performance of the Traction Inverter is evaluated using the MATLAB Simulink for Si based IGBT devices and SiC based MOSFET devices feeding Static load. Performance of VVVF drive is also evaluated for Si based IGBT devices and SiC based MOSFET devices. The results are discussed for application of SiC based devices in Traction Inverter.

5.1 Performance Evaluation of Si based IGBT devices and SiC based MOSFET devices feeding Static (RL) load:-

It is assumed that Converter (from AC to DC) is supplying constant DC voltage thus directly DC Voltage source is taken for model building. Universal bridge is used in Inverter mode. LC filter, Current measuring device, Voltage measuring device, power measuring device and RL (static) load are modeled in MATLAB using Power System Block set.

Si based IGBT Inverter:

The parameters are as below:

DC Voltage = 1900 V

Inverter: Snubber resistance = 10000 Ohm

Snubber capacitance = 1 X 10^{-6} F

Ron (Ohm) = 0.05 Ohm

Ton time = 1.0 X 10^{-6} sec

Toff time = 2.0 X 10^{-6} sec

PWM Generator: Carrier frequency = 800 Hz

Modulation Index = 0.8

LC filter: L = 3 x 10^{-3} H

C = 100 X 10^{-6} F

RL Load: = Equivalent to (200 KW x2) = 400 KW

Fig. 5.1 depicts the setup used to study the performance of the Traction Inverter for Si based IGBT devices feeding Static load

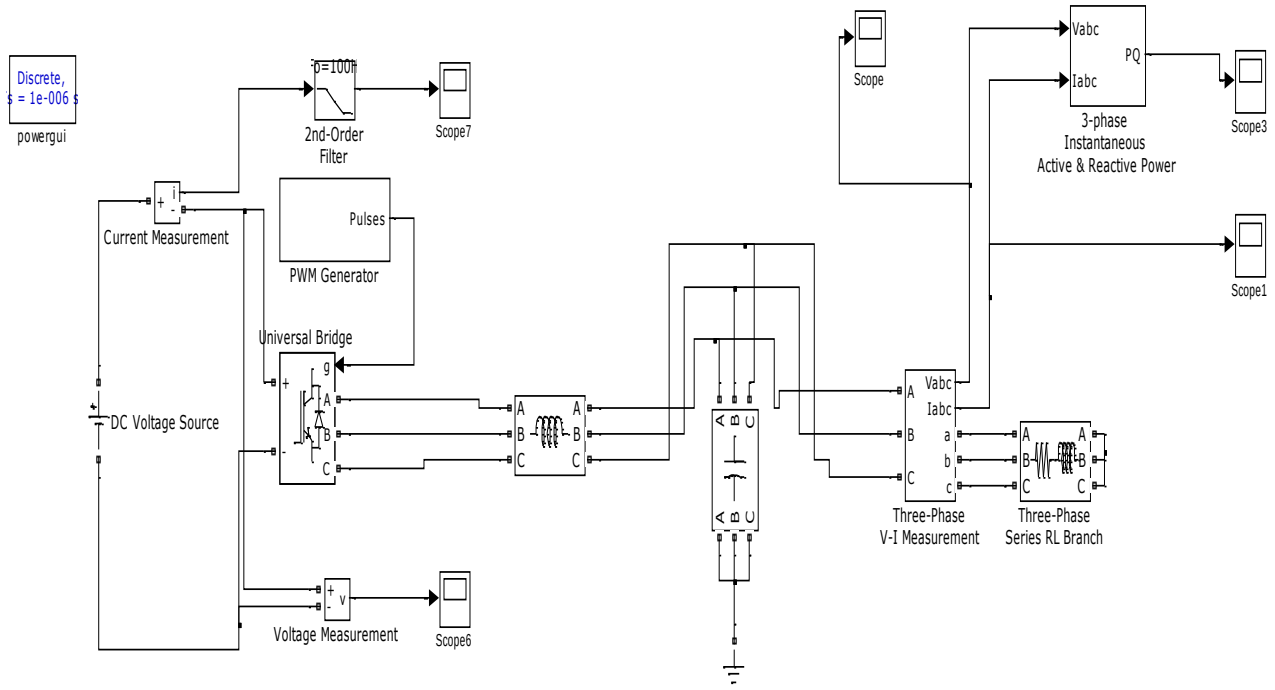

Figure 5.1 Simulink model for Static load (Si based IGBT)

The Output Voltage, Currant waveform and Output Power have been analyzed based on input Voltage and Input Current.

Input Side Waveforms:-

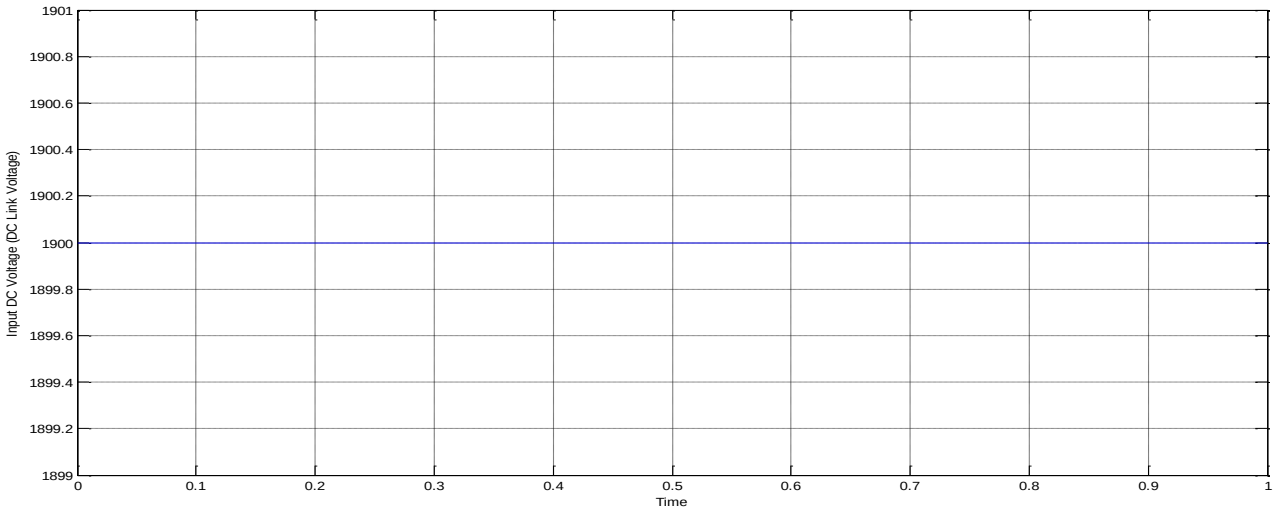

Figure 5.2 Input Voltage Waveform

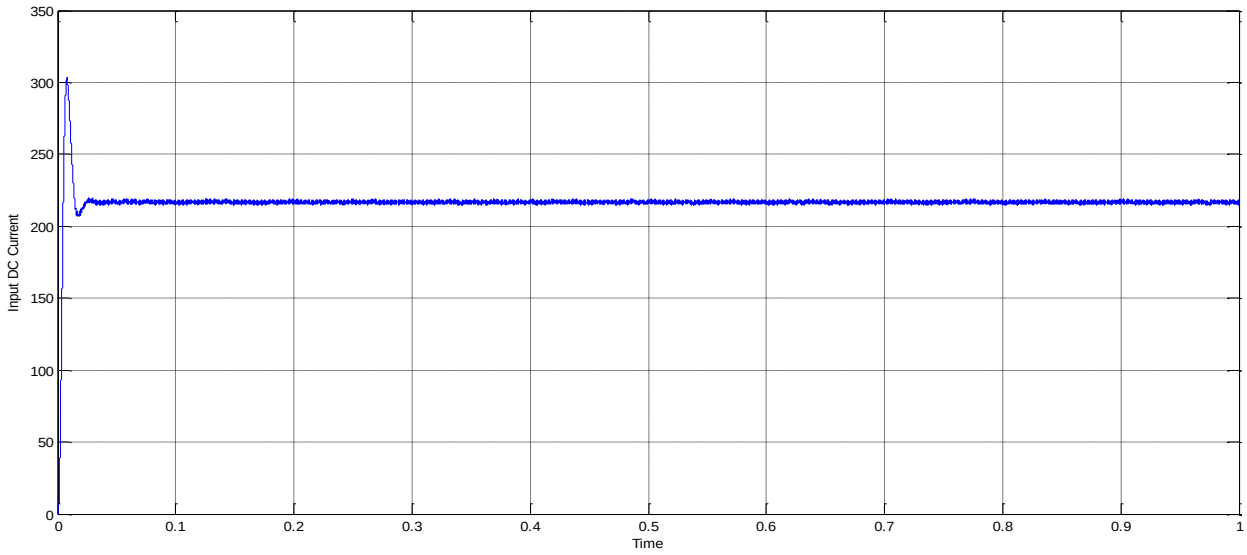

Figure 5.3 Input Current Waveform

Input Voltage is fixed DC Link Voltage = 1900 V, can be seen in waveform.

Input Current depends on load and corresponding input current = **217 Amps**.

Input Power = 1900 X 217 = 412300 Watts = **412.3 KW**

Output Side Waveforms:-

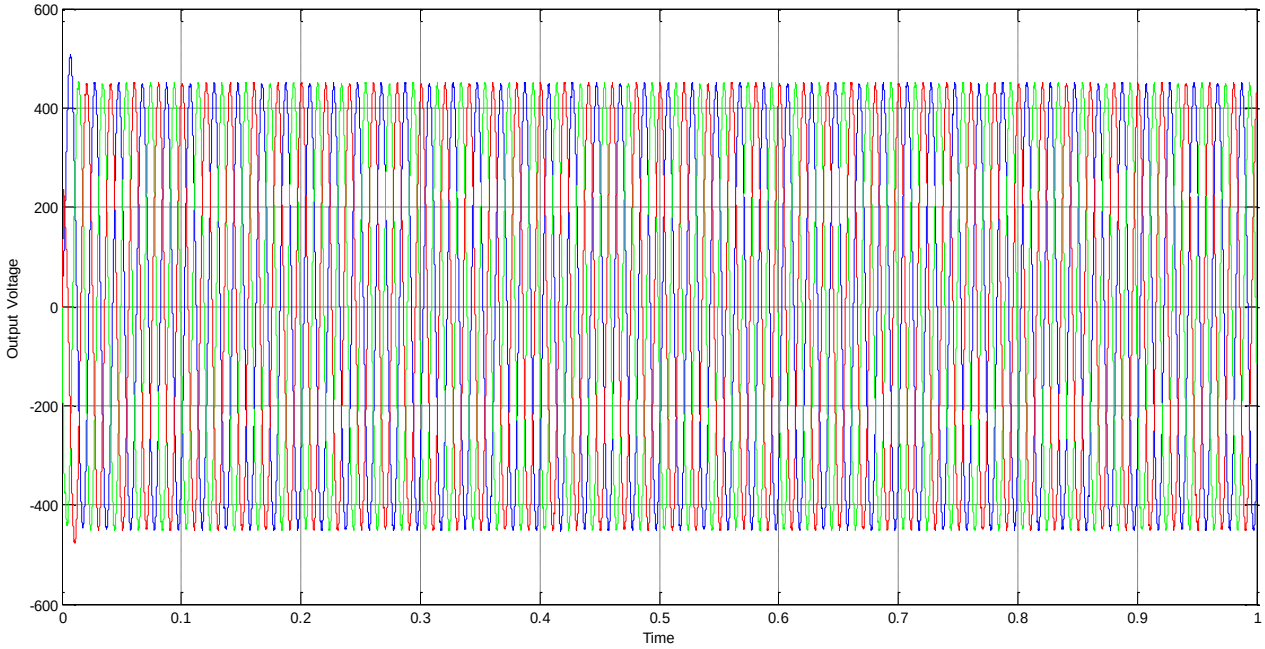

Figure 5.4 Output Voltage Waveform

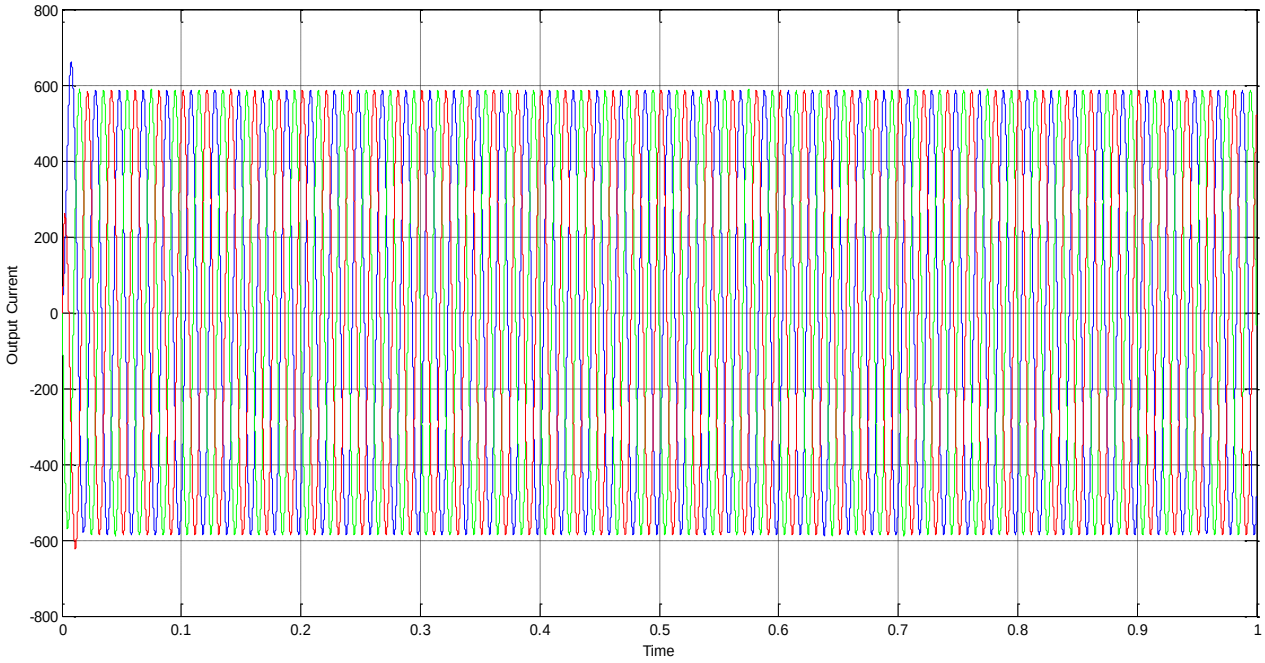

Figure 5.5 Output Current Waveform

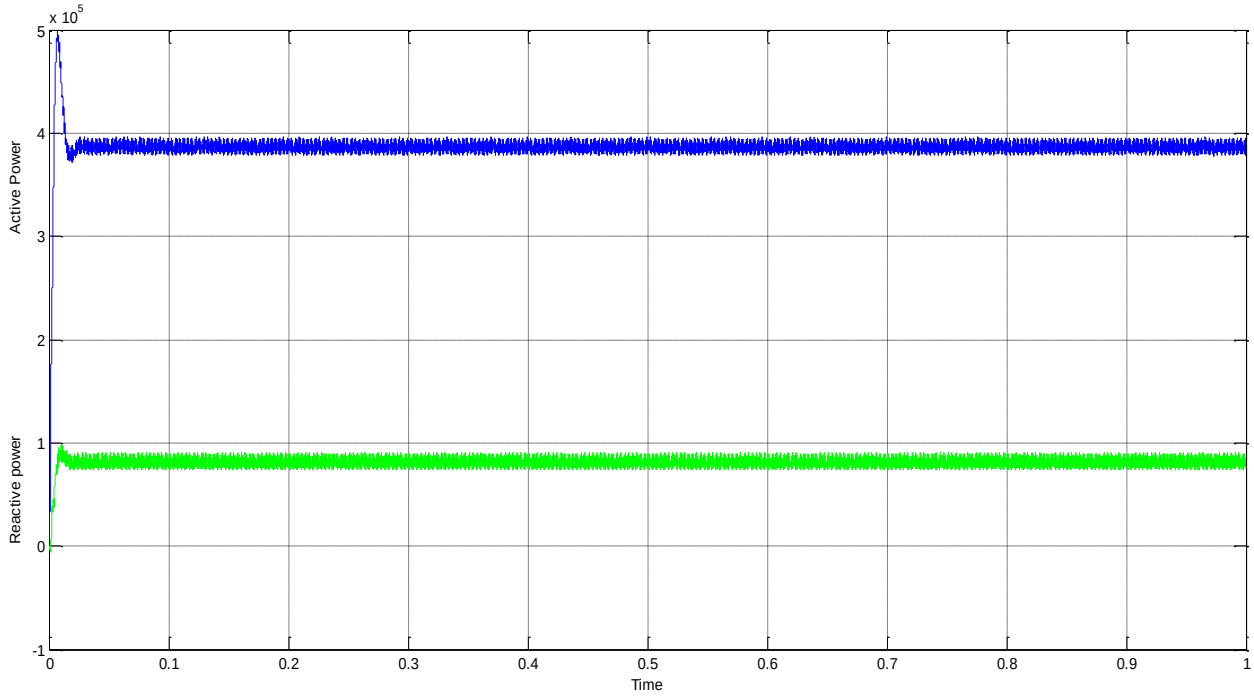

Figure 5.6 Output Power (Active and Reactive)

Output Voltage Vpeak = 454 V

Voltage Vrms = 321 V

Output Current Ipeak = 589 Amps

Current Irms = 416.5 Amps

Active Power = 3.9 X 10^5 Watts = **390 KW**

Inverter Efficiency = Output power / Input power

= 390/412.3

= **94.59 %**

SiC based MOSFET Inverter:

The parameters are as below:

DC Voltage = 1900 V

Inverter: Snubber resistance = 1000 Ohm

Snubber capacitance = 20 X 10^{-6} F

Ron (Ohm) = 0.0075 Ohm

Ton time = 4.5 X 10^{-9} sec

Toff time = 6.0 X 10^{-9} sec

PWM Generator: Carrier frequency = 10 KHz

Modulation Index = 0.8

LC filter: L = 1 x 10^{-3} H

C = 500 X 10^{-6} F

RL Load: = Equivalent to (200 KW x2) = 400 KW

Fig. 5.7 depicts the setup used to study the performance of the SiC based MOSFET devices feeding Static load.

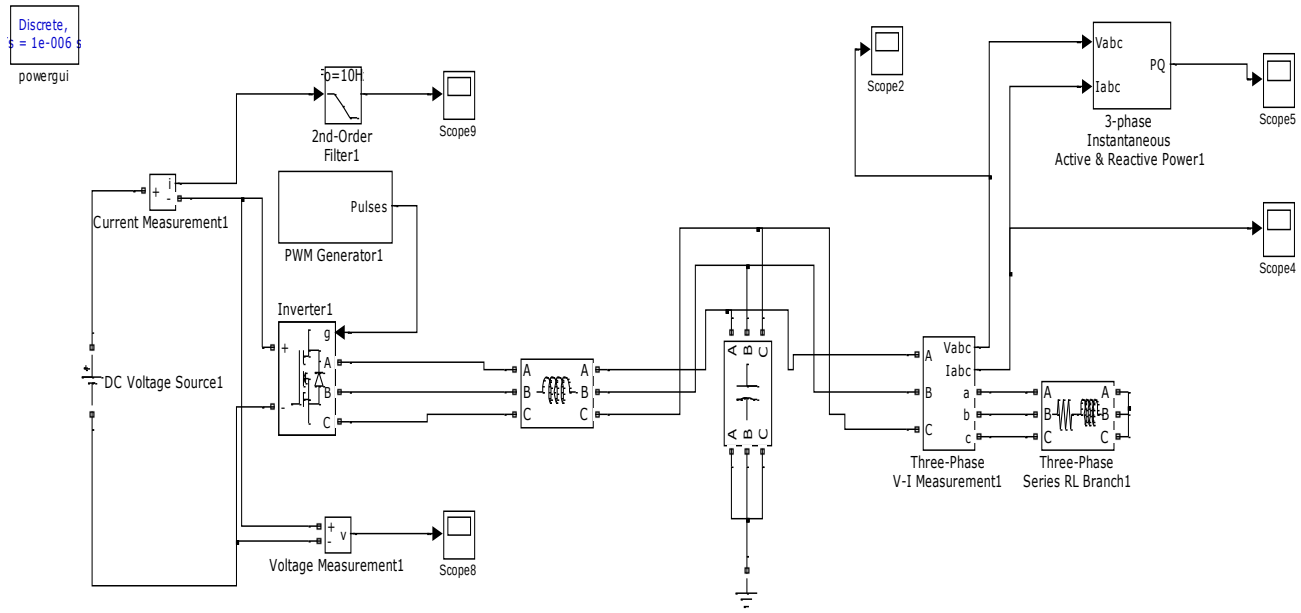

Figure 5.7 Simulink model for Static load (SiC based MOSFET)

The Output Voltage, Currant waveform and Output Power have been analyzed based on input Voltage and Input Current.

Input Side Waveforms:-

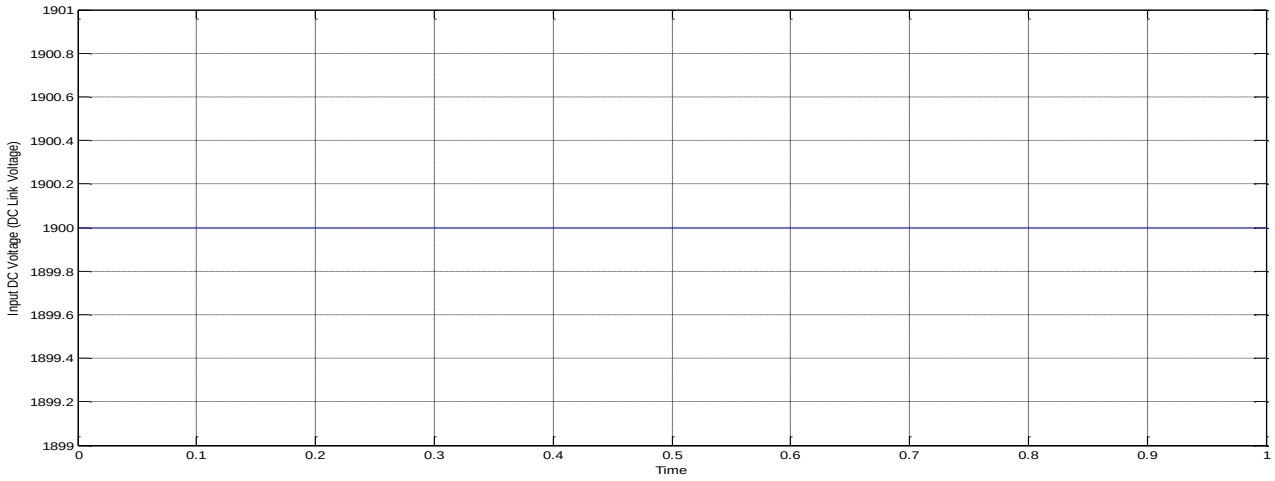

Figure 5.8 Input Voltage Waveform

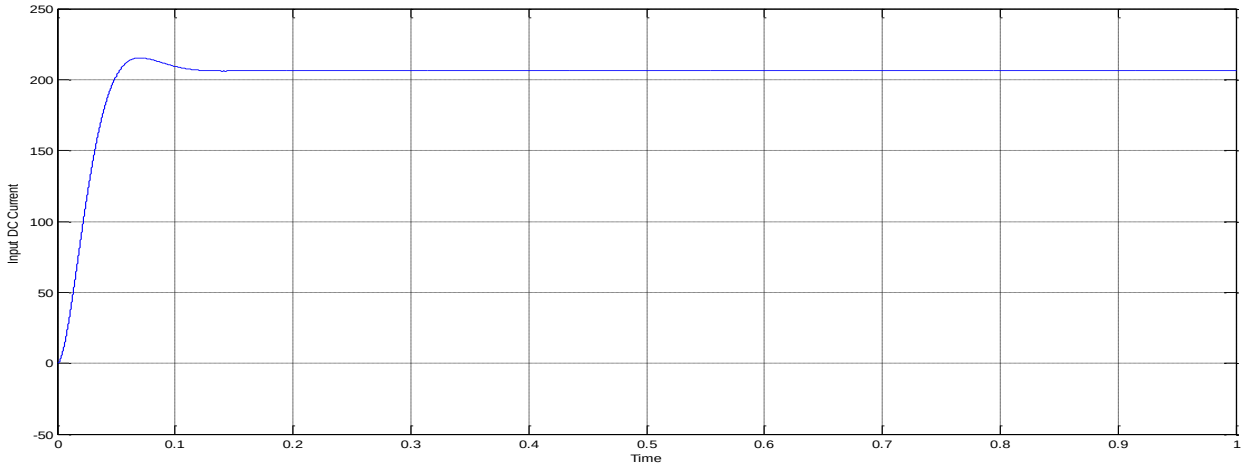

Figure 5.9 Input Current Waveform

Input Voltage is fixed DC Link Voltage = 1900 V, can be seen in waveform.

Input Current depends on load and corresponding input current = **208 Amps**.

Input Power = 1900 X 208 = 395200 Watts = **395.2 KW**

Output Side Waveforms:-

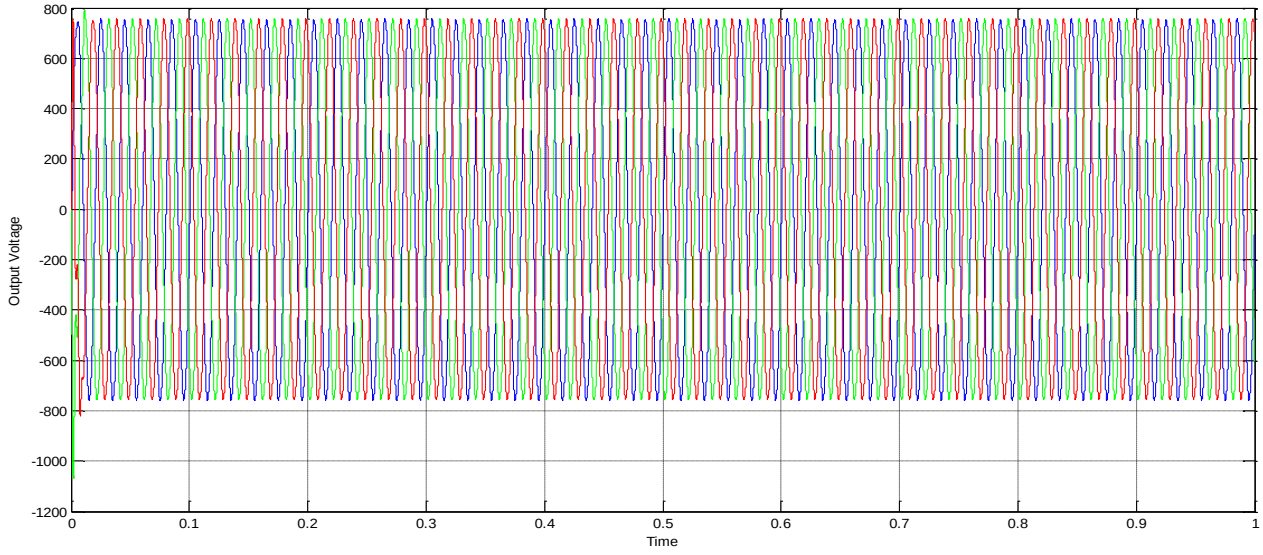

Figure 5.10 Output Voltage Waveform

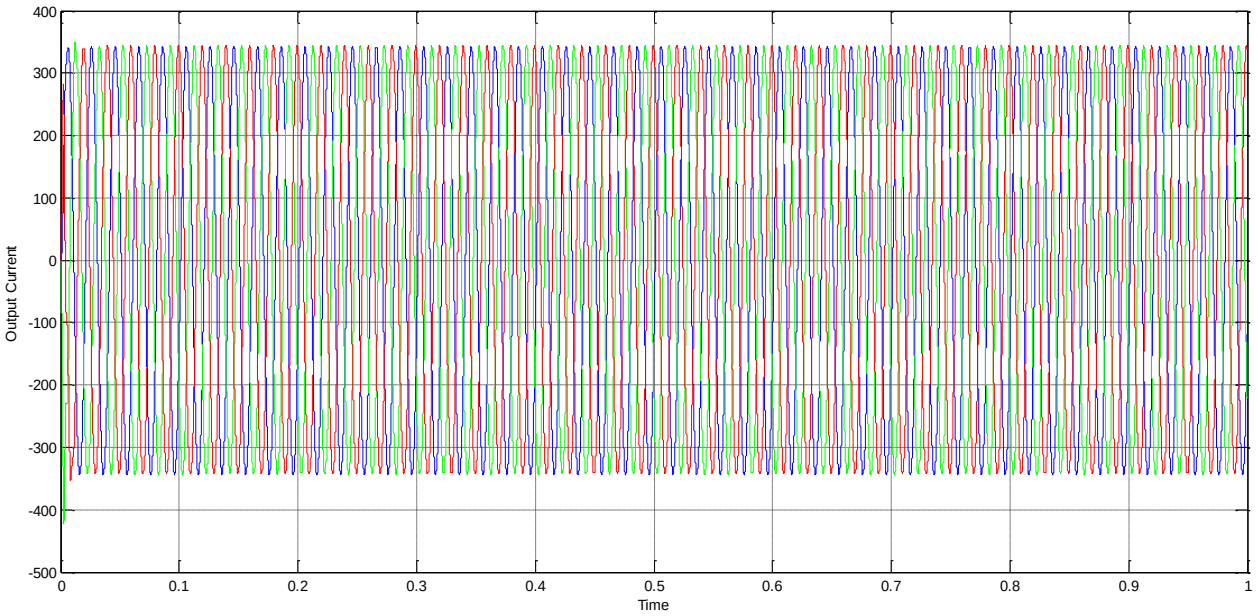

Figure 5.11 Output Current Waveform

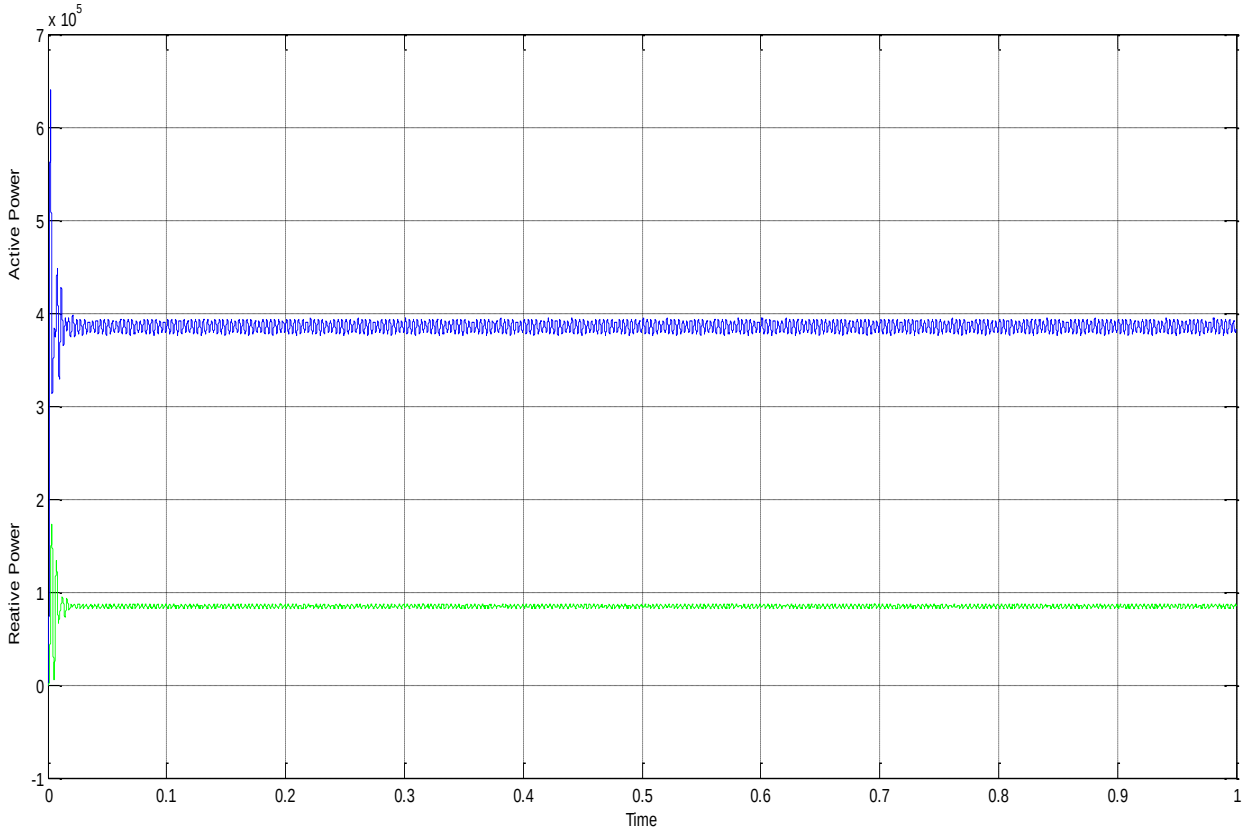

Figure 5.12 Output Power (Active and Reactive)

Output Voltage Vpeak = 760 V

Voltage Vrms = 537.4 V

Output Current Ipeak = 350 Amps

Current Irms = 247. 50 Amps

Active Power = 3.9 X 10^5 Watts = **390 KW**

Inverter Efficiency = Output power / Input power

= 390/395.2

= **98.68 %**

Summarized Result Table:

Device	Output power (Load Requirement)	Input power (Required to meet load)	Input current at fixed DC link Voltage (1900 V)	Inverter Efficiency
Si based IGBT	390 KW	412.3 KW	217 Amps	**94.59**
SiC based MOSFET	390 KW (Same)	395.2 KW **Reduction by 17.1 KW**	208 Amps **Reduction by 9 A**	**98.68**

CHAPTER-6

6 Performance Evaluation of Traction Motor (VVVF drive) with Si based IGBT device and with SiC based MOSFET device

It is assumed that Converter (from AC to DC) is supplying constant DC voltage thus directly DC Voltage source is taken for model building. Universal bridge is used in Inverter mode. LC filter, Current measuring device, Voltage measuring device, power measuring device and Traction Motor (Dynamic load) are modeled in MATLAB using Power System Block set. Motor is started initially with 100 Nm torque and later on torque is increased to 900 Nm.

Si based IGBT Inverter:

The parameters are as below:

DC Voltage = 1900 V

Inverter: Snubber resistance = 10000 Ohm

Snubber capacitance = 1 X 10^{-6} F

Ron (Ohm) = 0.05 Ohm

Ton time = 1.0 X 10^{-6} sec

Toff time = 2.0 X 10^{-6} sec

PWM Generator: Carrier frequency = 800 Hz

Modulation Index = 0.8

Traction Motor (Dynamic Load): = 220 KW , 1450 V, 72.5 Hz, 2% Slip

Stator Resistance = 0.1116 ohm

Inductance = 0.000317 H

Rotor Resistance = 0.1108 ohm

Inductance = 0.000305 H

Mutual Inductance = 0.0059 H

Fig. 6.1 and Fig. 6.2 depict the setup used to study the performance of the Traction Inverter for Si based IGBT devices feeding Traction Motor.

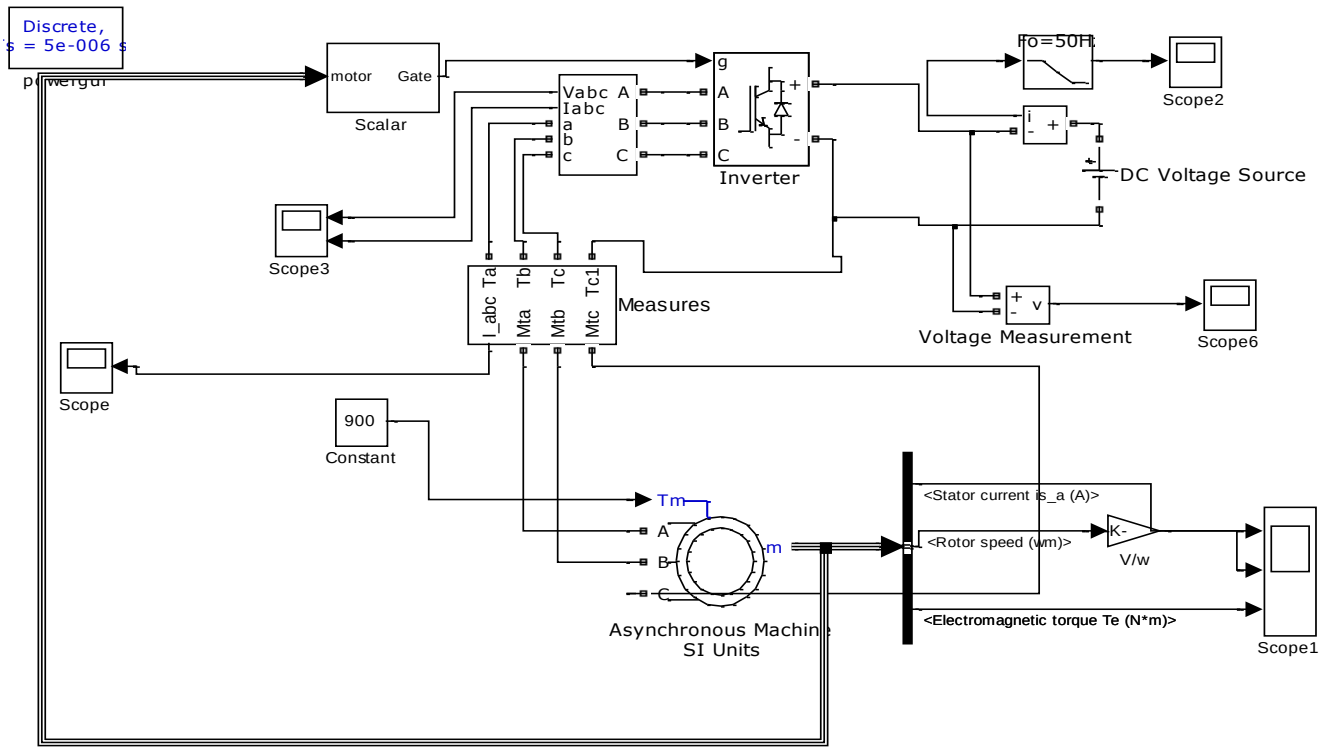

Figure 6.1 Simulink model for Traction Motor (Si based IGBT)

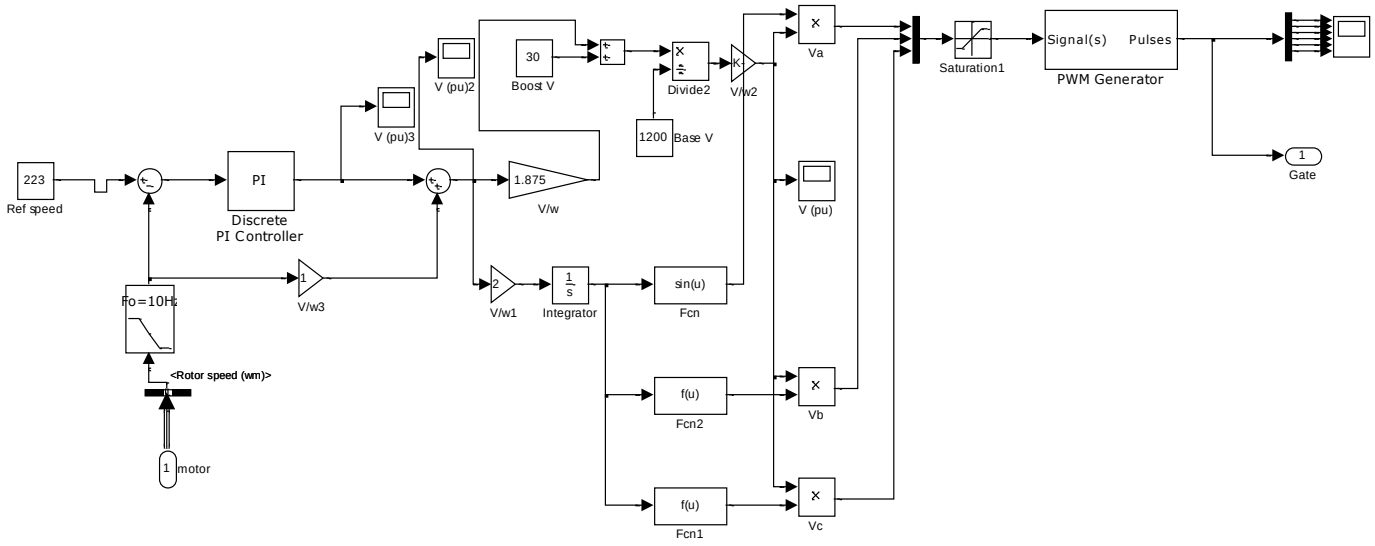

Figure 6.2 Simulink model for Control of VVVF drive (PWM for IGBT)

The Output Voltage, Currant waveform and Output Power have been analyzed based on input Voltage and Input Current.

Input Side Waveforms:-

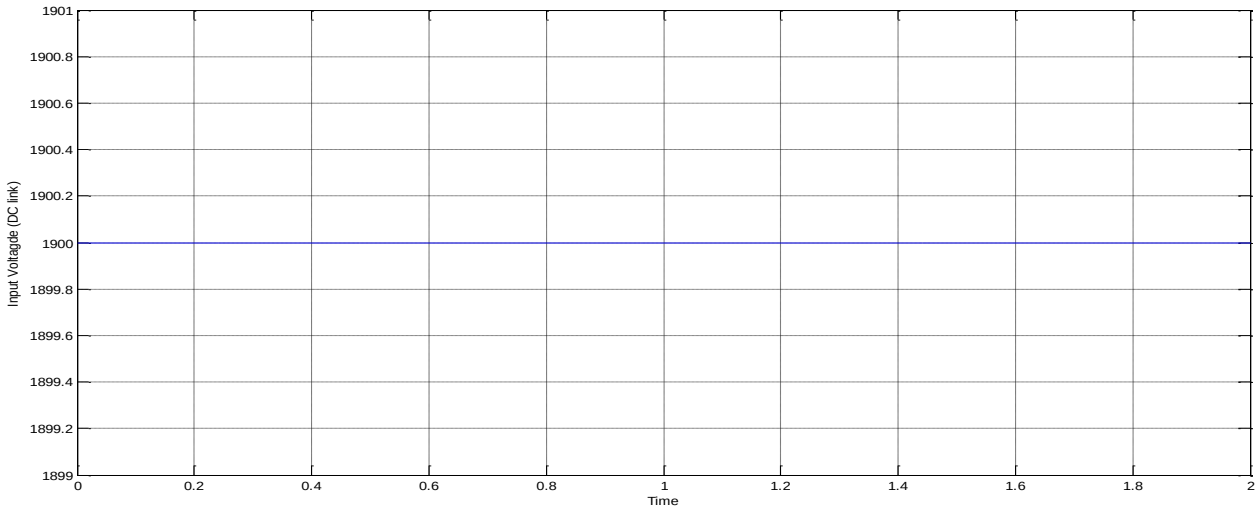

Figure 6.3 Input Voltage Waveform

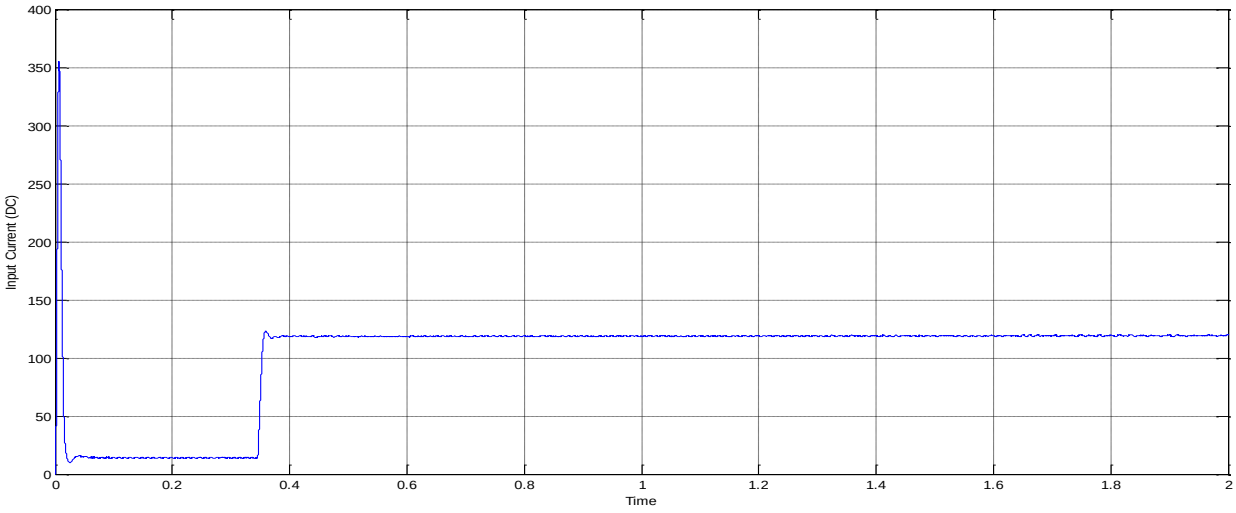

Figure 6.4 Input Current Waveform

Input Voltage is fixed DC Link Voltage = 1900 V, can be seen in waveform.

Input Current depends on load and corresponding input current = **118 Amps**.

Input Power = 1900 X 118 = 224200 Watts = **224.20 KW**

Output Side Waveforms:-

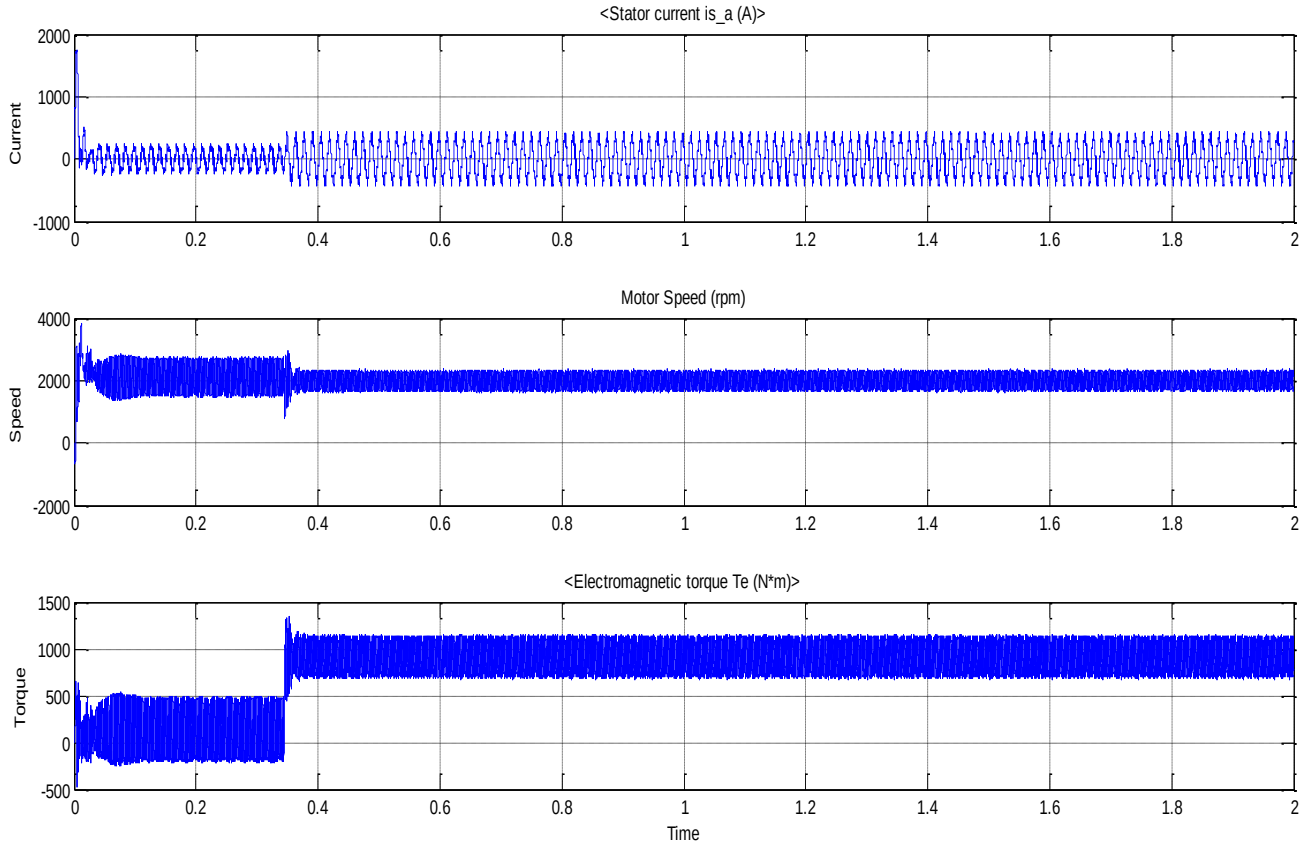

Figure 6.5 Output Waveform

Stator Current Ipeak = 430 Amps

Current Irms = 304 Amps

Motor Speed = 2000 rpm = 209.44 rad/sec

Output Torque = 900 Nm

Output Torque = Torque X speed

= 900 X 209.44 = 188496 watts = **188.496 KW**

Inverter Efficiency (including Motor) = Output power / Input power

= 188.496/224.20

= **84.075 %**

SiC based MOSFET Inverter:

The parameters are as below:

DC Voltage = 1900 V

Inverter: Snubber resistance = 1000 Ohm

Snubber capacitance = 20 X 10^{-6} F

Ron (Ohm) = 0.0075 Ohm

Ton time = 4.5 X 10^{-9} sec

Toff time = 6.0 X 10^{-9} sec

PWM Generator: Carrier frequency = 10 KHz

Modulation Index = 0.8

Traction Motor (Dynamic Load): = 220 KW , 1450 V, 72.5 Hz, 2% Slip

Stator Resistance = 0.1116 ohm

Inductance = 0.000317 H

Rotor Resistance = 0.1108 ohm

Inductance = 0.000305 H

Mutual Inductance = 0.0059 H

Fig. 6.6 and Fig. 6.7 depict the setup used to study the performance of the SiC based MOSFET devices feeding Traction Motor.

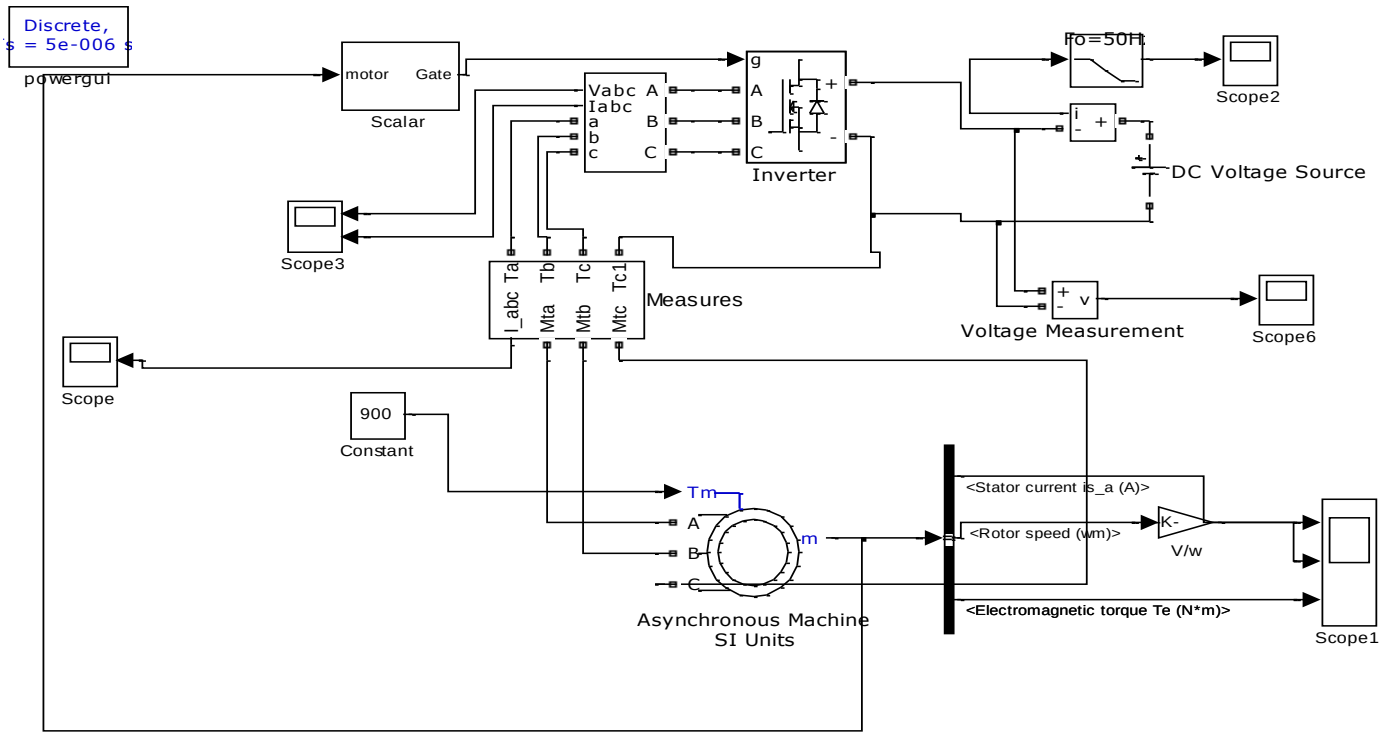

Figure 6.6 Simulink model for Traction Motor (SiC based MOSFET)

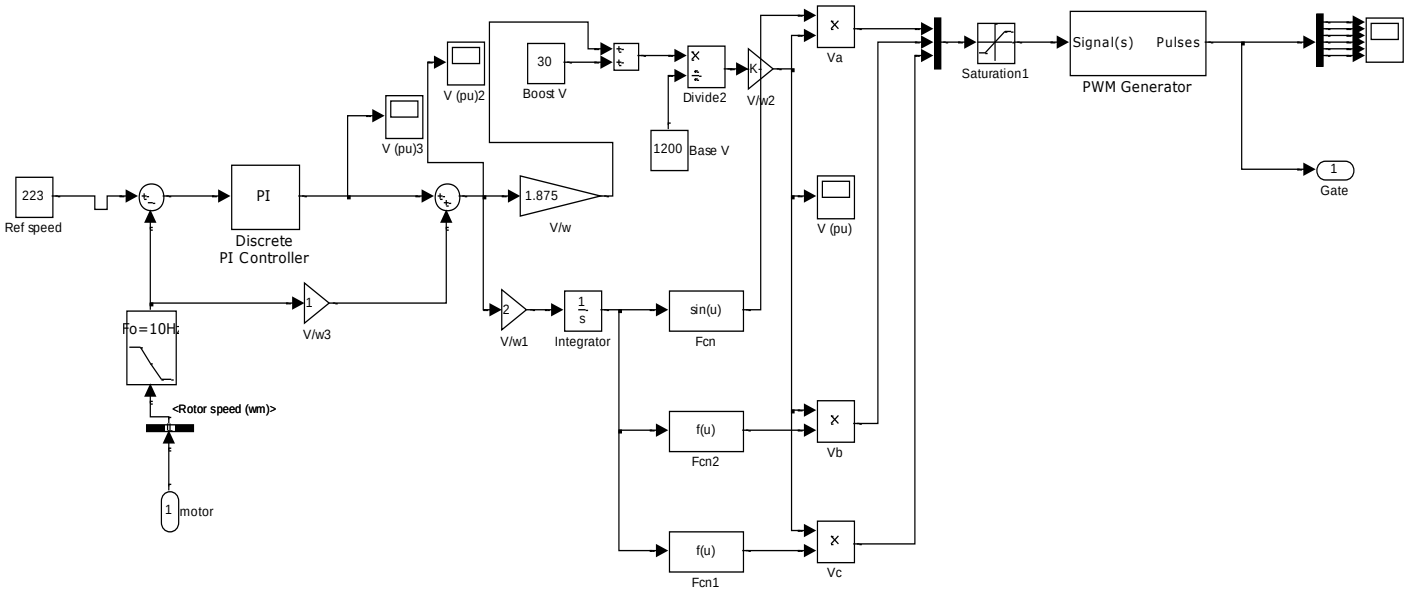

Figure 6.7 Simulink model for Control of VVVF drive (PWM for MOSFET)

The Output Voltage, Currant waveform and Output Power have been analyzed based on input Voltage and Input Current.

Input Side Waveforms:-

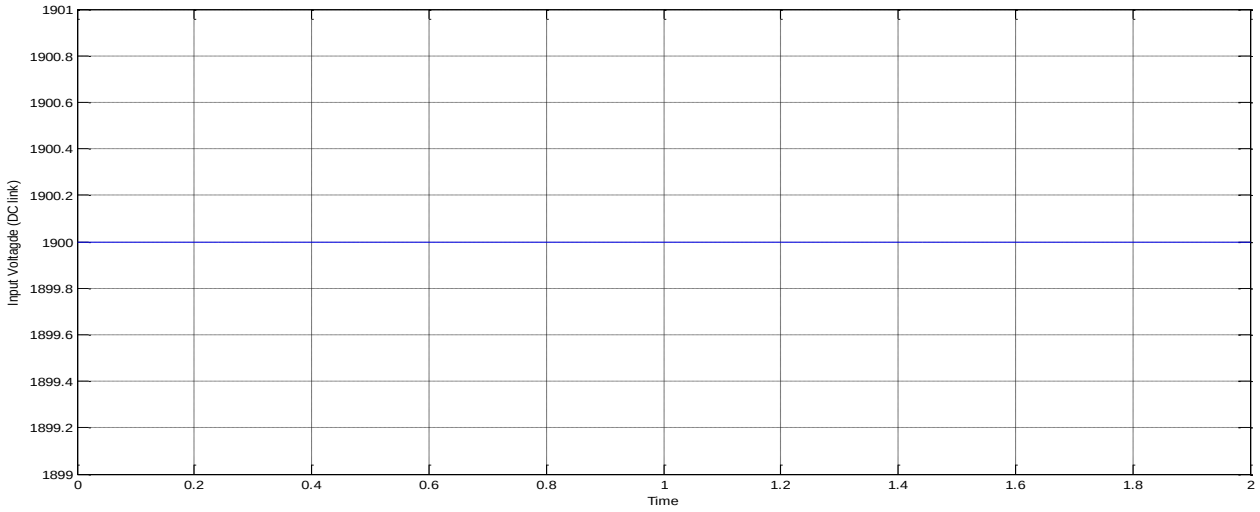

Figure 6.8 Input Voltage Waveform

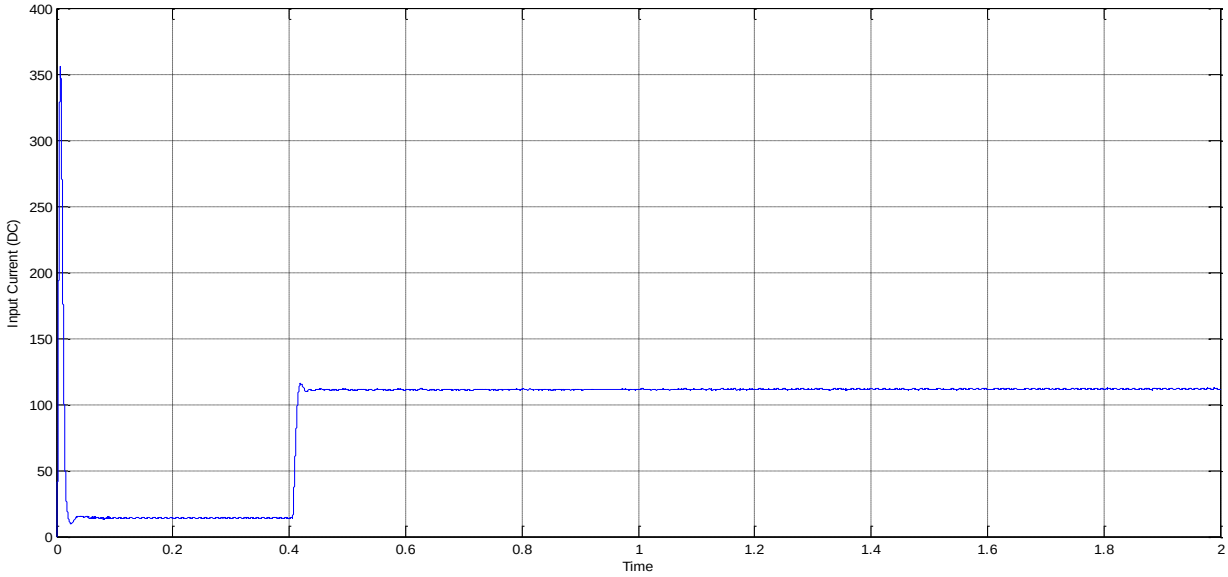

Figure 6.9 Input Current Waveform

Input Voltage is fixed DC Link Voltage = 1900 V, can be seen in waveform.

Input Current depends on load and corresponding input current = **111 Amps**.

Input Power = 1900 X 111 = 210900 Watts = **210.90 KW**

Output Side Waveforms:-

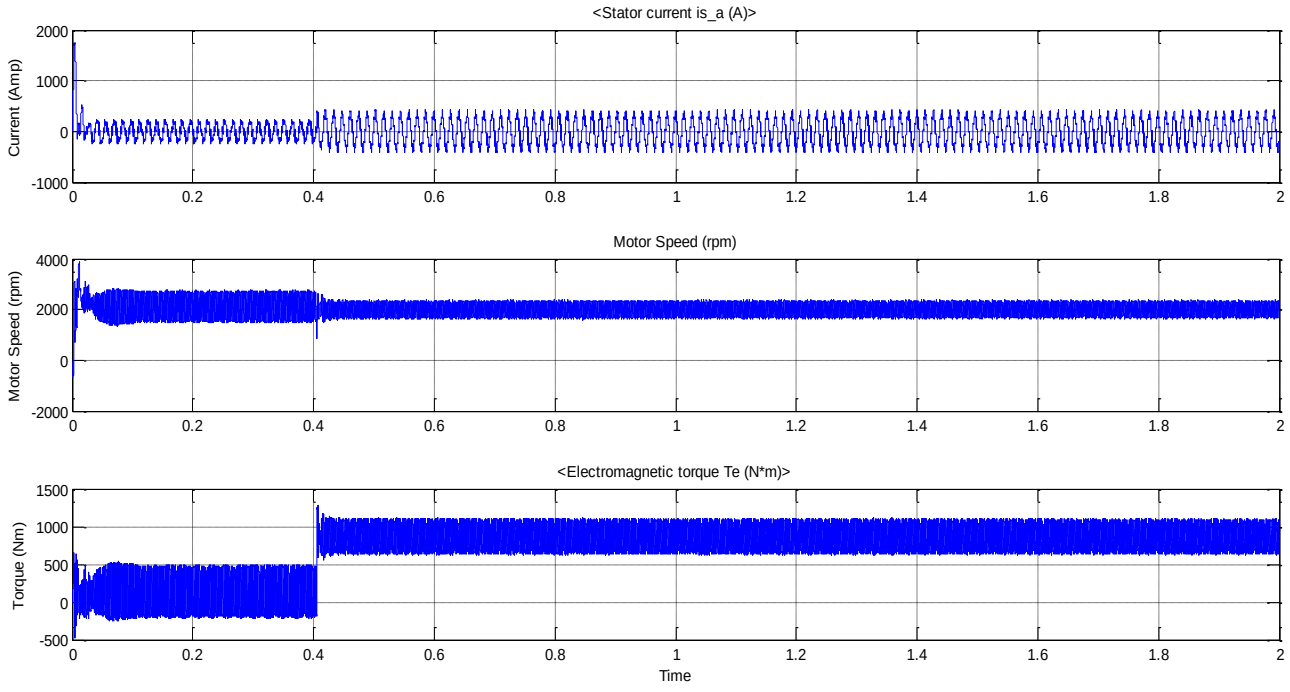

Figure 6.10 Output Waveform

Stator Current Ipeak = 412 Amps

Current Irms = 291.33 Amps

Motor Speed = 2000 rpm = 209.44 rad/sec

Output Torque = 900 Nm

Output Torque = Torque X speed

= 900 X 209.44 = 188496 watts = **188.496 KW**

Inverter Efficiency (including Motor) = Output power / Input power

= 188.496/210.90

= **89.376 %**

Summarized Result Table:

Device	Output power (Load Requirement)	Input power (Required to meet load)	Input current at fixed DC link Voltage (1900 V)	Inverter Efficiency
Si based IGBT	188.496 KW	224.20 KW	118 Amps	**84.075**
SiC based MOSFET	188.496 KW (Same)	210.90 KW **Reduction by 13.3 KW**	111 Amps **Reduction by 7 A**	**89.376**

CHAPTER-7

7 Performance Evaluation of Traction Motor (VVVF drive) in Regeneration mode with Si based IGBT device and with SiC based MOSFET device

It is assumed that Converter (from AC to DC) is supplying constant DC voltage thus directly DC Voltage source is taken for model building. Universal bridge is used in Inverter mode. LC filter, Current measuring device, Voltage measuring device, power measuring device and Traction Motor (Dynamic load) are modeled in MATLAB using Power System Block set. Motor is started initially with 100 Nm torque and later on torque is increased to 900 Nm.

After start of Motor, Motor is braked after 1 second and the Slope of speed getting reduced is calculated. Slope of Synchronous Speed is set higher than the slope of Motor Speed so that Motor is acting like a Generator.

Ns slope > N slope: - N > Ns thus Motor is acting like Generator

Si based IGBT Inverter:

The parameters are as below:

DC Voltage = 1900 V

Inverter: Snubber resistance = 10000 Ohm

Snubber capacitance = 1 X 10^{-6} F

Ron (Ohm) = 0.05 Ohm

Ton time = 1.0 X 10^{-6} sec

Toff time = 2.0 X 10^{-6} sec

PWM Generator: Carrier frequency = 800 Hz

Modulation Index = 0.8

Traction Motor (Dynamic Load): = 220 KW , 1450 V, 72.5 Hz, 2% Slip

Stator Resistance = 0.1116 ohm

Inductance = 0.000317 H

Rotor Resistance = 0.1108 ohm

Inductance = 0.000305 H

Mutual Inductance = 0.0059 H

Fig. 7.1 and Fig. 7.2 depict the setup used to study the performance of the Traction Inverter for Si based IGBT devices feeding Traction Motor (in Regeneration mode).

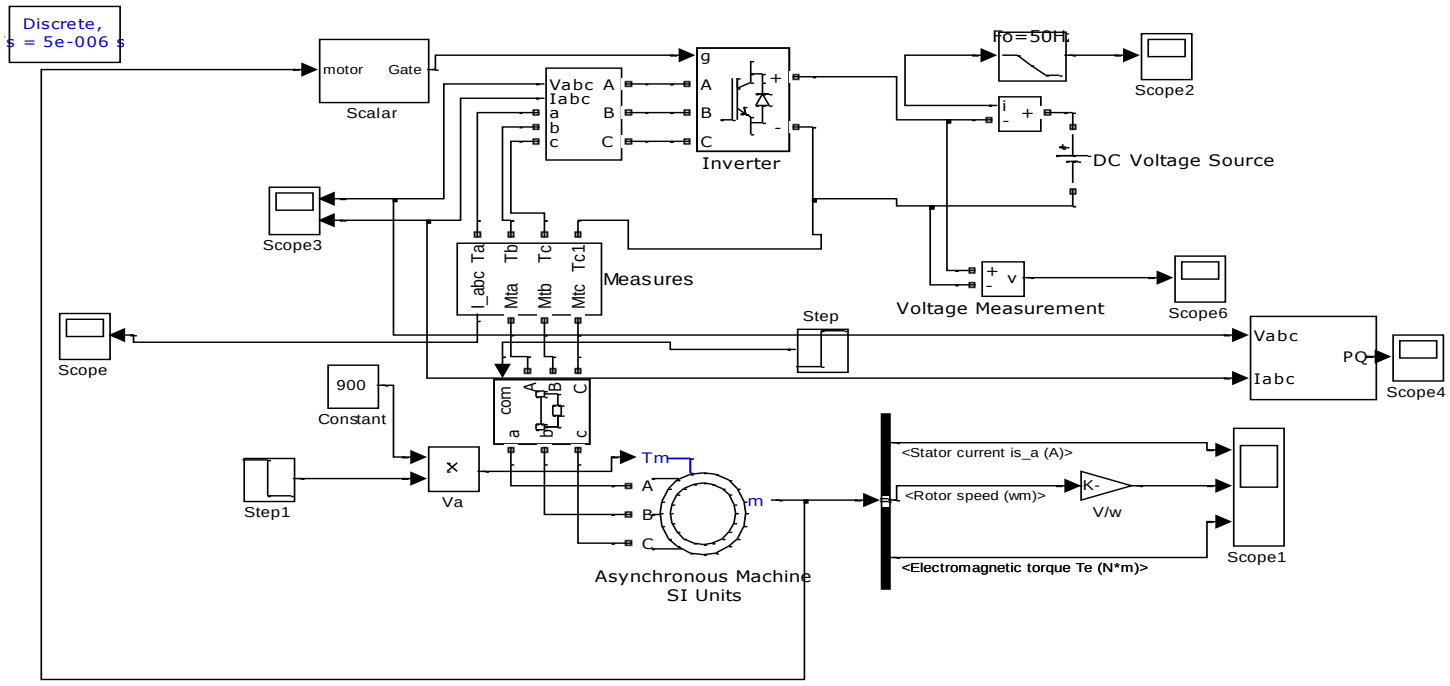

Figure 7.1 Simulink model for Traction Motor (Si based IGBT)

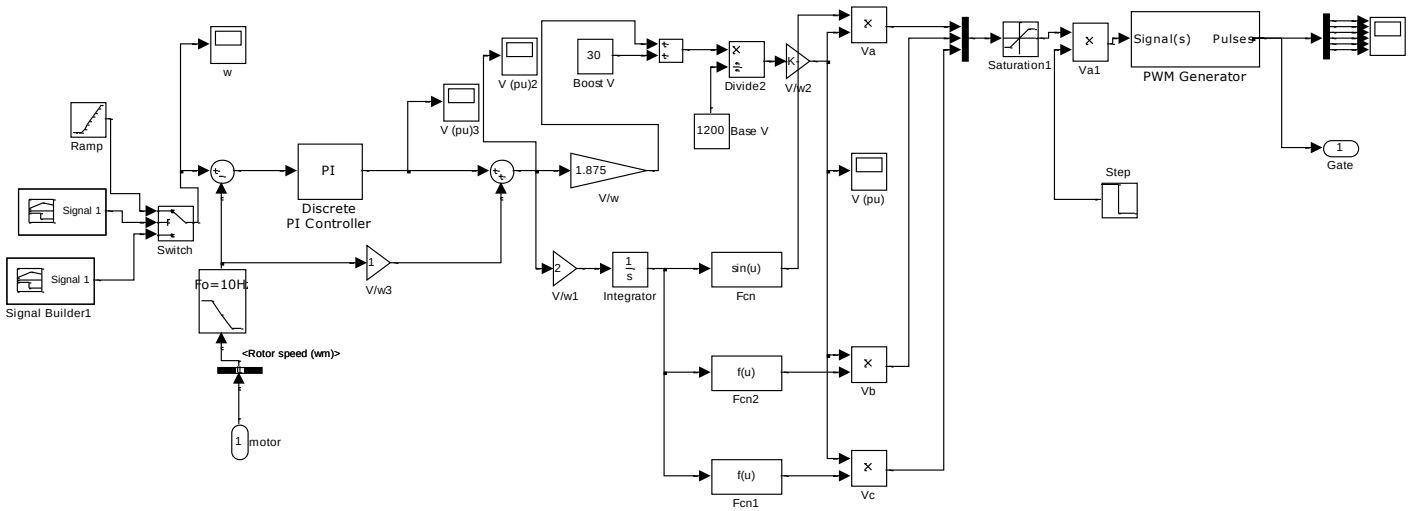

Figure 7.2 Simulink model for Control of VVVF drive (PWM for IGBT)

Slope of Synchronous speed (Ns) based on Actual Motor speed (N):

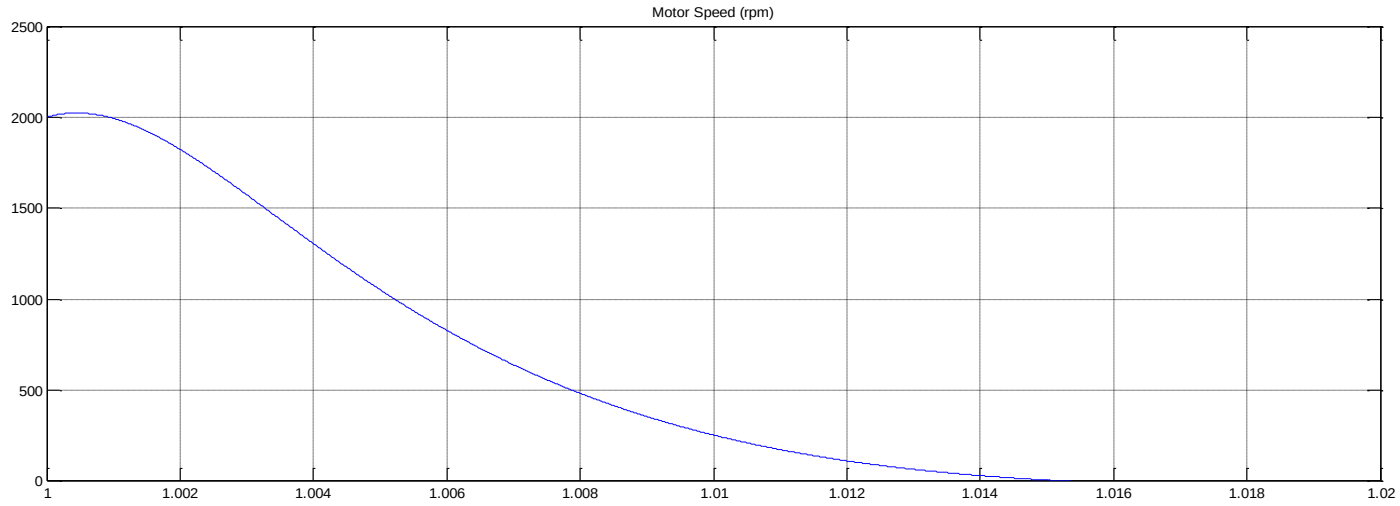

7.3 Motor speed (N) slope

Reduction of speed from 2000 rpm (209.44 rad/sec) to zero in approx 0.014 seconds, thus

Slope = 209.44/0.014 = 14960

So fixed slope for Ns > 14960, thus

Fixed slope for Synchronous speed Ns, = 15000

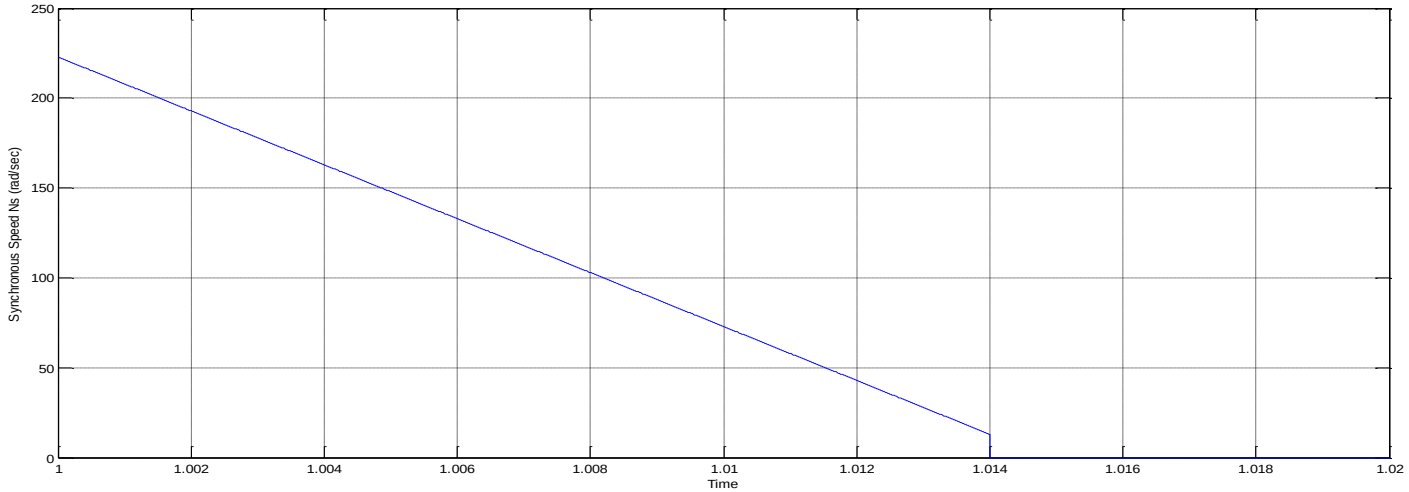

7.4 Synchronous Speed (Ns) Slope derived fromMotor speed (N) slope

The Output Voltage, Currant waveform and Output Power have been analyzed based on input Voltage and Input Current.

Input Side Waveforms:-

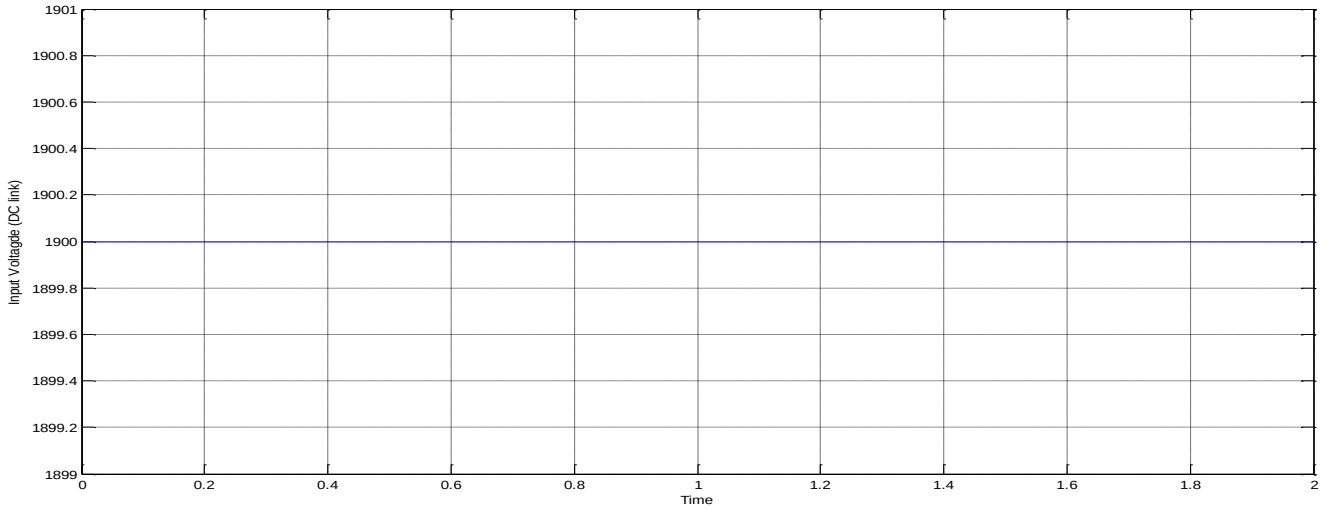

Figure 7.5 Input Voltage Waveform

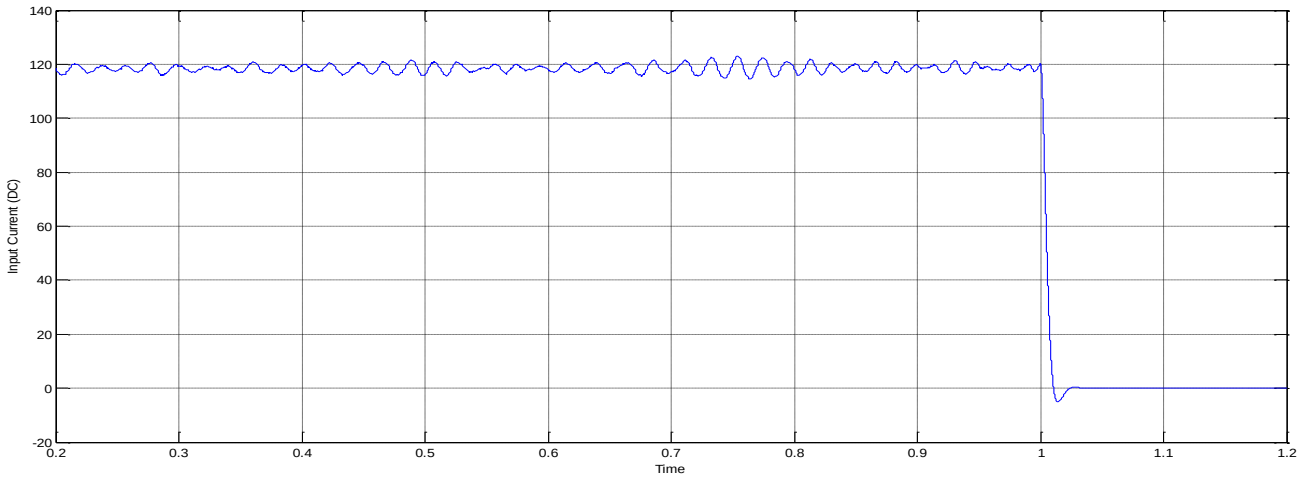

Figure 7.6 Input Current Waveform

Output Side Waveforms:-

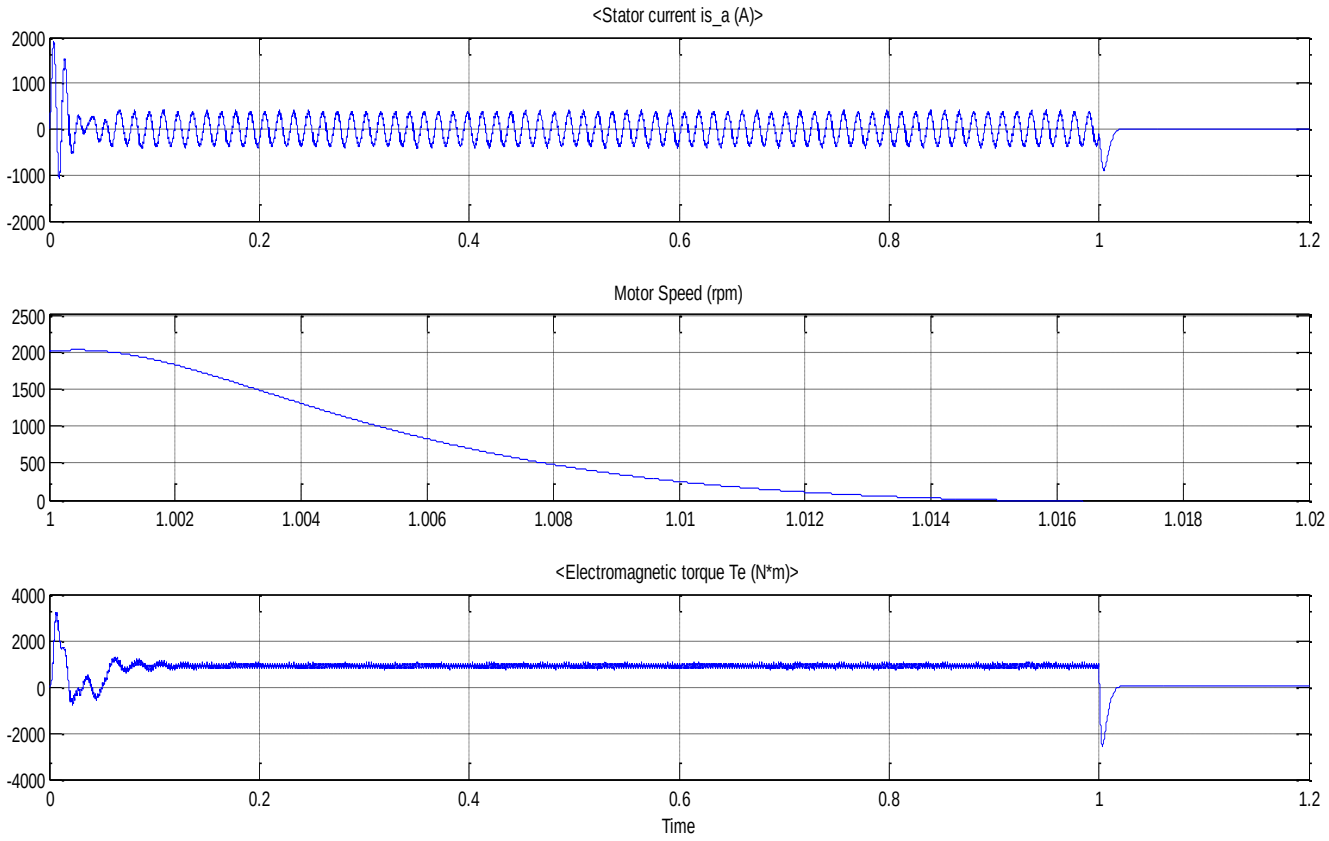

Figure 7.7 Output Waveform

Motor Speed = 2000 rpm = 209.44 rad/sec

Output Torque = 900 Nm

Regenerated Power Waveforms

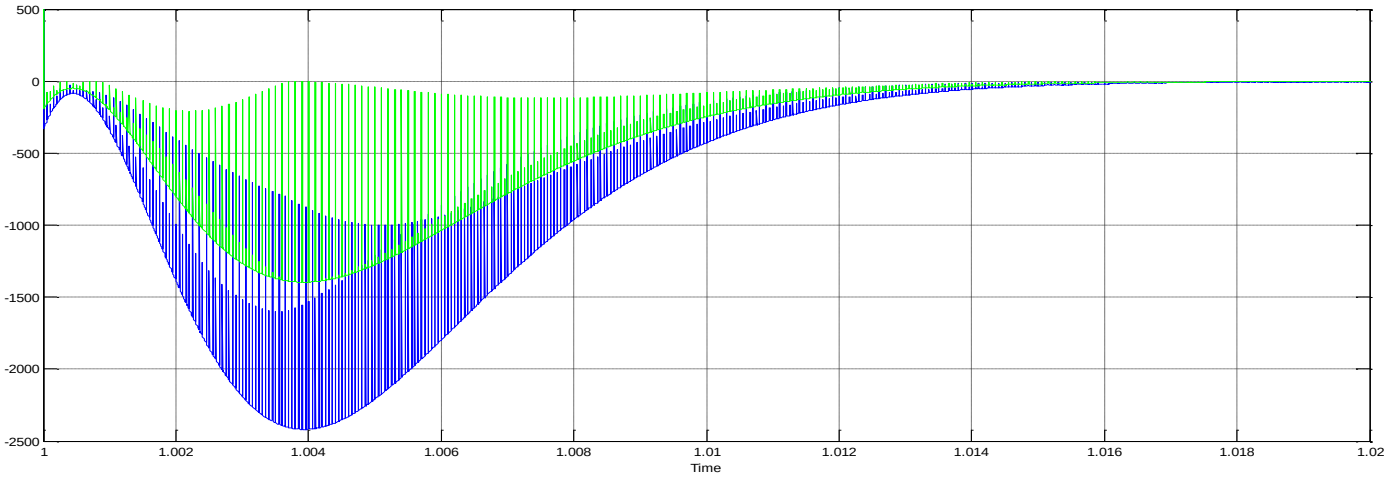

Figure 7.8 Regenerated Power Waveform

Regenerated Power (active) = 1390 Watts

SiC based MOSFET Inverter:

The parameters are as below:

DC Voltage = 1900 V

Inverter: Snubber resistance = 1000 Ohm

Snubber capacitance = 20 X 10^{-6} F

Ron (Ohm) = 0.0075 Ohm

Ton time = 4.5 X 10^{-9} sec

Toff time = 6.0 X 10^{-9} sec

PWM Generator: Carrier frequency = 10 KHz

Modulation Index = 0.8

Traction Motor (Dynamic Load): = 220 KW , 1450 V, 72.5 Hz, 2% Slip

Stator Resistance = 0.1116 ohm

Inductance = 0.000317 H

Rotor Resistance = 0.1108 ohm

Inductance = 0.000305 H

Mutual Inductance = 0.0059 H

Fig. 7.9 and Fig. 7.10 depict the setup used to study the performance of the SiC based MOSFET devices feeding Traction Motor(in Regeneration mode).

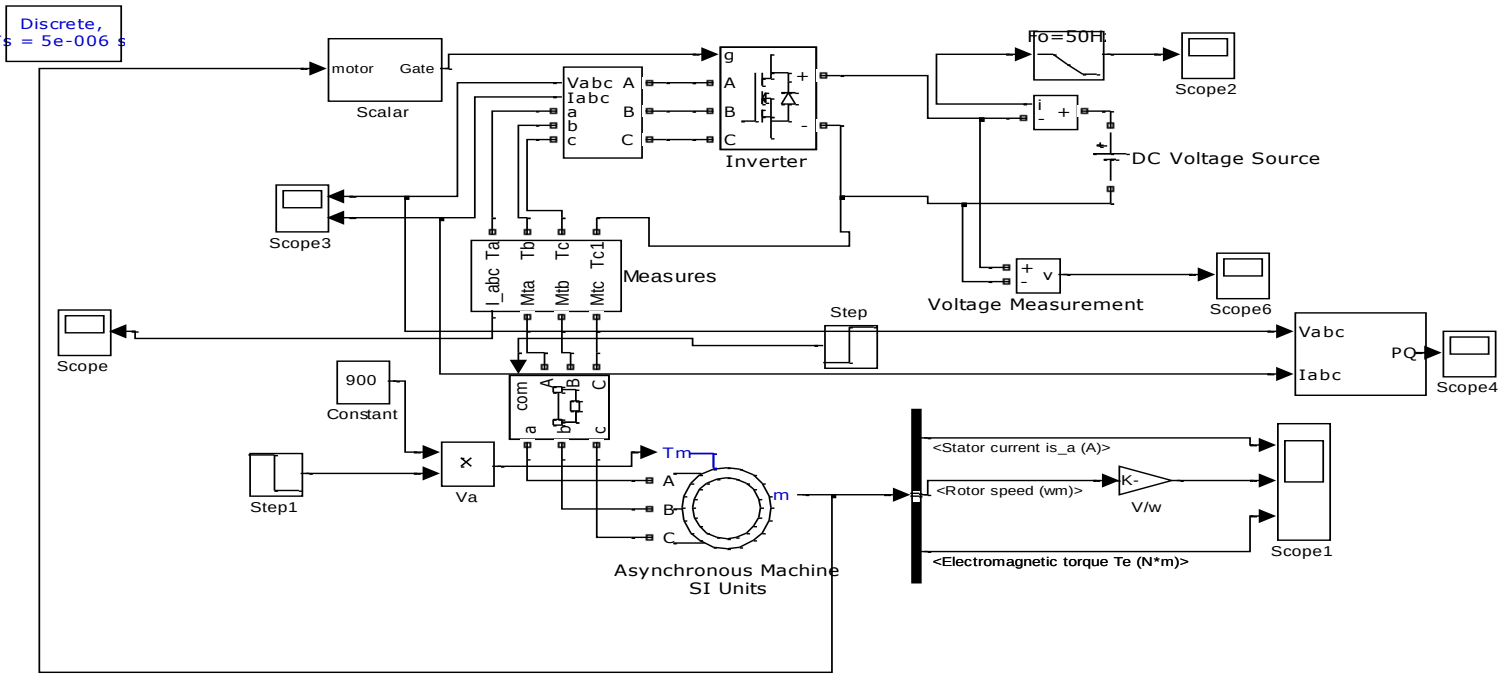

Figure 7.9 Simulink model for Traction Motor (SiC based MOSFET)

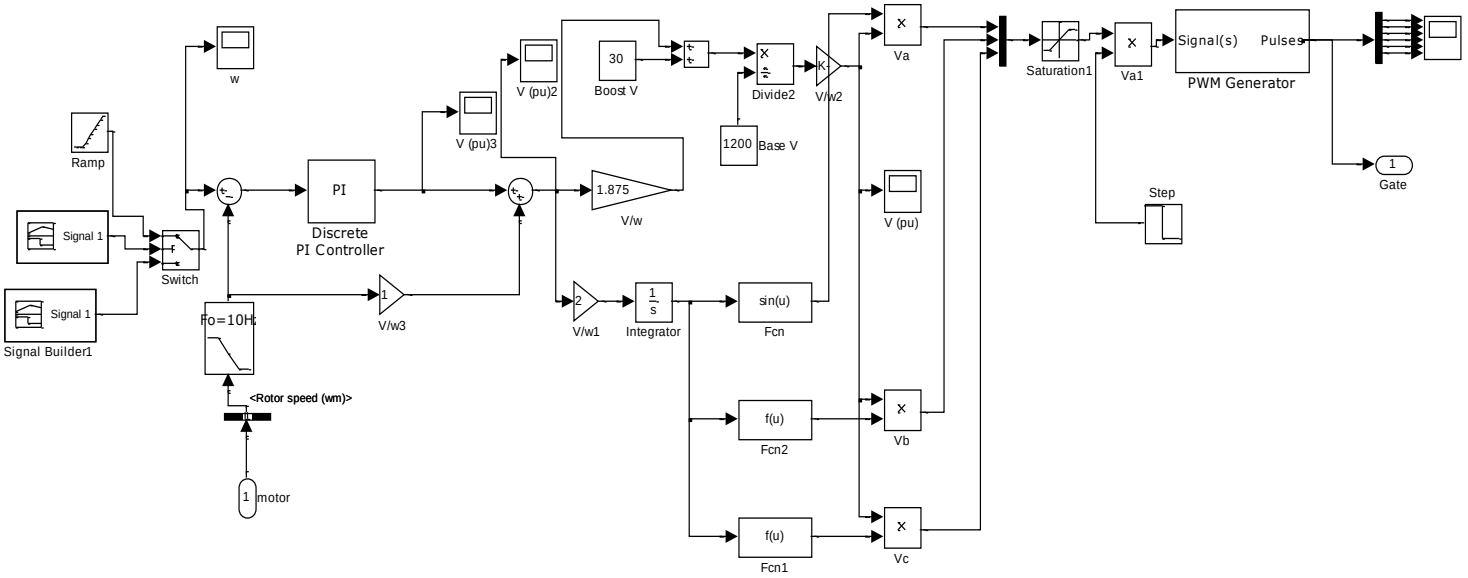

Figure 7.10 Simulink model for Control of VVVF drive (PWM for MOSFET)

Slope of Synchronous speed (Ns) based on Actual Motor speed (N):

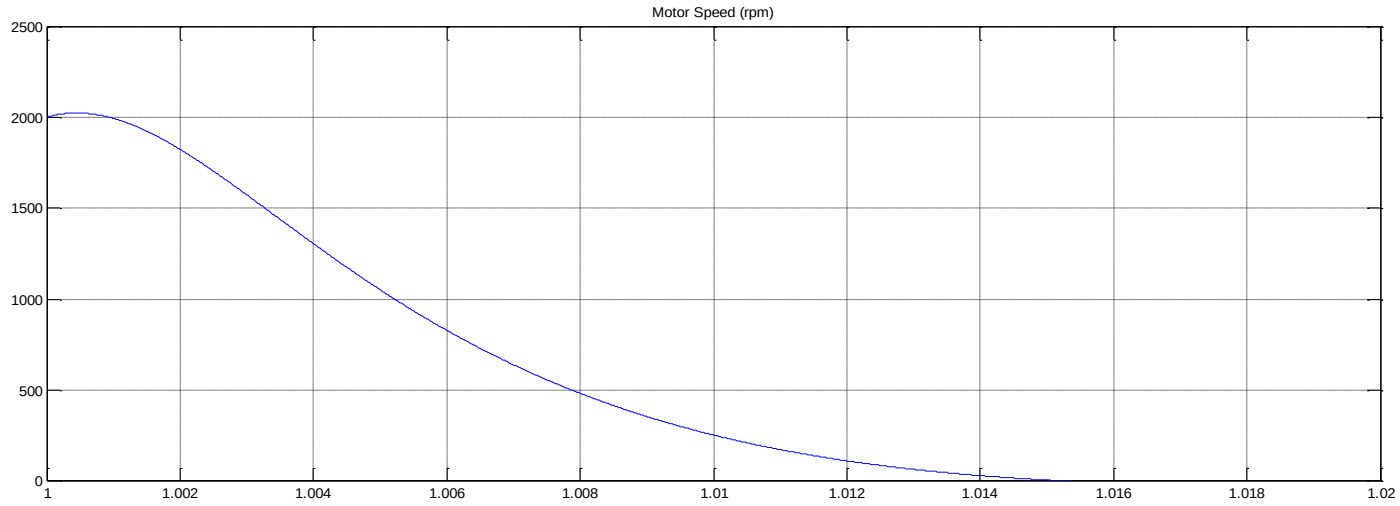

Figure 7.11 Motor speed (N) slope

Reduction of speed from 2000 rpm (209.44 rad/sec) to zero in approx 0.014 seconds, thus

Slope = 209.44/0.014 = 14960

So fixed slope for Ns > 14960, thus

Fixed slope for Synchronous speed Ns, = 15000

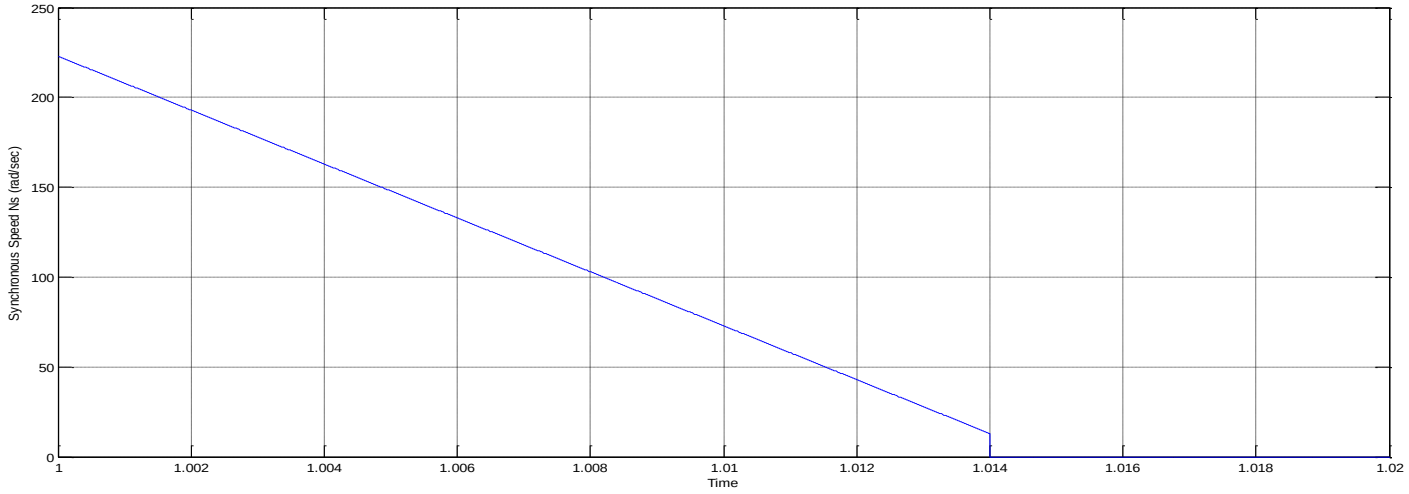

7.12 Synchronous Speed (Ns) Slope derived fromMotor speed (N) slope

The Output Voltage, Currant waveform and Output Power have been analyzed based on input Voltage and Input Current.

Input Side Waveforms:-

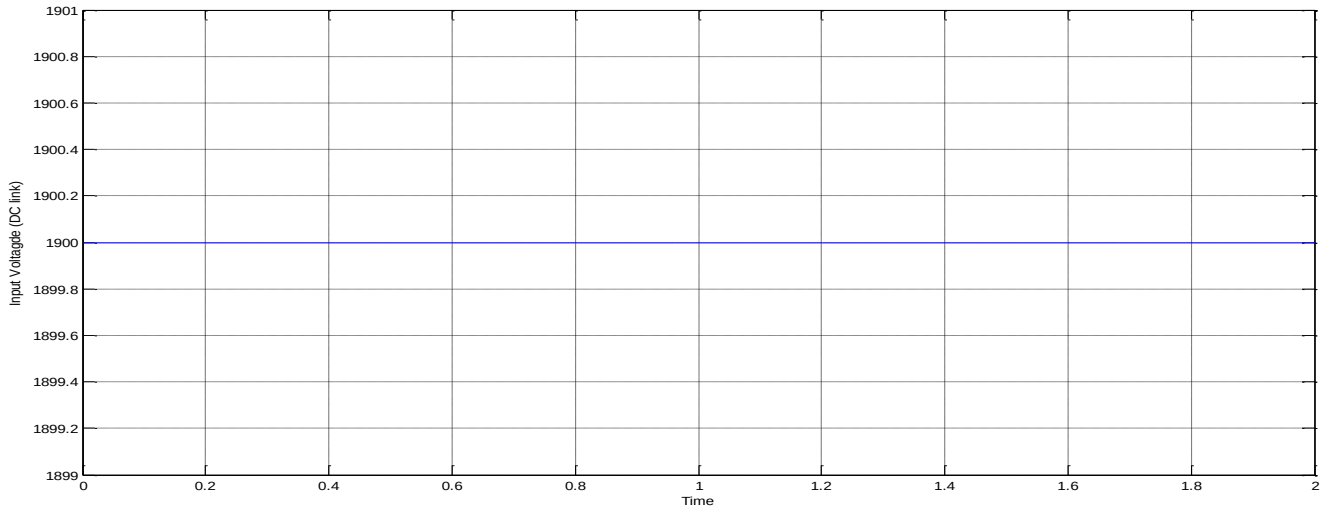

Figure 7.13 Input Voltage Waveform

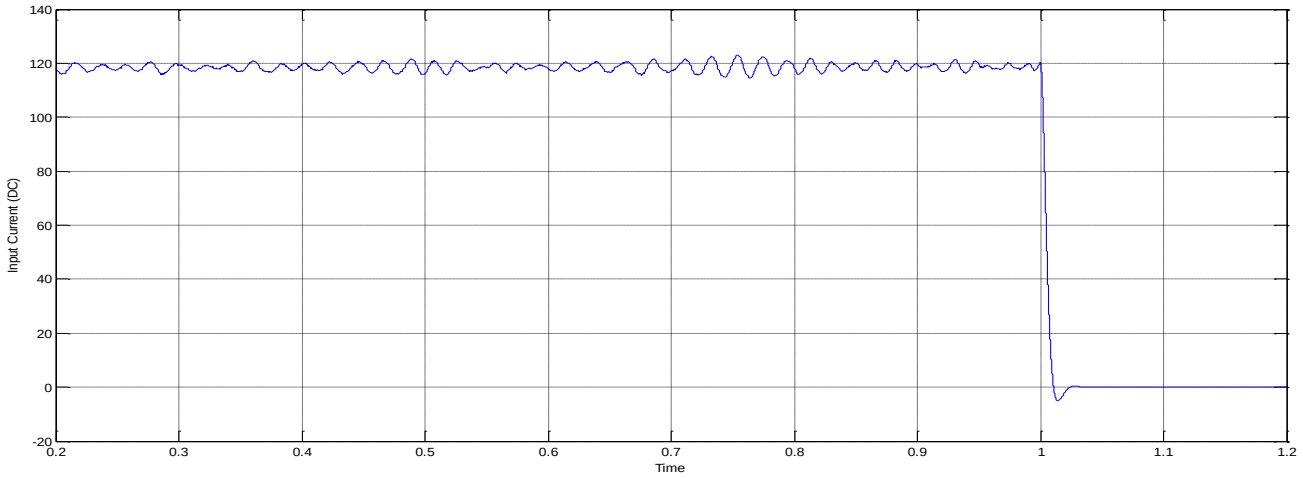

Figure 7.14 Input Current Waveform

Output Side Waveforms:-

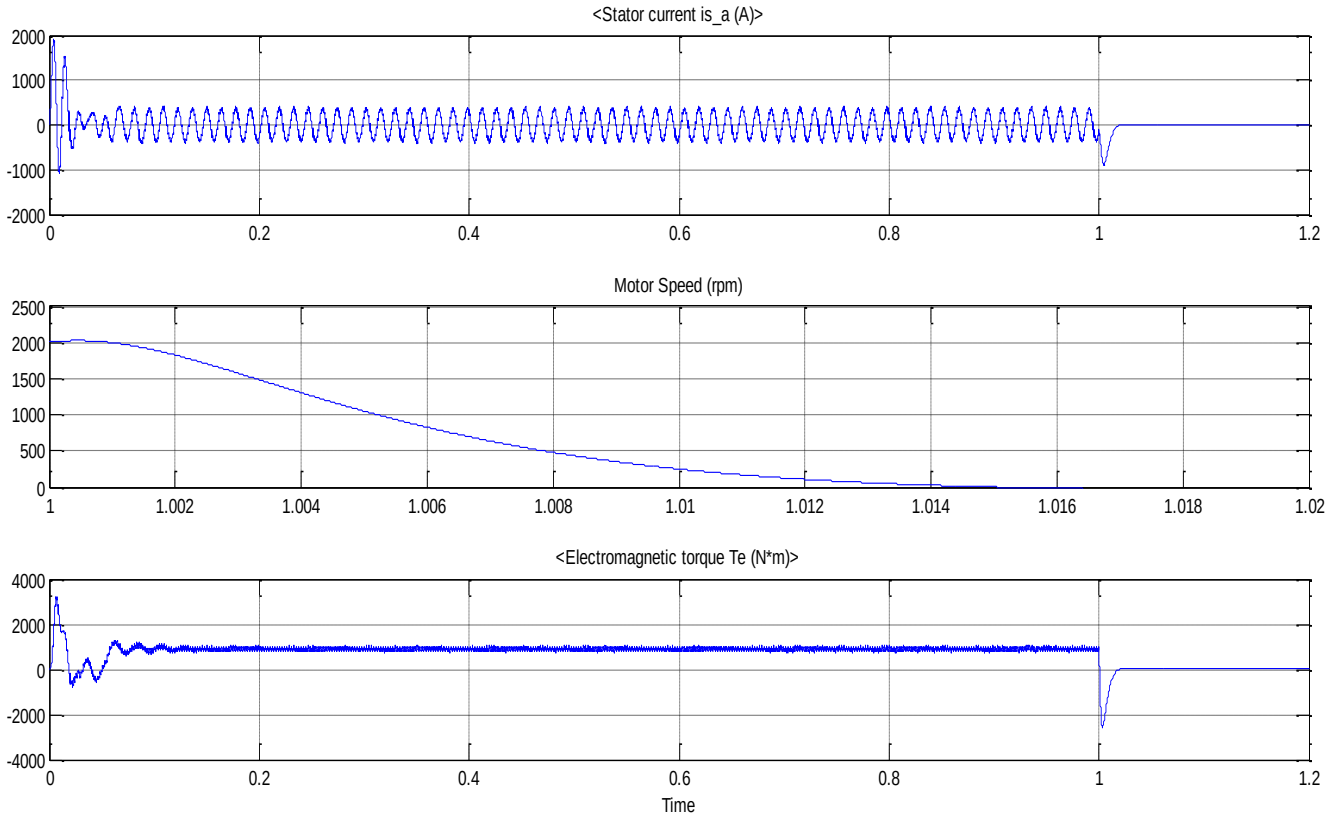

Figure 7.15 Output Waveform

Motor Speed = 2000 rpm = 209.44 rad/sec

Output Torque = 900 Nm

Regenerated Power Waveforms

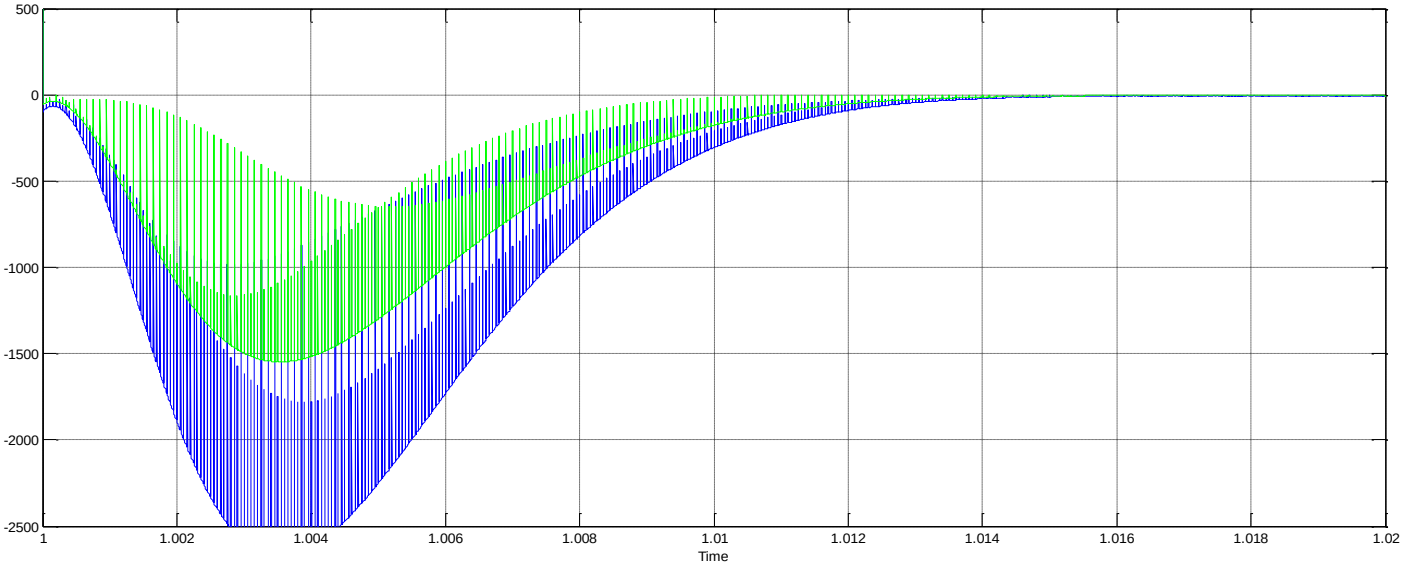

Figure 7.16 Regenerated Power Waveform

Regenerated Power (active) = 1550 Watts

Summarized Result Table:

Device	**Regenerated Power**	**Remarks**
Si based IGBT	1390 Watts	Simulated for same load condition.
SiC based MOSFET	1550 Watts **Saving of 160 Watts power**	
%age saving	**11.51%**	

CHAPTER-8

8 Main Conclusion and Future Scope of Study

8.1 General

System level benefits that will results from the use of SiC power electronics instead of Si devices are reduced losses, increased efficiency, and reduced size and volume. Also, the heat sink required for the drive can be reduced to one-third of the original size and the traction drive efficiency in a hybrid electric vehicle increases by 5 percentage points when SiC power devices replace Si power devices. The sizes of the passive components, which include the transformer and the filter components, decrease proportionally with the increase in switching frequency by using SiC devices show that.

8.2 Main Conclusion

The MATLAB/ Simulink environment using SimPower systems block set has been used to develop the model and carry out simulation work. It has been established by simulation that SiC based devices are more energy efficient and having very low losses compare to Si based devices.

The conclusions drawn from result of Static (RL) Load are as below:-

1. Requirement of around 4.5 % less power for feeding of same load (reduction of 17.1 KW power for feeding of 390 KW).
2. Requirement of almost same %age 4.5% less current if Voltage is fixed (reduction of 9 Amps from 217 Amps).
3. Increase in efficiency from 94.59% (Si based IGBT) to 98.68% (SiC based MOSFET) for feeding same load.

The conclusions drawn from result of Dynamic (Traction Motor) Load are as below:-

1. Requirement of around 5.9 % less power for feeding of same load (reduction of 13.3 KW power for feeding of 188.496 KW).
2. Requirement of almost same %age 5.9% less current if Voltage is fixed (reduction of 7 Amps from 118 Amps).
3. Increase in efficiency from 84.075% (Si based IGBT) to 89.376% (SiC based MOSFET) for feeding same load.

The conclusions drawn from result of Regeneration mode (Traction Motor) are as below:-

1. Increase of Regeneration from 1390 Watts in Si based IGBT to 1550 Watts in SiC based MOSFET for same load condition.
2. Saving of Energy in terms of Regeneration is 11.51% (Increase of 160 Watts regeneration from original regeneration of 1390 Watts).

As a wide bandgap semiconductor technology, SiC allows greater efficiency and reliability than conventional Silicon devices. The significant improvement in efficiency delivers further advantages by allowing the size of any cooling systems and other motor-control components to be reduced. Overall, this can allow the size of the inverter to be reduced by as much as 40 %.

The use of SiC based device will result of Saving of Energy around 38% (55% of Switching losses alone). Conduction loss also gets reduced as significant level.

Thus it is recommended to use SiC based devices for Traction Controller.

8.3 Future Scope of Work

This project was limited to only design improvement of Traction converter based on technology advancement; there are other factors also which determine the energy consumption of Train and energy efficiency.The possible potential points for energy loss:-

1) losses at source level (OCS and RSS)
2) losses in between OCS and Converter
3) losses at Converter level
4) limitation of Power Electronic devices
5) losses in between Converter and load
6) losses at load level (Traction Motors)

Out of above possible points, only point 3 and 4 have been discussed and covered in this project.
There is a need to look the entire factors in totality in conjunction with diversified and harsh requirement. This simulation needs to be put in practical field and to be evaluated practically before going into multiplication of same.

CHAPTER-9

9 References

1) Ahmed Elasser and T. Paul Chow, "Silicon Carbide Benefits and Advantages for Power Electronics Circuits and Systems", Proceedings of The IEEE, Vol. 90, No.6, June 2002, Pg. 969-986

2) Kenji Hamada, Shiro Hino, Naruhisa Miura, Hiroshi Watanabe, Shuhei Nakata, Eisuke Suekawa, Yuji Ebiike, Masayuki Imaizumi, Isao Umezaki, Satoshi Yamakawa, |3.3 kV/1500 A Power Modules for The World's First All-SiC Traction Inverter", Japanese Journal of Apllied Physics 54, 04DP07 (2015), Pg. 04DP07-1-04DP07-4

3) Tsuyoshi Funaki, Juan C. Balda, Jeremy Junghans, Anuwat Jangwanitlert, Sharmila Mounce, Fred D. Barlow, H. Alan Mantooth, Tsunenobu Kimoto, Takashi Hikihara, |Switching Characteristics of SiC JFET and Schottky Diode in High –Temperature DC-DC Power Converters", IEICE Electronics Express, Vol. 2, No.3, Pg. 97-102

4) Tsuyoshi Funaki, Juan C. Balda, Jeremy Junghans, Avinash S. Kashyap, Fred D. Barlow, H. Alan Mantooth, Tsunenobu Kimoto, Takashi Hikihara, "SiC JFET DC Characteristics Under Extremely High Ambient Temperatures", IEICE Electronics Express, Vol.1, No.17, Pg. 523-527

5) DMRC Design Documents and Manuals

6) S. Bernet, "Recent developments of high power converters for industry and traction applications," IEEE Trans. Power Electron., vol. 15, pp. 1102–1117, Nov. 2000.

7) H. Yilmaz, Owyang, M. F. Chang, J. L. Benjamin, and W. R. Van Dell, "Recent advances in insulated gate bipolar transistor technology," IEEE Trans. Ind. Applicat., vol. 26, pp. 831–834, Sept.–Oct. 1990.

8) B. P. Muni, A. V. Gokuli, and S. N. Saxena, "Gating and protection of IGBT in an inverter," in Proc. Int. Conf. Industrial Electronics, Control, and Instrumentation, vol. 1, 1991, pp. 662–667.

9) A. Petterteig, J. Lode, and T. M. Undeland, "IGBT turn-off losses for hard switching and with capacitive snubbers," in Proc. IEEE Industry Applications Society Annu. Meeting, vol. 2, 1991, pp. 1501–1507.

10) N. Hingorani, "Introducing custom power," IEEE Spectrum, vol. 32, pp. 41–48, June 1995.

11) F. Nozari and H. S. Patel, "Power electronics in electric utilities: HVDC Power Transmission Systems," Proc. IEEE, vol. 76, pp. 495–506, Apr. 1988.

12) L. Gyugyi, "Power electronics in electric utilities: Static Var Compensators," in Proc. IEEE, vol. 76, Apr. 1988, pp. 483–494.

13) M. Morikawa, K. Nakura, M. Ito, N. Machida, S. Yamada, S. Kudo, S. Shimizu, and I. Yoshida, "Highly efficient 2.2-GHz Si power MOSFETs for cellular base station applications," in Proc. IEEE Radio and Wireless Conf., 1999, pp. 305–307.

14) H. Matsunami, "Progress in wide bandgap semiconductor SiC for power devices," in Proc. 12th Int. Symp. Power Semiconductor Devices and ICs, 2000, pp. 3–9.

15) G. J. Campisi, "Status of silicon carbide power technology," in Proc. Power Engineering Society Summer Meeting, vol. 2, July 2000, pp. 1238–1239.

16) J. W. Palmour, R. Singh, R. C. Glass, O. Kordina, and C. H. Carter, "Silicon carbide for power devices," in Proc. 9th Int. Symp. Power Semiconductor Devices and ICs, 1997, pp. 25–32.

17) B. J. Baliga, "Power semiconductor device figure of merit for high frequency applications," IEEE Electron Device Lett., vol. 10, pp. 455–457, Oct. 1989.

18) Cree, Inc. Announces Introduction and Availability of 3 Inch 4H SiC Wafers [Online]. Available: http://www.compoundsemiconductor. net

19) Infineon Technologies Produces World's First Power Semiconductors in Silicon Carbide [Online]. Available: http://www.compoundsemiconductor. net

20) J. B. Fedison, T. P. Chow, A. K. Agarwal, S. H. Ryu, R. Singh, O.Kordina, and J.W. Palmour, "Switching characteristics of 3 kV 4H–SiC GTO thyristors," in Proc. 58th Annu. Device Research Conf., 2000, pp. 135–136.

21) S. H. Ryu, A. K. Agarwal, R. Singh, and J. W. Palmour, "3100V asymmetrical, gate turn-off thyristors in 4H–SiC," IEEE Electron Device Lett., vol. 22, pp. 127–129, Mar. 2001.

22) S. Seshadri, J. B. Casady, A. K. Agarwal, R. R. Siergiej, L. B. Rowland, P. A. Sanger,C.D. Brandt, J. Barrow, D. Piccone, R. Rodrigues, and T. Hansen, "turn-off characteristics of 1000 V SiC gate-turn-off thyristors," in Proc. 10th Int. Symp. Power Semiconductor Devices and ICs, 1998, pp. 131–134.

23) K. Chatty, T. P. Chow, R. J. Gutmann, E. Arnold, and D. Alok, "Accumulation-layer electron mobility in n-channel 4H–SiC MOSFETs," IEEE Electron Device Lett., vol. 22, pp. 212–214, May 2001.

24) R. Singh, K. G. Irvine, O.Kordina, J.W. Palmour,M. E. Levinshtein, and S. L. Rumyanetsev, "4H–SiC bipolar P-i-N Diodes with 5.5 KV blocking voltage," in Proc. 56th Annu. Device Research Conf., 1998, pp. 86–87.

25) K. Shenai, R. S. Scott, and B. J. Baliga, "Optimum semiconductors for high power electronics," IEEE Trans. Electron Devices, vol. 36, pp. 1811–1823, Sept. 1989.

26) A. Bhalla and T. P. Chow, "Examination of semiconductors for bipolar power devices," Proc. Inst. Phys. Conf., no. 137, p. 621, 1994.

27) A. Bhalla and T. P. Chow, "Bipolar power device performance: dependence on materials, lifetime and device ratings," in Proc. 6th Int. Symp. Power Semiconductor Devices and ICs, 1994, pp. 287–292.

28) T. P. Chow and R. Tyagi, "Wide bandgap compound semiconductors for superior high-voltage power devices," IEEE Trans. Electron Devices, vol. 41, pp. 1481–1482, 1994.

29) B. J. Baliga, Power Semiconductor Devices. Boston, MA: PWS Publishing, 1996.

30) [30] S. K. Ghandhi, Semiconductor Power Devices. New York: Wiley, 1977.

31) M. Bhatnagar, P. K. McLarty, and B. J. Baliga, "Silicon carbide high-voltage (400V) Schottky barrier diodes," IEEE Electron Device Lett., vol. 13, pp. 501–503, Oct. 1992.

32) R. Raghunathan, D. Alok, and B. J. Baliga, "High voltage 4H–SiC Schottky barrier diodes," IEEE Electron Device Lett., vol. 16, pp. 226–228, June 1995.

33) A. Itoh, T. Kimoto, and H. Matsunami, “Low power-loss 4H–SiC Schottky rectifiers with high blocking voltage,” in Proc. Inst. Phys.Conf., 1995, pp. 689–692.

34) K. Ueno, T. Urushidani, K. Hashimoto, and Y. Seki, “The guard-ring termination for the high-voltage SiC Schottky barrier diodes,” IEEE Electron Device Lett., vol. 16, pp. 331–332, July 1995.

35) C. E. Weitzel, J. W. Palmour, C. H. Carter Jr, K. Moore, K. J. Nordquist, S. Allen, C. Thero, and M. Bhatnagar, “Silicon carbide high power devices,” IEEE Trans. Electron Devices, vol. 43, pp. 1732–1741, Oct. 1996.

36) H. Mitlehner, W. Bartsch, M. Bruckmann, K. O. Dohnke, and U. Weinert, “The potential of fast high voltage SiC diodes,” in Proc. 9th Int. Symp. Power Semiconductor Devices and ICs, 1997, pp. 165–168.

37) V. Saxena and A. J. Steckl, “High voltage 4H SiC rectifiers using Pt and Ni metallization,” Mater. Sci. Forum, vol. 264–268, pp.937–940, 1998.

38) R. Singh and J. W. Palmour, “Planar terminations in 4H–SiC Schottky diodes with low leakage and high yields,” in Proc. 9th Int. Symp. Power Semiconductor Devices and ICs, 1997, pp. 157–160.

39) Q. Wahab, T. Kimoto, A. Ellison, C. Hallin, M. Tuominen, R. Yakimova, A. Henry, J. P. Bergmann, and E. Janzen, “A 3 kV Schottky barrier diode in 4H–SiC,” Appl. Phys. Lett., vol. 72, no. 4, pp. 445–447, Jan. 1998.

40) K. J. Schoen, J. M. Woodall, J. A. Cooper Jr., and M. R. Melloch, “Design considerations and experimental analysis of high-voltage SiC Schottky barrier rectifiers,” IEEE Trans. Electron Devices, vol. 45, pp. 1595–1604, July 1998.

41) V. Khemka, T. P. Chow, and R. J. Gutmann, “Effect of reactive ion etch-damage on the performance of 4H–SiC Schottky barrier diodes,” J. Electron. Mater., vol. 27, no. 10, pp. 1128–1135, Oct. 1998.

42) [42] H. Mitlehner, P. Friedrichs, D. Peters, R. Schorner, U. Weinert, B. Weis, and D. Stephani, “Switching behavior of fast high voltage SiC pn diodes,” in Proc. 10th Int. Symp. Power Semiconductor Devices and ICs, 1998, pp. 127–130.

43) J. H. Zhao, K. Tone, S. R.Weiner,M. A. Caleca, D. Honghua, and S. P.Withrow, “Evaluation of ohmic contacts to p-type 6H–SiC created by C and Al co implantation,” IEEE Electron Device Lett., vol. 18, pp. 375–377, Aug. 1997.

44) M. E. Levinshtein, J. W. Palmour, S. L. Rumyantsev, and R. Singh, “turn-on process in 4H–SiC thyristors,” IEEE Trans. Electron Devices, vol. 44, pp. 1177–1179, July 1997.

45) N. V. Dyakonova, M. E. Levinshtein, J. W. Palmour, S. L. Rumyantsev, and R. Singh, “Temperature dependence of turn-on process in 4H–SiC thyristors,” Electron. Lett., vol. 33, no. 10, pp. 914–915, 1997.

46) P. Neudeck,W. Huang, and M. Dudley, “Breakdown degradation associated with elementary screw dislocations in 4H–SiC p+/n junction rectifiers,” Solid-State Electron., vol. 42, no. 12, pp. 2157–2164,Dec. 1998.

47) H. Yano, T. Kimoto, H. Matsunami, M. Blasser, and G. Pensl,"MOSFET performance of 4H-, 6H-, and 15R–SiC processed by dry and wet oxidation," Mater. Sci. Forum, vol. 338-342, pp. 1109–1112, Oct. 1999.

48) G. Y. Chung, C. C. Tin, J. R. Williams, J. K. McDonald, M. Di Vantra, S. T. Pantelides, L. C. Feldman, and R. A.Weller, "Effect of nitride oxide annealing on the interface trap densities near the band edges in the 4H polytype of silicon carbide," Appl. Phys. Lett., vol. 76, no. 13, pp. 1713–1715, Mar. 2000.

49) L. Lipkin, "N2O processing improves the 4H–SiC : SiO2 interface," presented at the ICSCRM, Tsukuba, Japan, Oct.-Nov. 2001.

50) D. Stephani, "Status, prospects and commercialization of SiC power devices," presented at the 59th Annu. Device Research Conf., South Bend, IN, June 2001.

51) Proc. Materials Research Society, vol. 640, Silicon Carbide—Materials, Processing, and Devices, Boston, MA, 2000.

52) A. Elasser,M. Ghezzo, N. Krishnamurty, J. Kretchmer, A.W. Clock, D. M. Brown, and T. P. Chow, "Switching characteristics of silicon carbide power p–i-n diodes," Solid-State Electron., vol. 44, no. 2, pp. 317–323, Feb. 2000.

53) H. Kapels, R. Rupp, L. Lorenz, and I. Zverev, "SiC Schottky diodes: A milestone in hard switching applications," in Proc. Power Conversion and Intelligent Motion Conf., Nuremberg, Germany, June 2001, pp. 95–100.

54) W. Wright, J. Carter, P. Alexandrov, P. Pan, M. Weiner, and J. H. Zhao, "Comparison of Si and SiC diodes during operation in threephase inverter driving ac induction motor," Electron. Lett., vol. 37, no. 12, pp. 787–788, June 2001.

55) W.Wondrak, R. Held, E. Niemann, and U. Schmid, "SiC devices for advanced power and high-temperature applications," IEEE Trans. Ind. Electron., vol. 48, no. 2, pp. 307–308, Apr. 2001.

56) K. Shenai, P. Neudeck, and G. Schwarze, "Design and technology of compact high power converters," IEEE Aerosp. Electron. Syst. Mag., vol. 16, pp. 27–31, Mar. 2001.

57) C. M. Johnson <etal>, "Recent progress and current issues in SiC semiconductor devices for power applications," IEE Proc. Circuits Devices Systems, vol. 148, no. 2,, pp. 101–108, Apr. 2001.

58) R. Rupp, "SiC Schottky diodes reach the market," Compound Semiconductor Mag., vol. 7, no. 3, Apr. 2001.

59) "Microsemi launches second-generation line of silicon carbide power Schottkies," Compound Semiconductor Mag., press release, May 16, 2001.

60) T. P. Chow, "SiC and GaN high-voltage power switching devices," in Proc. Int. Conf. Silicon Carbide and Related Materials, Research Triangle Park, NC, 1999, pp. 1155–1160.

61) J. Wang and B. W. Williams, "Evaluation of high-voltage 4H–SiC switching devices," IEEE Trans. Electron Devices, vol. 46, pp. 589–597, Mar. 1999.

62) M. J. Schutten and D. A. Torrey, "Edge-resonant power converter with novel magnetics," in Proc. IEEE Power Electronics Specialist Conf., June 1997, pp. 769–774.

63) M. J. Schutten, M. Kheraluwala, R. L. Steigerwald, and D. A. Torrey, "EMI comparison of hard switched, edge-resonant and load resonant dc/dc converters using a common power stage," in Proc. IEEE Industry Applications Society Conf., vol. 2, 1998, pp. 1588–1595.

64) V. Vlatkovic, M. J. Schutten, and R. Steigerwald, "Auxiliary series resonant converter: A new converter for high-voltage, high-power applications," in Proc. IEEE Applied Power Electronic Conf., 1996, pp. 493–499.

65) High Voltage Diode Data Sheet, Philips. [Online]. Available: http://www.semiconductors.philips.com/acrobat/datasheets/ BY8100_2.pdf

66) Y. Sugawara, D. Takayama, K. Asano, R. Singh, J. Palmour, and T. Hayashi, "12—19kV 4H–SiC pin diodes with low power loss," in Proc. Int. Symp. Power Semiconductor Devices and ICs, 2001, pp. 27–30.

67) K. Shenai and M. Trivedi, "Silicon carbide power electronics for high temperature applications," in Proc. IEEE Aerospace Conf., vol. 5, 2000, pp. 431–437.

68) P. G. Neudeck, "Progress toward high temperature, high power SiC devices," in Proc. Inst. Phys. Conf., vol. 141, Compound Semiconductors, 1994, pp. 1–6.

69) R. Sei-Hyung, A. K. Agarwal, J.W. Palmour, and M. E. Levinshtein, "1.8 kV, 3.8 A bipolar junction transistors in 4H–SiC," in Proc. 13th Int. Symp. Power Semiconductor Devices and ICs, 2001, pp. 37–40.

70) M. R. Werner and W. R. Fahrner, "Review on materials, microsensors, systems, and devices for high-temperature and harsh-environment applications," IEEE Trans. Ind. Electron., vol. 48, pp. 249–257, Apr. 2001.

71) Benefits of silicon carbide electronics to aircraft, NASA. [Online]. Available: http://www.grc.nasa.gov/WWW/SiC/aircraftbenefit.html

72) N. G. Hingorani, "High-voltage dc transmission: A power electronics workhorse," IEEE Spectrum, vol. 33, pp. 63–72, Apr. 1996.

73) E. R. Brown, "Megawatt solid-state electronics," Solid-State Electron., vol. 42, no. 12, pp. 2119–2130, 1998.

74) M. M. Freeman and M. R. Perschbacher, "Hybrid power—an enabling technology for future combat systems," in Proc. 12th IEEE Int. Pulsed Power Conf., vol. 1, 1999, pp. 17–22.

75) M. Ghezzo, "Silicon carbide megawatt power devices for combat vehicles," General Electric CRD, Final Rep. DARPA Contract MDA972-98-C-0001, July 2001.

76) T. Burke, K. Xie, J. R. Flemish, H. Singh, T. Podelsak, and J. H. Zhao, "Silicon carbide power devices for high temperature, high power density switching applications," in Proc. IEEE 22nd Power Modulator Symp., 1996, pp. 18–21.

77) T. Burke, K. Xic, H. Singh, T. Podlesak, and J. Flemish, "Silicon carbide thyristors for electric guns," IEEE Trans. Magn., vol. 33, pp. 432–437, Jan. 1997.

78) A.Welleman, U. Schlapbach, and E. Ramezani, "Plug and play solid state switching system for laser applications," in Proc. 12th IEEE Int. Pulsed Power Conf., vol. 1, 1999, pp. 150–152

79) Y. Chung, C. Yang, and H. Kim, "All solid state switched pulser for air pollution control system," in Proc. 12th IEEE Int. Pulsed Power Conf., vol. 1, 1999, pp. 177–180.

80) T. F. Podlesak and F. M. Simon, "Single shot and burst repetitive operation of involute gate 125mm symmetric thyristors up to 221kA with a di=dt of 2k A/ s," in Proc. 12th IEEE Int. Pulsed Power Conf., vol. 1, 1999, pp. 206–209.

81) C. R. Hummer, H. Singh, and D. Piccone, "Thyristors for pulsed power applications," in Proc. 24th Int. Power Modulator Symp., 2000, pp. 78–80.

82) R. B. True, R. J. Hansen, and G. R. Good, "The Hobetron-a high power vacuum electronic switch," IEEE Trans. Electron Devices, vol. 48, pp. 122–128, Jan. 2001.

83) Samir Hazra, Sachin Madhusoodhanan, Subhashish Bhattacharya," Design Considerations and Performance Evaluation of 1200 V, 100 A SiC MOSFET Based Converter for High Power Density Application", 2013.

84) Rasmus Ørndrup Nielsen,"Efficiency and Cost Comparison of Si IGBT and SiC JFET Isolated DC/DC Converters", 2013.

85) Szymon Piasecki, "Jacek Rąbkowski, Grzegorz Wrona, Tadeusz Płatek," SiC-Based Support Converter for Passive Front-End AC Drive Applications", 2013.

86) Hesam Mirzaee, "Design Comparison of High-Power Medium-Voltage Converters Based on a 6.5-kV Si-IGBT/Si-PiN Diode, a 6.5-kV Si-IGBT/SiC-JBS Diode, and a 10-kV SiC-MOSFET/SiC-JBS Diode", 2014.

87) Jonathan K. Hayes1, Andrés Escobar-Mejía2, Juan Carlos Balda3, Atanu Dutta4, Simon S. Ang5," Realization of a SiC Module-Based Indirect Matrix Converter with Minimum Parasitic Inductances", 2014.

88) Héctor Sarnago," SiC BJT-based Full-ZCS Quasi-Resonant Converter with Improved Efficiency for Induction Heating Applications.

89) Luigi Abbatelli, Michele Macauda, Giuseppe Catalisano," Fully SiC based High Efficiency Boost Converter", 2014.

90) Di Han, "Comprehensive Efficiency, Weight, and Volume Comparison of SiC- and Si-Based Bidirectional DC–DC Converters for Hybrid Electric Vehicles", 2014.

91) Luigi Abbatelli," Cost Benefits on High Frequency Converter system based on SiC MOSFET approach", 2014.

92) Emre Gurpinar," Performance Analysis of SiC MOSFET Based 3-Level ANPC Grid-Connected Inverter with Novel Modulation Scheme", 2014.

93) Liyao Wu, "Efficiency Evaluation of the Modular Multilevel Converter Based on Si and SiC Switching Devices for Medium/High-Voltage Applications", 2015.

94) Sachin Madhusoodhanan, "Solid-State Transformer and MV Grid Tie Applications Enabled by 15 kV SiC IGBTs and 10 kV SiC MOSFETs Based Multilevel Converters", 2015.

95) Liyao Wu, Jiangchao Qin, and Maryam Saeedifard," Loss Comparison of Si- and SiC-Based Modular Multilevel Converter for Medium/High-Voltag Applications", 2015.

96) Georgios Kampitsis, Michail Antivachis, Sotirios Kokosis," An Accurate Matlab/Simulink Based SiC MOSFET Model for Power Converter Applications", 2015.

97) Samir Hazra, High Switching Performance of 1700-V, 50-A SiC Power MOSFET Over Si IGBT/Bi MOSFET for Advanced Power Conversion Applications", 2016

98) Sachin Madhusoodhanan, Krishna Mainali, Awneesh Tripathi, Dhaval Patel, Arun Kadavelugu, Subhashish Bhattacharya," Performance Evaluation of 15 kV SiC IGBT based